Characterization of the life-cycle stages of the coccolithophore *Emiliania huxleyi* and their responses to Ocean Acidification

Dissertation

zur Erlangung des akademischen Grades eines

Doktors der Naturwissenschaften

- Dr. rer. nat. -

Am Fachbereich 2 (Biologie/Chemie)

der Universität Bremen

Vorgelegt von

Sebastian Rokitta im September 2012

Sebastian Rokitta, Dipl. Biol.

Alfred-Wegener-Institut für Polar- und Meeresforschung

in der Helmholtz-Gemeinschaft

ERC Nachwuchsgruppe PhytoChange / Marine Biogeosciences

Am Handelshafen 12, 27570 Bremerhaven, Germany

Sebastian.Rokitta@awi.de

Table of Contents

PREFACE

Disclaimer

I hereby assure that I myself have performed the work described in this doctoral thesis. All external resources used as well as the contributions made to the publications are appropriately stated.

_____

Acknowledgements

I am exceptionally grateful to Björn Rost. Besides for your guidance, I thank you for your contagious curiosity that made me embrace ever new and exciting topics. Thank you for creating a wonderful working atmosphere that stimulated my creativity and thinking.

I also thank Uwe John for his supervision and counsel throughout the whole time. Our inspiring discussions have always motivated me. Thanks for the academic freedom you two gave to me, and for the support I received from you with many respects, also aside from pure science.

I would also like to thank professors Kai Bischof and Dieter Wolf-Gladrow for reviewing this thesis and being part of the promotion committee. Dieter, I have always enjoyed being part of the Biogeosciences group, which is not at last due to the unconventional way of your administration. I am indebted to this great group of people, for the open and collegial working environment and the fun that arose from it. Special thanks go to Albert Benthien, for his help and advice in so many things and the fun we had as fellow commuters. I would also like to thank Silke Thoms and Lena Holtz, who have not only sparked my interest for the dark arts of numerical modeling but also for the fruitful cooperation we had and will have.

I want to express my gratitude to the technical staff of the group, especially Klaus-Uwe and Uli Richter, Jana Hölscher, Laura Wischnewski and all others that construct apparatuses, operate machines and run analyses. You all deserve great acknowledgments, for my work and that of others would not have been possible without you.

I acknowledge the help and supervision I received from Scarlett Trimborn, Dedmer van de Waal and Sven Kranz, the senior (and partly former) members of the PhytoChange project. Thanks for your constructive criticism and the challenging discussions regarding methods, procedures and manuscript drafting. These were not always easy but have significantly influenced my interpretation and reasoning and improved the overall quality of my work. A lot of what I learned during the time of my PhD was due to the 'never-let-loose'-attitude which I adapted from you, Sven.

On the other side, I want to say 'thank you' to the younger members of the PhytoChange project, Clara Hoppe, Meri Eichner, Mirja Hoins, Doro Kottmeier and Tim Eberlein. It is a great pleasure and a delighting feeling to give to you what was previously given to me. Thank you Clara for being a kind and trustful office companion; our exciting discussions and arguments of whatever nature always gave me new insights or at least perspectives. Thank you Doro for being a dedicated and enthusiastic student, it is great to work with you and I look forward to our future explorations.

I want to thank my cooperation partners, namely Colomban De Vargas and Ian Probert from the Biological Station Roscoff (France), for contributing their expertise to the

projects I conducted and the interesting discussion that arose. I also like to thank Peter von Dassow from the University of Santiago (Chile) for the great time we had creating loads of interesting data. I look forward to processing these finally.

I also would like to thank Sinead Collins from the University of Edinburgh (Scotland) and Gordon Wolfe from the University of Chico (California, USA). The constructive and thorough input and ideas I got from you have always been helpful and I hope we can continue this fruitful cooperation.

I also like to thank all the other people at the AWI that make this institute such a great place, especially Christoph Wagner, an exceptional non-scientist who became an estimated friend over the time.

At last, but at most, I am indebted and deeply grateful to the two women in my life: My wife Nike and my daughter Emilia. You not only gave me a 'real-life' outside science, but indeed made it a rich, exciting and beautiful adventure. You gave me not only the freedom but also the power to pursue my goals. That I could succeed in this quest is also your accomplishment and merit. Thank you, I love you!

Summary

Anthropogenic carbon dioxide emissions cause a chemical phenomenon known as Ocean Acidification (OA). The associated changes in seawater chemistry are believed to have significant impact especially on coccolithophores, unicellular calcifying primary producers that take an outstanding role in the regulation of the marine carbon pumps. This thesis investigated the calcifying diploid and the non-calcifying haploid life-cycle stages of the globally dominant coccolithophore *Emiliania huxleyi*, and their responses to OA. Emphasis was put on investigating the role of energy-availability (i.e., irradiance) in the manifestation of OA-responses. A suite of methods was applied to resolve the effects on the phenomenological level (growth, elemental quotas and production), the physiological level (photosynthesis, carbon acquisition) and the level of gene expression (transcriptomics).

In publication I, haploid and diploid cells were compared using microarray-based transcriptome profiling to assess stage-specific gene expression. The study identified genes related to distinct cell-biological traits, such as calcification in the diplont as well as flagellae and lipid respiration in the haplont. It further revealed that the diploid stage needs to make more regulatory efforts to epigenetically administrate its double amount of DNA, and therefore strongly controls its gene expression on the basis of transcription. The haplont in turn, possessing only a single sized genome, does not require these administrative efforts and seems to drive a more unrestricted gene expression. The proteome is apparently regulated on the basis of rapid turnover, i.e., post-translational. The haploid and diploid genomes may therefore be regarded as cellular 'operating systems' that streamline the life-cycle stages to occupy distinct ecological niches.

Publication II investigated the responses of the life-cycle stages to OA under limiting and saturating light intensities. Growth rates as well as quotas and production rates of carbon (C) and nitrogen (N) were measured. In addition, inorganic C acquisition and photosynthesis were determined with a ^{14}C-tracer technique and mass spectrometry-based gas-flux measurements. Under OA, the diploid stage shunted resources from calcification towards biomass production, yet keeping the production of total particulate carbon constant. In the haploid stage, elemental composition and production rates were more or less unaffected although major physiological acclimations were evident, pointing towards efforts to maintain homeostasis. Apparently, both life-cycle stages pursue distinct strategies to deal with OA. As a general pattern, OA-responses were strongly modulated by energy availability and typically most pronounced under low light. A concept explaining the energy-dependence of responses was proposed.

In publication III, microarray-based transcriptome profiling was used to screen for cellular processes that underlie the observed phenomenological and physiological responses observed in the life-cycle stages (publication II). In the diplont, the increased biomass production under OA seems to be caused by production of glycoconjugates and lipids.

The lowered calcification may be attributed to impaired signal-transduction and ion-transport mechanisms. The haplont utilized genes and metabolic pathways distinct from the diploid stage, reflecting the stage-specific usage of certain portions of the genome. With respect to functionality and energy-dependence, however, the transcriptomic OA-responses resembled those of the diplont. In both stages, signal transduction and ion-homeostasis were equally OA-sensitive under all light intensities. The effects on carbon metabolism and photophysiology, however, were clearly modulated by light availability. These interactive effects can be explained with the influence of both OA and light on the cellular 'redox hub', a major sensory system controlling the network of metabolic sources and sinks of reductive energy.

In the general discussion, the newly gained views on the life-cycle stages are synthesized and biogeochemical implications of light-dependent OA-effects on coccolithophore calcification are considered. Furthermore, emerging physiological response patterns are identified to develop unifying concepts that can explain the energy-dependence of physiological effects. Finally, the critical role of redox regulation in the responses to changing environmental parameters is argued and research perspectives are given how to further resolve effects of the changing environment on marine phytoplankton.

Zusammenfassung

Anthropogene Kohlenstoffdioxidemissionen verursachen das chemische Phänomen der Ozeanazidifizierung (OA). Man geht davon aus, dass die damit verbundenen Veränderungen in der Seewasserchemie einen signifikanten Einfluss auf Coccolithophoriden haben. Diese einzelligen, kalkbildenden Primärproduzenten haben einen großen Einfluß auf die marinen Kohlenstoffpumpen. In dieser Dissertation wurden diploide, kalzifizierende und haploide, nicht-kalzifizierende Kernphasenstadien der Coccolithophoride *Emiliania huxleyi* charakterisiert, und ihre Reaktionen auf OA untersucht. Im besonderen Fokus stand die Frage, welche Rolle die Energieverfügbarkeit (d.h. Lichtintensität) für die Ausprägung dieser OA-Reaktionen spielt. Eine Reihe von Methoden wurde angewendet, um die Effekte auf den Ebenen von Phänomenologie (Wachstumsrate, Elementzusammensetzung, Produktionsraten), Physiologie (Photo-synthese, Kohlenstofferwerb) und Genexpression (Transkriptomik) zu beschreiben.

In Publikation I wurden die Transkriptomprofile der haploiden und diploiden Kernphasenstadien mittels Microarrays verglichen, um stadien-abhängige Unterschiede in der Genexpression zu erfassen. Die Studie konnte Gene identifizieren, die den spezifischen Merkmalen zuzuordnen sind (Kalzifizierung im Diplonten, Flagellen und erhöhte Lipidrespiration im Haplonten). Die Studie konnte weiterhin zeigen, dass der Diplont aufgrund der doppelten Genomgröße mehr epigenetische Regulation betreiben muss, und seine Genexpression daher auf der Ebene der Transkription steuert. Der Haplont hingegen, der nur ein einfaches Genom besitzt, benötigt derartige Regulation

nicht und betreibt die Transkription vergleichsweise uneingeschränkt. Das Proteom wird offenbar durch steten Abbau, d.h. auf post-translationaler Ebene kontrolliert. Das haploide und das diploide Genom sind folglich als zelluläre ‚Betriebssysteme' zu sehen, die die Stadien in die Lage versetzen, verschiedene ökologische Nischen zu besetzen.

In Publikation II wurden die Reaktionen der Kernphasenstadien auf OA unter limitierenden und saturierenden Lichtintensitäten untersucht. Hierzu wurden Wachstumsraten sowie der Gehalt und die Produktionsraten von partikulärem Kohlenstoff (C) und Stickstoff (N) gemessen. Zusätzlich wurden der Erwerb von inorganischem Kohlenstoff und die Photosynthese mittels ^{14}C-Tracertechniken und massenspektrometrischen Gasfluss-messungen charakterisiert. Unter OA verlagerte der Diplont Ressourcen von der Kalzifizierung zur Biomasseproduktion, hielt jedoch die Gesamtproduktion von partikulärem Kohlenstoff konstant. Obwohl im Haplonten physiologische Reaktionen klar erkennbar waren, blieben Elementzusammensetzungen und Produktionsraten unverändert. Offenbar verfolgen beide Ploidiestadien unterschiedliche Strategien im Umgang mit OA. Im Allgemeinen waren die Reaktionen auf OA stark durch die Energieverfügbarkeit moduliert und typischerweise unter niedrigen Lichtintensitäten besonders ausgeprägt. Basierend auf den Ergebnissen wurde ein Konzept zur Energieabhängigkeit physiologischer Reaktionen vorgeschlagen.

In Publikation III wurden mittels Microarrays Transkriptomprofile erfasst und verglichen, um die Prozesse aufzuklären, die hinter den beobachteten phänomenologischen und physiologischen Reaktionen stehen (Publikation II). Im Diplonten wird die gesteigerte Biomasseproduktion unter OA offenbar durch die gesteigerte Produktion von Glycoconjugaten und Lipiden verursacht. Die reduzierte Kalzifizierung kann der Beeinträchtigung von Signaltransduktion und Ionentransportmechanismen zugeordnet werden. Der Haplont expremiert andere Gene und betreibt andere Stoffwechselwege als der Diplont, was die kernphasenspezifische Nutzung genomischer Ressourcen widerspiegelt. In beiden Stadien waren Signaltransduktion und Ionentransport-mechanismen OA-sensitiv, unabhängig von der Lichtintensität. Die Effekte auf den Kohlenstoffmetabolismus und die Photophysiologie hingegen waren klar energiemoduliert. Diese interaktiven Effekte können mit dem Einfluß von OA und Licht auf den ‚redox hub' erklärt werden, ein wesentliches Sensorsystem, welches das Netzwerk von metabolischen Quellen und Senken reduktiver Energie kontrolliert.

In der allgemeinen Diskussion werden die neu gewonnenen Erkenntnisse über die Kern-phasenstadien synthetisiert und die biogeochemischen Implikationen von lichtmodu-lierten OA-Effekten auf die Kalzifizierung betrachtet. Ferner werden hervortretende Muster identifiziert und vereinheitlichende Konzepte erarbeitet, welche die Energieabhängigkeit physiologischer Effekte formulieren. Abschließend wird die zentrale Rolle der Redoxregulation bei Reaktionen auf Umweltbedingungen diskutiert und es werden Forschungsansätze aufgezeigt, mit denen die Reaktionen von marinem Phytoplankton auf den globalen Wandel detaillierter untersucht werden können.

List of abbreviations

ATP	adenosine triphosphate
$CaCO_3$	calcium carbonate mineral
CCM	carbon-concentrating mechanism
C_i	inorganic carbon
CO_2	carbon dioxide
CO_3^{2-}	carbonate ion
DIC	dissolved inorganic carbon
DNA	deoxyribonucleic acid
GL	glycolysis
HCO_3^-	bicarbonate
H_2CO_3	true carbonic acid
µatm	microatmosphere
$NADP^+$/NADPH	nicotineamide-adenine-dinucleotide-phosphate, redox pair
NAD^+/NADH	nicotinamide-adenine-dinucleotide, redox pair
NH_4^+	ammonium
NO_3^-	nitrate
OA	Ocean Acidification
Ω	saturation state of a mineral
pCO_2	carbon dioxide partial pressure
pK_a	pK value of an acid
PIC	particulate inorganic carbon
POC	particulate organic carbon
ppmv	parts per million (volume-based), a mixing ratio
PPP	pentose phosphate pathway
TA	total alkalinity
TPO_4	total phosphate

List of figures

INTRODUCTION

Global change and the Anthropocene

One key event in human evolution was when hominids learned to control fire, around 0.5-1.5 million years ago (James et al. 1989). Ever since, heating, lighting and cooking was fuelled by the combustion of organic matter, a chemical process that became indispensable to our daily life. Technologies of modern history, especially steam power and electricity, allowed conversion of heat into kinetic and electric energy, providing unprecedented labor force and innovative applications. The new technologies promoted welfare, raised people´s living standards and soon enabled the transition of agrarian societies into industrialized ones. While wood and peat have been the dominant fuel for hundreds of thousands of years, the use of fossil fuels like coal and oil became common in the early nineteenth century. These fuels possess a much higher energy-density and especially petrochemistry paved the way for internal combustion motors. Broadly applied in land- and air transportation, motors enabled worldwide resource flows and product distribution and have ultimately initiated the era of economic globalization we live in: It is nowadays impossible to grasp where the hundreds of individual components of modern products (e.g. a cell phone) originate from, or how much pollution, labor force and transportation was involved in providing them.

Whereas beneficial aspects of industrialization and globalization (e.g., reduced child mortality, higher education, increasing gross domestic products and increased life expectancy) are highly valuated and appreciated, the cascading negative effects of globalization, the so-called 'global change' has been almost unrecognized and neglected for long time. The term 'global change' comprises the vast number of human activities that influence principal components of the Earth system, i.e. atmosphere, cryosphere, hydrosphere, geosphere, biosphere as well as the biogeochemical cycles of elements throughout. Because the human civilization has over the past decades significantly influenced these components, it is meanwhile considered a geophysical force itself, being of systemic relevance for the fate of the planet (Steffen et al. 2004). For these reasons, the youngest history is being termed the 'Anthropocene', the era of mankind (Crutzen 2002). The effects of global change occur over longer time scales and usually remote from their source. They cumulate in ecosystems in a bottom-up manner and have effects on variable spatial and temporal scales, making the exploration of global change most challenging.

The human carbon perturbation

Among the plethora of environmental impacts, the massive release of carbon dioxide (CO_2) into the atmosphere due to fossil fuel combustion and changed land use may be the most striking one. Atmospheric CO_2 partial pressure (pCO_2) was tightly coupled to glacial-interglacial cycles over at least the last 850.000 years, fluctuating roughly between 180 and 280 µatm (Lüthi et al. 2008; Figure 1 showing the past 400.000 years). Nowadays it is driven by anthropogenic CO_2 emissions and has increased from ~280 µatm in the mid of the 18th century to around 395 µatm in 2012 (Mauna Loa Observatory, Scripps Institution of Oceanography). These levels are higher than seen in the last 850.000 years and likely several million years (Kump et al. 2009). Cumulated over a time of few hundred years, mankind has released estimated 500 Pg of carbon in the form of CO_2 (Allen et al. 2009). At the current release rates (~10 Pg C per year; Peters et al. 2012), which are ~30 times higher than those that have commonly occurred in the known geological past (Doney et al. 2009), the next 500 Pg of anthropogenic carbon will be emitted in 50 years, probably less.
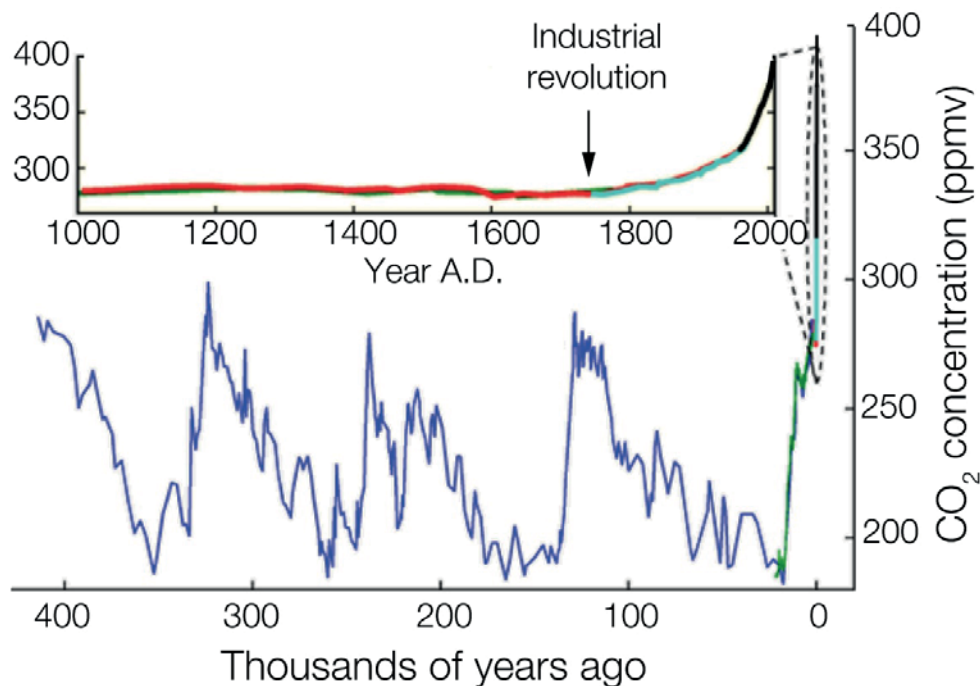
Figure 1: Reconstructions of atmospheric CO_2 concentrations; Redrawn from Rohde (2006); Blue: Vostok ice core (Fischer et al. 1999); Green: Taylor Dome core (Monnin et al. 2004); Red: Law Dome ice core (Etheridge et al. 1998); Cyan: Siple Dome ice core (Neftel et al. 1994); Black: Mauna Loa Observatory data (Keeling and Whorf 2004); CO_2 concentrations have been growing exponentially since the 18th century, the beginning of industrialization.

One primal effect of this extraordinary atmospheric CO_2 input is the intensification of the CO_2-derived greenhouse effect, i.e., atmospheric heat-retention. Without this greenhouse effect, Earth would exhibit significantly lower, uninhabitable temperatures (Lacis et al. 2010; Pierrehumbert 2011). The anthropogenic greenhouse effect, however, promotes additional warming and deglaciation and thereby interferes with the natural glacial-interglacial cycling (Petit et al. 1999). Such 'global warming' also imposes secondary effects, especially on aquatic ecosystems: High temperatures in upper water layers lead to stronger stratification and prevent deep wind-driven overturning. Due to reduced vertical mixing, the supply of macronutrients N and phosphorus (P) from deeper waters is reduced and organisms in the upper layer become on average more exposed to solar irradiation. In addition to these physical effects, CO_2 also causes a chemical phenomenon in seawater that was recognized decades ago (Revelle and Suess, 1957; Broecker and Peng 1982), but only recently received broader attention: The phenomenon of ocean acidification (OA), which to be understood, requires a brief introduction to seawater carbonate chemistry.

Seawater carbonate chemistry

Like other gases, atmospheric CO_2 dissolves in seawater, a process that is described by Henry's law. Unlike most other gases, CO_2 reacts with water (H_2O) and forms true carbonic acid (H_2CO_3), an acid that rapidly dissociates and thereby speciates into bicarbonate (HCO_3^-), carbonate ions (CO_3^{2-}) and H^+ (Figure 2). Consequently, an invasion or outgassing of CO_2 alters the pH of aquatic solutions. Vice versa, pH manipulations alter the speciation of the carbonate system. CO_2 (including H_2CO_3), HCO_3^- and CO_3^{2-} are collectively referred to as dissolved inorganic carbon (DIC).
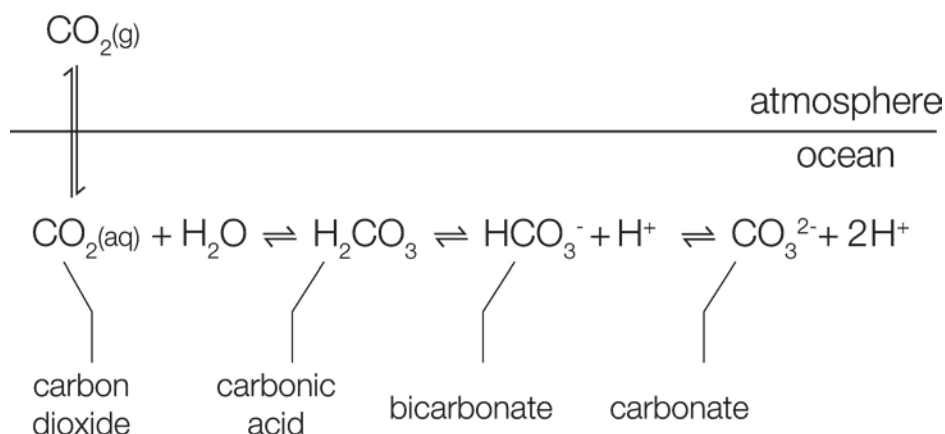
Figure 2: Ocean-atmosphere equilibration of CO_2 and speciation of carbonic acid.

Whereas CO_2 is the dominant species at pH values below the first dissociation point ($pK_{a,1} \approx 6.1$), CO_3^{2-} dominates above the second dissocation point ($pK_{a,2} \approx 9.1$) and HCO_3^- in between (Figure 3; pK_a values taken from Mehrbach et al. 1973 refit by Dickson and Millero 1987; temperature = 20°C, pressure = 1dbar, salinity = 32). The speciation into carbonates allows water to take up more inorganic carbon than would be possible due to solubility of CO_2 alone.
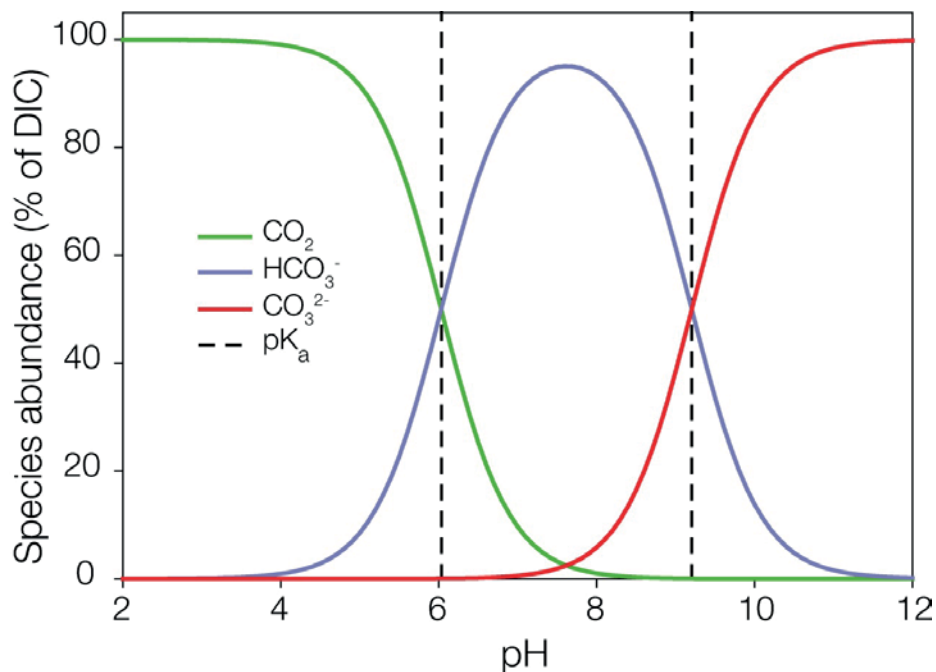
Figure 3: Bjerrum plot, showing DIC speciation over pH (temperature = 20°C, pressure = 1 dbar, salinity = 32).

The described uptake of CO_2 into water can be tremendously enhanced by alkalinity, a chemical property of fresh- and especially seawater. Alkalinity may be described operationally, as an amount of negative charges that is able to accept the H^+ released in the dissociation reactions of carbonic acid (Figure 2). This removal of reaction products facilitates a massive invasion of CO_2 into the water: If simple (TA = 0), saline water is left to equilibrate with the ambient atmosphere (395 µatm CO_2; temperature = 20°C, pressure = 1 dbar, salinity = 32), it exhibits DIC concentrations of ~0.016 mmol kg^{-1}. If seawater with a typical alkalinity background of 2.35 mmol kg^{-1} is used instead, it takes up ~2.1 mmol DIC kg^{-1}, i.e., more than the 130-fold amount that non-alkaline water can take up.

The origins of oceanic alkalinity are geological weathering processes. Typical weathering scenarios are the formation of slightly acidic rain in the atmosphere (Equation 1) and subsequent dissolution of silicate minerals such as olivine (Mg_2SiO_4; Equation 2) or carbonate minerals like limestone ($CaCO_3$; Equation 3).

Eq. 1 $$CO_2 + H_2O \rightarrow HCO_3^- + H^+$$

Eq. 2 $$Mg_2SiO_4 + 2\,HCO_3^- + 2\,H^+ \rightarrow 2\,Mg^{2+} + 2\,HCO_3^- + H_2SiO_4^{2-}$$

Eq. 3 $$CaCO_3 + HCO_3^- + H^+ \rightarrow Ca^{2+} + 2\,HCO_3^-$$
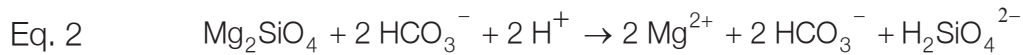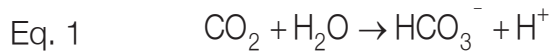
In both cases, due to their lower or equal pK_a value, the weak bases that are released from the mineral accept the H^+ that originate from carbonic acid. The resulting carbonates, having donated original protons, are washed to the ocean together with the metal cations released from the mineral, i.e., electroneutral. Consequently, the oceans contain an excess of proton acceptors (i.e., bases derived from weak acids with $pK_a<4.5$) over proton donors. This is in fact the traditional definition of total alkalinity (TA) as given by Dickson (1981; Equation 4):

Eq. 4
$$TA = [HCO_3^-] + 2\,[CO_3^{2-}] + [B(OH)_4^-] + [OH^-] + [HPO_4^{2-}] + 2\,[PO_4^{3-}]$$
$$+ [H_3SiO_4^-] + [NH_3] + [HS^-] - [H^+] - [HSO_4^-] - [HF] - [H_3PO_4]$$

TA (given in mol kg^{-1}) is a conservative parameter, because the number of relevant negative charges in 1 kg of seawater is independent of volume changes caused by varying temperature and pressure. However, single constituents within in the TA expression (e.g., HCO_3^-, CO_3^{2-} or $B(OH)_4^-$; Equation 4) are themselves not conservative, because pK_a values of their acid-base systems are influenced by temperature and pressure. To overcome this, Dickson's definition was re-expressed in an *explicit conservative* way by Wolf-Gladrow et al. (2007; Equation 5):

Eq. 5
$$TA_{ec} = [Na^+] + 2\,[Mg^{2+}] + 2\,[Ca^{2+}] + [K^+] + 2\,[Sr^{2+}] + ...$$
$$- [Cl^-] - [Br^-] - [NO_3^-] - ...$$
$$+ [TPO_4] + [TNH_3] - 2\,[TSO_4] - [THF] - [THNO_2]$$

TA is thereby defined by Dickson's definition but combined with an overall charge balance. DIC species do not appear at all, because CO_2 invasion or -release do not affect the concentrations of conservative ions or uncharged species (such as TPO4). This expression also makes it possible to easily grasp effects of biological processes in terms of their effect on alkalinity. It can for example be seen that the production of 1 unit $CaCO_3$ reduces TA by 2 units because two charges are removed from solution (cf. Equation 5), whereas only one mol of C is required. This and other biological effects on carbonate chemistry are illustrated in Figure 4 (Zeebe and Wolf Gladrow 2001; Rost et al. 2008).
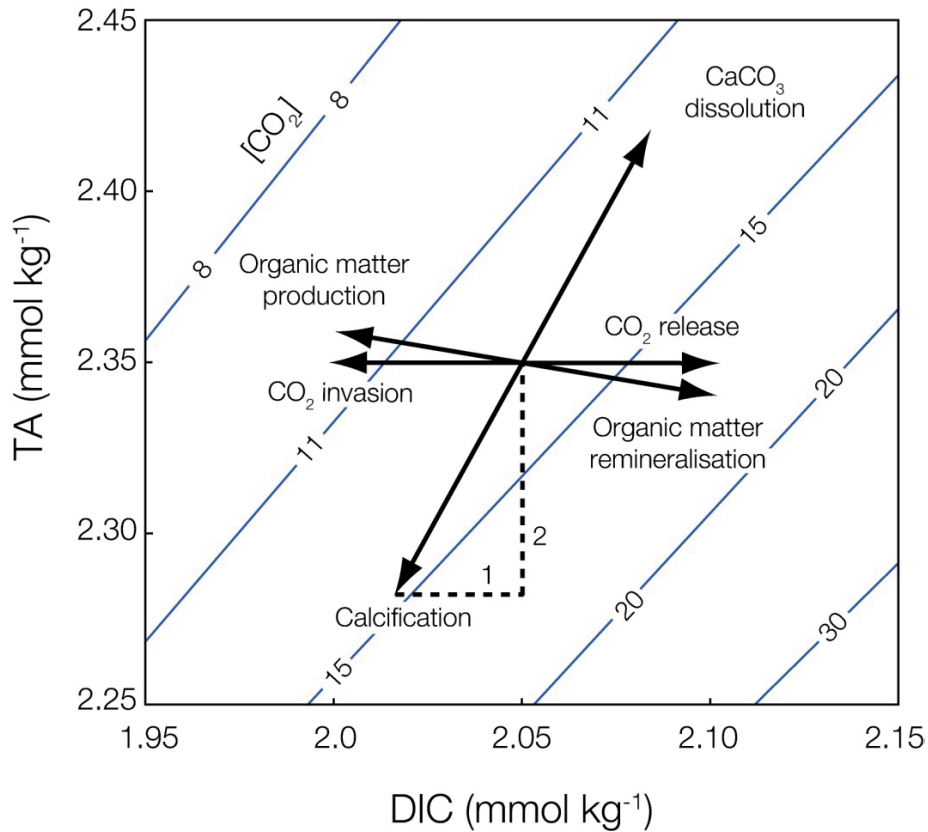
Figure 4: Processes affecting DIC and TA (background isoclines indicate $[CO_2]$ in $\mu mol\ kg^{-1}$): Whereas CO2 invasion and release can increase or decrease [DIC], the production and dissolution of $CaCO_3$ can decrease or increase both, [DIC] and TA, in a 1:2 stoichiometry. Biomass production and remineralization decrease or increase [DIC], respectively, but also slightly increase or decrease TA due to the uptake or release of NO_3^- (Equation 5). Redrawn from Zeebe and Wolf Gladrow (2001).

Given this brief introduction, the chemical and geochemical implications of anthropogenic CO_2 emissions for the marine environment are elaborated in the following section.

Ocean Acidification

The human carbon perturbation causes an invasion of CO_2 into the sea and increases aqueous $[CO_2]$, [DIC] and $[HCO_3^-]$ while it decreases pH and $[CO_3^{2-}]$. The term 'Ocean Acidification' summarizes this combination of shifting chemical parameters (Figure 3). Because relative increases in [DIC] and $[HCO_3^-]$ will be only marginal (<10%), these are believed to have little overall effect on biota. The prominent relative changes in the remaining parameters, however, are believed to have qualitatively different effects on marine biota: The increased $[CO_2]$, i.e., 'ocean carbonation', may benefit marine primary

productivity, by possibly enhancing diffusive CO_2 supply for photosynthesis (Raven et al. 2005) or by reducing the CO_2 leakage from cells that use carbon-concentrating mechanisms (CCM) to actively accumulate inorganic carbon (C_i; Rost et al. 2006).

Regarding oceanic pH, values have already dropped from values of ~8.2 (corresponding to preindustrial pCO$_2$ of 280 µatm) to contemporary values of ~8.1 (around 395 µatm) and will continue to drop to values around 7.9 (expected by the end of the century at ~800 µatm) and beyond (Figure 5). The drop of 0.3 pH units translates roughly into a doubling of [H^+] that will not only affect acid-base chemistry and bioavailability of macro- and micronutrients, but may as well affect the conformation and thereby the catalytic activity of cellular enzymes and transporters.
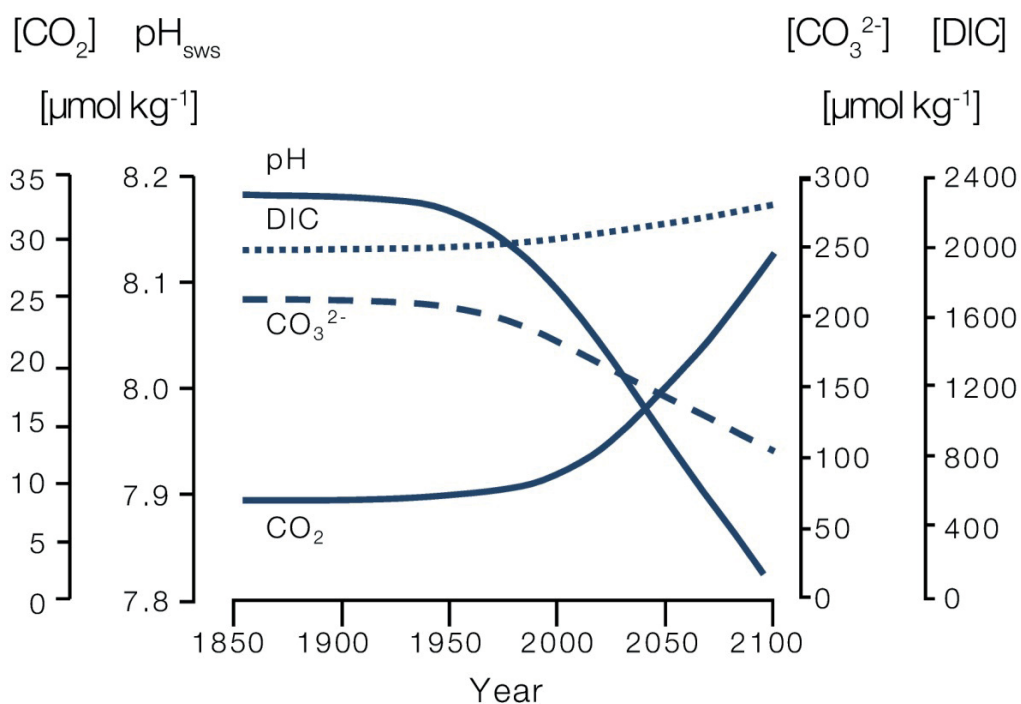
Figure 5: Ocean Acidification, here projected over time, affects marine chemistry by altering especially [CO_2], pH and [CO_3^{2-}]. Redrawn from Wolf-Gladrow et al. 1999, concentrations reflect the IS92A 'business as usual' CO_2 emission scenario (IPCC 1995).

Calcifying organisms have been shown to exhibit an exceptional sensitivity towards OA (Kroecker et al. 2011; Nisumaa et al. 2011). Reduced calcification is usually attributed to the decrease in saturation state (Ω) of $CaCO_3$ due to lowered [CO_3^{2-}] (Equation 6). The saturation state Ω relates the concentrations of Ca^{2+} and CO_3^{2-} in a solution to their concentrations at saturation and thereby reflects the degree of under- or oversaturation with respect to a specific mineral.

Eq. 6
$$\Omega = \frac{[Ca^{2+}] \times [CO_3^{2-}]}{[Ca^{2+}]_{sat} \times [CO_3^{2-}]_{sat}}$$

As long as $\Omega > 1$, the water is supersaturated and $CaCO_3$ will not dissolve. If $\Omega < 1$, the water becomes corrosive and dissolution is favored. In contemporary oceans, the saturation states of surface water for calcitic (trigonal crystal structure) and aragonitic (rhomboedric crystal structure) $CaCO_3$ are about 4.8 and 3.2, respectively (Ridgwell and Zeebe 2005). However, ongoing OA will cause saturation states to drop. In fact, due to higher CO_2 solubility at low temperatures, undersaturation of polar surface waters is expected within the 21st century (Orr et al. 2005). Although only 'true' undersaturation will cause dissolution, already a lowered saturation state must to some extent affect the biological mineralization processes, simply because $CaCO_3$ precipitation under low pH is thermodynamically *less* favored (Ridgwell and Zeebe, 2005).

Cells of multicellular heterotrophic organisms exhibit steep outwards-directed CO_2 gradients due to respiration. Also, their tissues possess epithelia that protect internal physiology from outside perturbations. Unicellular organisms, in turn, are separated from the outside world by only a ~10 nm thick lipid double layer, through which they must facilitate nutrient uptake and environmental sensing. Due to this qualitatively different nature of exposure, microbes, especially primary producing phytoplankton will be differently affected by the environmental perturbations in the carbonate system than multicellular organisms. The biogeochemical importance of phytoplankton activities will be outlined in the following section.

Phytoplankton-driven carbon pumps

The term 'plankton' (from greek, *'wanderer'*) comprises the vast diversity of organisms that possess negligible motility and are subject to wave drift in the pelagic zones of aquatic ecosystems. The prefix 'phyto' from (from greek, *'plant'*) implies photoauto-trophy, the ability to use sunlight and CO_2 as sources of energy and carbon for vital processes. These definitions narrow down the group of organisms to somewhat unicellular photosynthesizing organisms, which however encompasses a morphologically, taxonomically and functionally diverse group. A reasonable simplistic approach in the context of global change research is therefore to categorize phytoplankton based on its role in biogeochemical cycling of key elements, here primarily the vertical 'pumping' of carbon.

Whereas the physical carbon pump is driven by temperature-dependent differences in CO_2 solubility, i.e., abiotically, a significant proportion of the marine carbon pumping is mediated by biology. In biologically mediated carbon pumping, phytoplankton uses CO_2 to build up biomass that can be fed into the marine food webs. Some of the formed

biomass can form aggregates with other organic matter, like detritus and marine snow. These aggregates sink to depth and are thereby exported from the upper ocean. The consumption of DIC in the photic zone, the depth-export of particulate organic carbon (POC) and the subsequent remineralization by zooplankton and microorganisms establish vertical depth gradients of [DIC]. The concomitant DIC depletion of surface waters allows further uptake of atmospheric CO_2 (Organic carbon pump; Broecker and Peng 1982). Due to the simplistic categorization it becomes clear that all in fact phytoplankton species contributing to marine primary productivity (~50 Pg C per year; Field et al. 1998) also participate in driving the organic carbon pump. It must be noted, however, that by far not all POC is ultimately transported to the ocean floor. Instead, the majority is remineralized at intermediate depths and only a small fraction (1-3%) reaches the ocean floor (De La Rocha and Passow 2007).
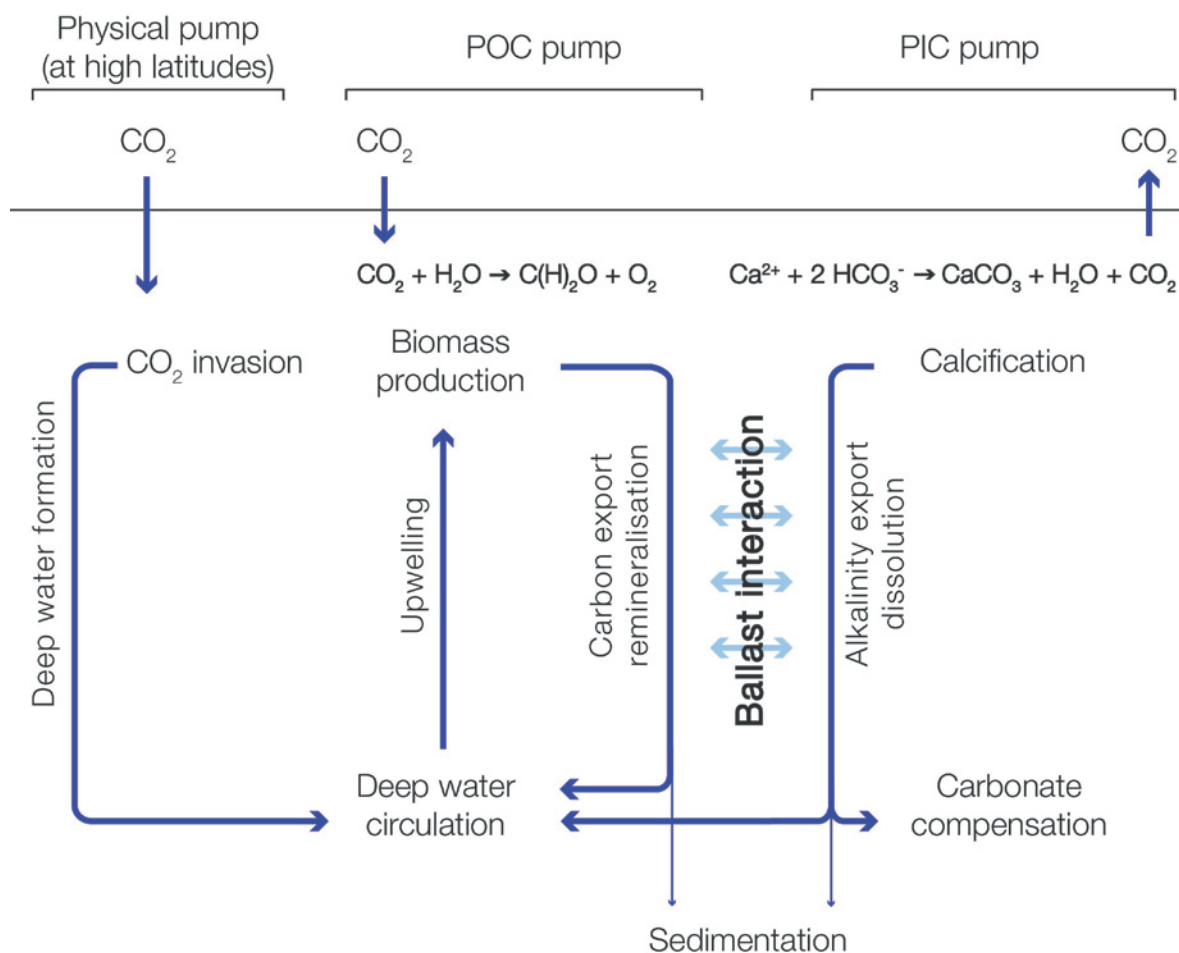
Figure 6: Marine carbon pumps; the physical pump is driven by the uptake of CO_2 into cold water and subsequent deep water formation at high latitudes; the POC pump is driven by primary production and consumes CO_2; the PIC pump is driven by calcification and increases $[CO_2]$. Ballasting influences the efficiency of the POC pump and co-regulates the partitioning of CO_2 between atmosphere and oceans.

In addition to the organic carbon pump, a calcification-driven 'inorganic carbon pump' is active, which has an opposing effect on the partitioning of CO_2 between atmosphere and ocean. The formation of particulate inorganic carbon (PIC, i.e., $CaCO_3$) removes not only DIC from the seawater but also Ca^{2+} and thereby reduces alkalinity (Equation 5), hence the 'DIC uptake capacity'. In consequence, extensive calcification (e.g., by a bloom of calcifying algae) can increase $[CO_2]_{aq}$ and eventually even cause CO_2 outgassing into the atmosphere (Zondervan et al. 2001). Due to its high density, however, PIC imposes additional ballast effects when incorporated into sinking POC aggregates. This ballasting significantly enhances export efficiencies of the organic carbon pump and ultimately co-regulates atmospheric CO_2 drawdown (Klaas and Archer, 2002). Estimates of global PIC production range between 1.1 ± 0.3 Pg per year (Feely et al. 2004) to 1.6 ± 0.3 Pg per year (Balch et al. 2007), i.e., less than 5% of the annual marine POC production. Despite being a small fraction of the overall produced particulate carbon, the $CaCO_3$-ballasting seems to be essential for an efficient transfer of aggregates to depth and thus is a main determinant of the relative pumping strengths (Honjo et al. 2008, Lam et al. 2011).

A number of multicellular organisms, like mussels, corals and pteropods contribute to marine calcification but the majority of PIC is formed in the open oceans, by unicellular organisms like foraminifers and coccolithophores. Whereas foraminifers are symbiont-bearing heterotrophs, coccolithophores are unicellular calcifying phytoplankton. Thus, they not only contribute significantly to global primary production (POC pump) but are also responsible for approximately half of the annual marine calcification (Milliman et al. 1993; PIC pump). Impacts of OA on the POC and PIC productivity of these organisms would have large implications for the biogeochemical cycling of carbon. The coccolithophores and hallmarks in their evolution will be briefly introduced in the upcoming section.

Evolutionary history of coccolithophores

Coccolithophores are a sub-group of haptophytes, one of several early eukaryotic clades of the so-called 'chromalveolates', ancient secondary-endosymbiotic algae. Although evolutionary dating is still under debate, recent analyses suggest that haptophytes have emerged from the other chromalveolate lineages as early as 1,900 million years ago (De Vargas et al. 2004). Molecular dating studies based on plastidary and nuclear genes indicate that around 1 billion years ago, haptophytes started to thrive as facultative photoautotrophs by utilizing the plastids of their prey, so that phototrophic haptophytes with a cell cover of organic scales have probably been existent at least since the late Proterozoic, 650 million years ago (De Vargas et al. 2004). The Permian-Triassic mass extinction event (251 million years ago; Bowring et al. 1998) drastically changed planetary conditions. Giant volcanic eruptions in today's Siberia endured over probably hundreds of thousands of years (Benton and Twitchett 2003) and triggered a 'super

greenhouse scenario'. A global atmospheric warming by estimated ~6°C (Benton and Twitchett 2003) caused oceanic circulation to cease and the subsequent ocean-wide anoxia wiped out 96% of marine species diversity (Tanner et al. 2004). For eukaryotic phototrophs, however, countless ecological niches were opened for colonization.
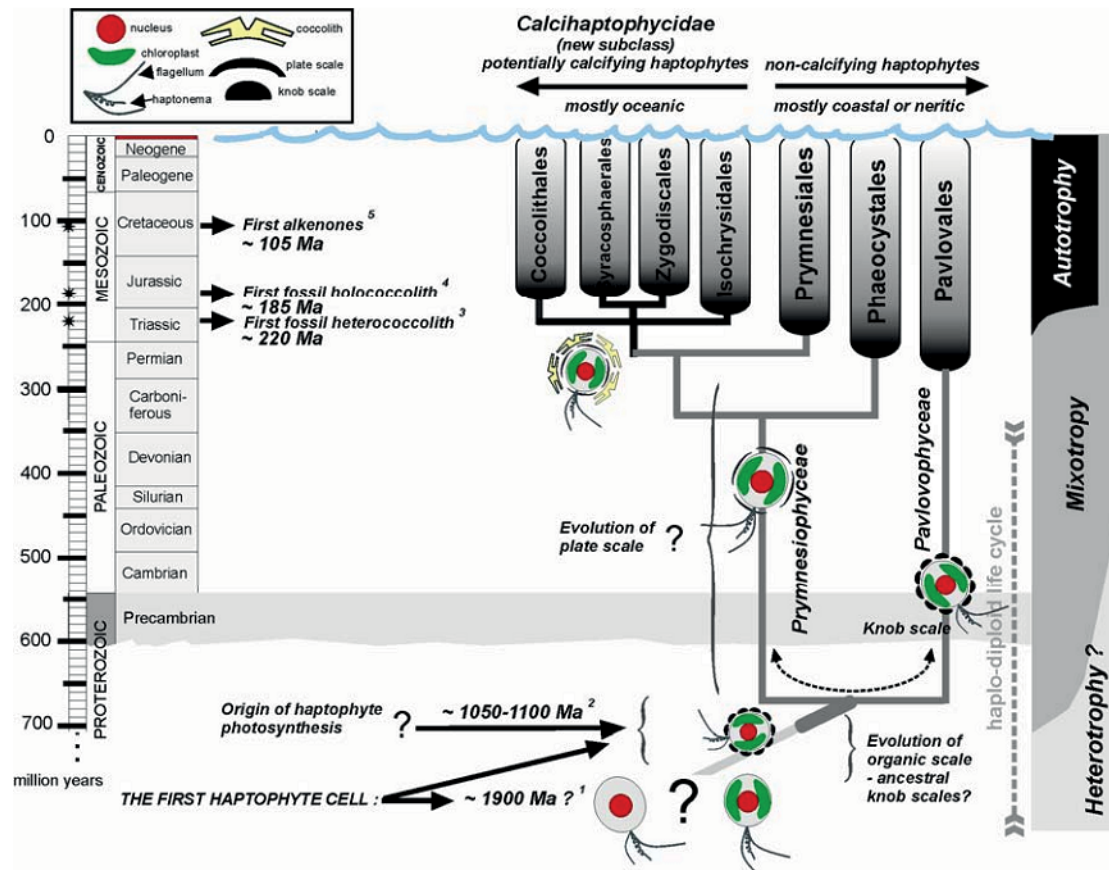
Figure 7: Phylogeny of haptophytes based on molecular clock approaches (De Vargas et al. 2004).

Over the following 20 million years, the eukaryotic phototrophs experienced a strong radiation that also gave rise to the extant lineages of haptophytes (Figure 7). Around 200-230 million years ago, calcifying haptophytes, the coccolithophores emerged (De Vargas et al. 2004; Bown et al. 2004). The striking feature of this new kind of microalgae was the ability to precipitate $CaCO_3$ within cellular vesicles to build minute calcite platelets. Upon exocytosis, these coccoliths interlock into an outer shell, the coccosphere (Figure 8). As all modern groups of coccolithophores cluster together in phylogenetic trees, it is well accepted that coccolith production is a unifying trait of this phylum. However, as evolutionary loss and re-invention of coccolith-production occurred frequently, also non-calcifying coccolithophores exist (De Vargas et al. 2004). This multiple invention of coccolith-production and also different modes of $CaCO_3$ precipitation have led to larger debate about cellular facilitation of the process and

23

promoted the opinion that it is a product of cell-biological 'bricolage': It is commonly noted that intracellular calcification was probably not a 'de novo' evolutionary invention but just the product of 'new associations of persisting biochemical processes' (Westbroek and Marin 1998). In other words, cell machinery was first invented for other purposes (e.g., organic scales for protection or stabilization) but later incidentally functioned in calcification (e.g., served as a nucleation matrix for $CaCO_3$ crystals). This hypothesis is supported by the evidence of more than 25 independent cases of evolution of intracellular calcification across the phylogenetic tree of eukaryotes (Knoll 2003).
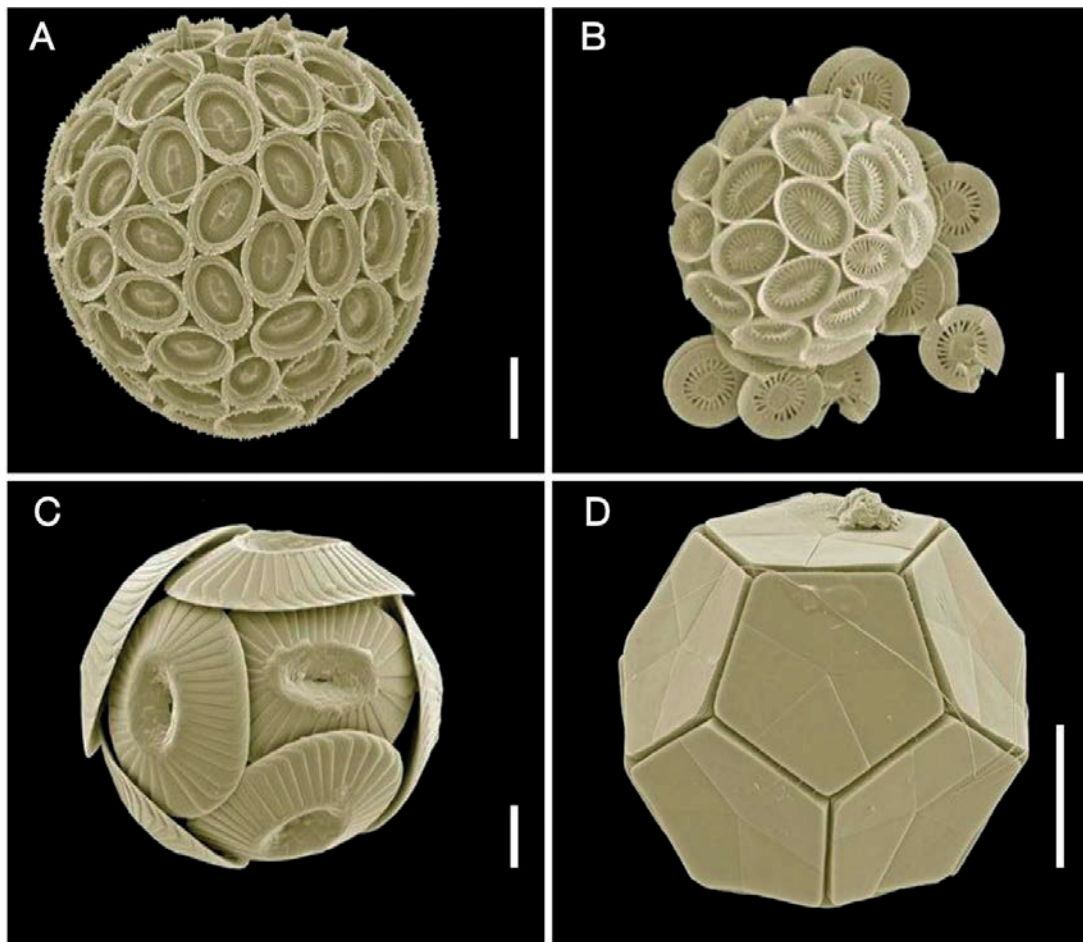
Figure 8: Scanning electron micrographs of coccolithophores; A: *Coronosphaera* spec.; B: *Syracosphaera* spec.; C: *Coccolithus spec.*; D: *Braarudosphaera* spec.; Scale bar = 5 µm; Photos: J. Young.

Before the massive appearance of calcifiers 200-230 million years ago, processes of calcification were constrained to the shallow coastal ecosystems, where seawater chemistry in the relatively warm shelf seas permitted an abiotic precipitation and preservation of $CaCO_3$ deposits. It is believed that the global rise of calcifiers and the dominance of coccolithophores from the Jurassic to the late Cretaceous (175-65 million

years ago) was thermodynamically favored by the very high oceanic [Ca^{2+}] of 30-60 mmol kg^{-1} and the resulting $CaCO_3$ supersaturation (Stanley and Hardie 1998; Ridgwell and Zeebe 2005). With this marine supersaturation, coccolithophores were able to emigrate from their shallow coastal habitats and conquer the open oceans. Indeed, it was the coccolithophores who have switched the major site of global carbonate deposition from shallow shelf seas to the deep ocean (Broecker and Peng 1982). They have thereby introduced the 'carbonate compensation' as a new planetary stabilizer of the carbon cycle and revolutionized biogeochemical regulation of ocean carbonate chemistry (Ridgwell and Zeebe 2005). As phototrophy has over time displaced the originally heterotrophic lifestyle and became a quasi-obligate feature of coccolithophores, it can be seen that the evolutionary history of coccolithophores is truly a story of 'coastal hunters that have become oceanic farmers' (De Vargas et al. 2004).

Over time, the taxonomic composition of phytoplankton in the oceans has of course changed, most remarkably, however, after the Cretaceous-Paleogene extinction event (~65 million years ago) that is believed to have been caused by a bolide impact (Smit and Hertogen 1980). Again, large-scale changes in the terrestrial and marine ecosystems occurred and changed the face of the planet. Especially the emergence and global radiation of sweet grasses (Poaceae) is believed to have significantly accelerated terrestrial silicate weathering and hence, increased the riverine input into the oceans (Falkowski et al. 2004). In addition, a concomitant sea level lowering diminished areas of shelf seas. These factors enabled the dominance of diatoms and seem to have caused the global numerical recession of coccolithophores. Coccolithophores have diversified into around 200 extant species (Young et al. 2003), occupied different ecological niches within the annual marine succession, and nowadays coexist with other phytoplankton in most oceanic regions. After briefly recapitulating the history of coccolithophores here, the evolutionary very young but most dominant species in today's oceans, *Emiliania huxleyi*, will be introduced in the upcoming section.

The *Emiliania huxleyi* morphospecies complex

Emiliania huxleyi (Figure 9) has emerged only 250.000-270.000 years ago (Thierstein et al. 1977) from the older genus *Gephyrocapsa*, both being the only known coccolithophores able to form significant blooms. *E. huxleyi* has persisted over the last two glacial-interglacial cycles and became dominant in coccolithophore assemblages around 70.000 years ago (Bijma et al. 2001). Despite being a very young species in terms of geological and evolutionary timescales, it has rapidly pervaded the global oceans and nowadays accounts for 30-50% (by number) of the total coccolithophore assemblages in most regions, and up to 100% in sub-polar waters (Winter and Siesser 1994; Mohan et al. 2008).

Figure 9: Scanning electron micrograph of *Emiliania huxleyi* strain RCC1216; Photo: C. Hoppe.

The pronounced dispersal of the species has been accompanied by the establishment of versatile ecotypes or 'strains' that inhabit different regions of the global oceans (Hagino et al. 2011). Recent sequencing efforts have shown that the fitness advantages of this `*E. huxleyi* morphospecies complex' derive from a high genetic variability and genomic organization: All members of the morphospecies complex share a conserved common genome, the so-called 'core genome' harboring those genes that are of vital function and are considered to more or less define the basic characteristics of the species. However, in all ecotypes examined to date there is considerable amount of additional deoxyribonucleic acid (DNA), i.e. extended genomic information, which encodes protein machinery that shapes the fitness of particular ecotypes. This highly variable 'pan-genome' seems to facilitate the rapid radiation of this species and to provide the genetic flexibility that ensures its ecological success (Read et al. under review; see appendix).

The ecological success may be attributed to some physiological key traits identified in most or all *E. huxleyi* ecotypes that make cells excellent competitors under many environmental conditions. Photosynthesis can, for example, not easily be inhibited by high irradiances: Even at intensities that equal or exceed direct sunlight (1000-1700 µmol photons m^{-2} s^{-1}; Nanninga and Tyrrell 1996; Nielsen 1995), cells can thrive with high growth rates. Another key feature is the possession of an efficient phosphate uptake system that not only enables highly affine uptake but also allows scavenging of organically bound phosphates (Riegman et al. 2000; Xu et al. 2010). Furthermore, *E. huxleyi* tolerates nitrogen-deprivation much better than diatoms, for instance, maintaining photosystem functionality over more than five weeks of nitrogen starvation (Löbl et al. 2010). To overcome metal-, and especially iron (Fe) limitation, *E. huxleyi* is able to substitute Fe-containing enzymes by functionally equivalent forms that bind

other metal cofactors (Read et al. under review). The presence of highly specialized morphotypes confirms that in the case of *E. huxleyi*, neither the individuals, nor the whole species, but rather the genetically distinct populations are the ecological units upon which evolutionary selection is acting (Brand 1982).

The dualism of biomass and calcite production in diploid *E. huxleyi*

During their blooms, populations of diploid *E. huxleyi* not only produce significant amounts of biomass but also $CaCO_3$ for their shells. Thereby, as outlined, they participate in and exert control on both biological carbon pumps. Whereas the biogeochemical consequences of coccolithophore growth are relatively well understood (Rost and Riebesell 2004), the cell-physiological role and control of calcification, as well as the deriving ecological consequences remain a conundrum that prohibits explicit statements on the evolutionary purpose of calcification. Because the accumulation of Ca^{2+} and C_i in intracellular vesicles and also the exocytosis of coccoliths demand energy and involve regulation, calcification in coccolithophores *must* have a certain benefit for the cells; otherwise it cannot be explained why a non-purposeful, yet energy-intensive process could have persisted for more than 200 million years under the strong selection pressure imposed in the marine habitats.

However, investigations on the ecological purpose(s) of the coccosphere have thus far not yielded any deeper insights. Hypotheses on coccosphere functions, e.g., in grazing protection or light refraction, could not be experimentally confirmed (Harris 1994; Young 1994). Other ideas proposed that cells use the coccosphere to regulate their buoyancy, as a controlled sinking might provide means to escape high irradiances or reach depths with higher nutrient concentrations (Balch et al. 1996; Young 1994). However, calculated sinking rates vary considerably amongst authors and are numerically negligible compared to wind-driven mixing and wave turbulence. It therefore seems unlikely that a coordinated sinking in response to environmental situations is a reasonable evolutionary purpose of calcification. While the ecological advantages of calcification remain elusive, researchers investigated its physiological responses in typical marine environmental scenarios, such as varying nutrient availabilities or light intensities.

If P limits growth, cells cannot replicate their genomes and typically get arrested in their mitotic cycle. Photosynthesis can continue, but because division is prohibited, cells usually accumulate little biomass and secrete photosynthate, i.e. carbohydrate (Staats et al. 2000). Due to the relatively unaffected calcification, cells become strongly overcalcified (Paasche and Brubak 1994). Interestingly, this phenomenon is often misinterpreted in a way that 'P-limitation enhances calcification' while it rather increases only the degree of calcification and not necessarily the rate of $CaCO_3$ production. Under N-limitation, effective photosynthesis and biomass production are inhibited due to deficits in chlorophyll pigments and protein machinery. Similar to P-limitation,

calcification can *in principle* proceed, as it does not consume N compounds as substrates. Still, as the process relies on energy provided by photosynthesis, membranes and protein machinery, N-limitation also impacts the process of calcification. Apparently, the relative impairment of biomass production is stronger than the impairment of calcification, i.e., PIC production and coccolith thickness decrease as a secondary effect (Paasche 1998).

Calcification has also for long been regarded as a CCM that enables the cells to utilize HCO_3^- and provide CO_2 to photosynthetic dark reactions according to Equation 7 (e.g., Sikes et al. 1980; Brownlee et al. 1994; Anning et al. 1996; Buitenhuis et al. 1999).

Eq. 7 $$Ca^{2+} + 2\ HCO_3^- \rightarrow CaCO_3 + CO_2 + H_2O$$

This hypothesis, however, also had to be withdrawn, not only because experiments showed that reduced calcification under low $[Ca^{2+}]$ does not impair the production of biomass at all (Trimborn et al. 2007), but also because CO_2-limitation of biomass production (under high pH) could not be avoided despite a stimulated calcification (Rost et al. 2002). In addition, calcification was thought to provide a sink for excess energy under high irradiances (Paasche 2002; Rost and Riebesell 2004). However, the energetic coupling of the two processes was shown to be unidirectional: While calcification requires energy from photosynthesis, photosynthesis in turn can operate even when calcification is inhibited by low $[Ca^{2+}]$ (Trimborn et al. 2007; Leonardos et al. 2009). Hence photosynthesis does not depend on calcification as an extra energy sink.

Anthropogenic OA prompted researchers to investigate the responses of biomass production and calcification to the projected changes in carbonate chemistry. The first major study with this specific research question found that OA stimulated biomass production and decreased calcite production (Riebesell et al. 2000). The decreased cellular PIC:POC ratio was used to substantiate and argue 'decreased calcification of marine plankton' with ongoing OA. However, further studies observed different, non-uniform response patterns between coccolithophore species (Langer et al. 2006) and even between strains of the *E. huxleyi* morphospecies complex (Langer et al. 2009), indicating that OA responses can vary significantly even on the species and strain level. Recent findings have also shown that physiological reactions to OA can be significantly modulated depending on light intensity, i.e., energy availability (Kranz et al. 2010). This highlights the urgent need to go beyond descriptive assessments of POC and PIC productions and to get an understanding of physiological processes and their interaction on the sub-cellular level.

Haplo-diplontic life cycling in *E. huxleyi*

The physiological traits of the diploid, calcifying stage of *Emiliania huxleyi* make it a strong competitor in regimes that often occur in the course of the annual marine succession. A usual scenario is the development of a diatom-dominated spring bloom due to nutrient-upwelling. After its collapse, waters are usually left with low amounts of macronutrients, especially silicate, prohibiting further growth of diatoms. In these low-nutrient regimes that become more stratified as the season progresses, *E. huxleyi* can typically thrive and outgrow other phytoplankton, creating blooms with cell densities of some 10.000, sometimes up to 100.000 cells mL^{-1} (Townsend et al. 1994; Nanninga and Tyrrell 1996; Paasche 2002; Tyrrell and Merico 2004). Blooms of calcifying *E. huxleyi* can sustain considerable populations of zooplanktic herbivores and are, due to their high growth rates, typically not regulated by grazing (Nejstgaard et al. 1997). Instead, blooms are regularly terminated by viruses that have co-evolved with the morphospecies complex. These are able to infect a broad range of host ecotypes, take control over cellular machinery and induce cell lysis (Castberg et al. 2002; Kegel et al. 2010). Viral lysis has been recognized a crucial component in marine succession, imposing a top-down regulation of coccolithophore blooms and enabling the transition to the next stage of ecological succession (Martínez et al. 2007).

Such viral bloom-terminations also bear large implications for the ecology and evolution of the species. Like other coccolithophores, *Emiliania huxleyi* pursues a haplo-diplontic life cycle. Unlike in other coccolithophores, the haploid stage is a scale-bearing, yet uncalcified cell that possesses flagellae to actively swim (Klaveness 1972; Green et al. 1996). The most striking property of the haplont is its resistance to viral attacks, pointing towards an important ecological function of this extensive life-cycling: As growing diploid populations continuously produce haploid cell stages, the 'background population' of haploid individuals will function as a new founding population in the case of a virally-mediated termination of the diploid bloom, a behavior that was termed the 'Cheshire cat escape strategy' (Frada et al. 2008; 2012). Such a 'double-life' is very seldom among eukaryotes, which are mostly arrested in either the diploid or the haploid life-cycle stage. The haploid life-cycle stages produced by meiosis can function as gametes to undergo syngamy and produce new diploid cells. At the same time, they are autonomous life-forms, able to propagate by mitotic division and to found independent populations. Although neither meiosis, nor syngamy has ever been directly observed, syngamic events can be inferred by comparative molecular techniques (Medlin et al. 1996; Barker et al. 1994). The evolutionary manifestation of life-cycling strongly implies major ecological benefits, not only because of providing an escape strategy in case of viral affection, but also because morphologically and physiologically dissimilar stages in life cycling generally increase the ecological range of the species as a whole (Valero et al. 1992). The haplont may thereby not only resemble the morphology, but possibly also the lifestyle of ancestral 'hunting' haptophytes (Paasche 2002).

Aims of this thesis

The human carbon perturbation drastically changes the environmental conditions in marine habitats. Especially the globally significant calcifier *Emiliania huxleyi* has been shown to exhibit diverse OA-responses with respect to processes biomass and calcite production. An understanding of these processes, of their mutual interaction and the mechanistics of OA-responses is however still lacking. The haploid life-cycle stage of *E. huxleyi* that specially contributes to the species' evolutionary success is also poorly characterized.

This thesis therefore aims to characterize and compare the haploid and diploid life-cycle stages of *E. huxleyi* with a focus on their reactions to future Ocean Acidification. Strong emphasis is put on the light-modulation of these responses, in order to investigate the influence of cellular energization on the relative intensity of physiological responses. To explore the physiological processes beyond a descriptive assessment of PIC and POC production, different *in-vivo* methods were used to assess underlying physiological processes and parameters like C_i acquisition, preferred C_i source and photosynthetic energy generation. Acquired phenomenological and physiological data are complemented by gene expression profiling. This allows the interpretation of the observed OA-responses in the context of (de-)activated genes and associated molecular functions.

To accomplish the aims of this thesis, cells of haploid and diploid *E. huxleyi* (strains RCC1216 and RCC1217) were acclimated to an experimental matrix of present day vs. future carbonate chemistry (pCO_2 of 380 vs. 1000 µatm) under limiting and high light intensities (50 vs. 300 µmol photons m^{-2} s^{-1}). Such a matrix-approach extends the one-dimensional investigation of an OA response into a second dimension: By assessing OA responses at two levels of energy availability, the *differences in responses* can be interpreted in the context of cellular energization state. In publication I, the haploid and diploid life-cycle stages were compared based on their differential gene expression. To this end, cells were grown under limiting and saturating light intensity and were compared by means of microarray-based transcriptome profiling. In publication II, cells of both life-cycle stages were investigated towards their phenomenological and physiological responses to OA and the modulation of these responses by light intensity. To that end, elemental quotas and production rates were assessed and complemented with physiological data: C_i affinities, preferred C_i sources and photosynthetic energy generation were assessed using membrane-inlet mass-spectrometry and ^{14}C tracer techniques. In publication III, the OA responses of the life-cycle stages and their modulation by light intensity were examined on the level of gene expression. This was done to pinpoint biochemical pathways that underlie the observed responses (Publication II) and to characterize the interplay of physiological functions and cellular energization.

This suite of methods yields a holistic picture of cellular functioning and therefore greatly increases explanatory power. Results of the studies are used to identify overarching OA-response patterns and unifying physiological concepts. Ideally, these concepts are not restrained to *E. huxleyi* but may be applicable in broader physiological contexts. This thesis therefore also seeks to gain a deeper understanding of general microalgal physiology. Such an understanding is required to improve numerical models that help estimating the relative strengths of the marine carbon pumps in future oceans.

PUBLICATIONS

List of publications

The presented doctoral thesis is based on the following publications:

I: Rokitta, S. D., De Nooijer, L. J., Trimborn, S., De Vargas, C., Rost, B. and John, U. 2011. Transcriptome analyses reveal differential gene expression patterns between life-cycle stages of Emiliania huxleyi (Haptophyta) and reflect specialization to different ecological niches. Journal of Phycology **47**:829-38.

II: Rokitta, S. D. and Rost, B. 2012. Effects of CO_2 and their modulation by light in the life-cycle stages of the coccolithophore *Emiliania huxleyi*. Limnology and Oceanography **57**:607-18.

III: Rokitta, S. D., U. John and B. Rost. 2012b. Ocean Acidification Affects Redox-Balance and Ion-Homeostasis in the Life-Cycle Stages of *Emiliania huxleyi*. PLoS ONE 7(12): e52212. doi:10.1371/journal.pone.0052212

The first author´s contribution to the publications

For all publications, the experimental concepts and approaches were devised together with the coauthors. The first author conducted experiments, performed the analyses and evaluated data. The manuscripts were drafted by the first author and discussed with the coauthors.

Publication I: Transcriptome analyses reveal differential gene expression patterns between life-cycle stages of *Emiliania huxleyi* (Haptophyta) and reflect specialization to different ecological niches

TRANSCRIPTOME ANALYSES REVEAL DIFFERENTIAL GENE EXPRESSION PATTERNS BETWEEN THE LIFE-CYCLE STAGES OF *EMILIANIA HUXLEYI* (HAPTOPHYTA) AND REFLECT SPECIALIZATION TO DIFFERENT ECOLOGICAL NICHES[1]

Sebastian D. Rokitta[2]

Alfred Wegener Institute for Polar and Marine Research, Am Handelshafen 12, 27570 Bremerhaven, Germany

Lennart J. de Nooijer

Department of Geosciences at Utrecht University, P.O. Box 80021, 3508 Utrecht, the Netherlands

Scarlett Trimborn

Alfred Wegener Institute for Polar and Marine Research, Am Handelshafen 12, 27570 Bremerhaven, Germany

Colomban de Vargas

CNRS, UMR7144 & Université Pierre et Marie Curie, Station Biologique de Roscoff, Équipe EPPO, Place George Teissier, 29680 Roscoff, France

Björn Rost and Uwe John

Alfred Wegener Institute for polar and marine research, Am Handelshafen 12, 27570 Bremerhaven, Germany

Coccolithophores, especially the abundant, cosmopolitan species *Emiliania huxleyi* (Lohmann) W. W. Hay et H. P. Mohler, are one of the main driving forces of the oceanic carbonate pump and contribute significantly to global carbon cycling, due to their ability to calcify. A recent study indicates that termination of diploid blooms by viral infection induces life-cycle transition, and speculation has arisen about the role of the haploid, noncalcifying stage in coccolithophore ecology. To explore gene expression patterns in both life-cycle stages, haploid and diploid cells of *E. huxleyi* (RCC 1217 and RCC 1216) were acclimated to limiting and saturating photon flux densities. Transcriptome analyses were performed to assess differential genomic expression related to different ploidy levels and acclimation light intensities. Analyses indicated that life-cycle stages exhibit different properties of regulating genome expression (e.g., pronounced gene activation and gene silencing in the diploid stage), proteome maintenance (e.g., increased turnover of proteins in the haploid stage), as well as metabolic processing (e.g., pronounced primary metabolism and motility in the haploid stage and calcification in the diploid stage). Furthermore, higher abundances of transcripts related to endocytotic and digestive machinery were observed in the diploid stage. A qualitative feeding experiment indicated that both life-cycle stages are capable of particle uptake (0.5 μm diameter) in late-stationary growth phase. Results showed that the two life-cycle stages represent functionally distinct entities that are evolutionarily shaped to thrive in the environment they typically inhabit.

Key index words: endocytosis; life-cycle stages; microarray; quantitative RT-PCR; transcriptome profiling

Abbreviations: cRNA, complementary RNA; EMS, endomembraneous system; GPA, calcium binding protein with a high glutamic acid, proline, and alanine content; KOG, eukaryotic orthologous genes; PKS, polyketide synthase; qRT-PCR, quantitative real-time polymerase chain reaction

Phytoplankton are responsible for the majority of marine primary production and play an important role in the global cycling of biogenic elements (Falkowski and Raven 2007). As in all phytoplankton, the production of biomass results in the export of particulate organic carbon to depth (the so-called organic carbon pump). Coccolithophores further produce particulate inorganic carbon by precipitation of calcium carbonate. This process results in the removal of dissolved inorganic carbon from surface waters and sustains the vertical gradients of dissolved inorganic carbon and alkalinity in the oceans (Rost and Riebesell 2004). This phenomenon, known as the carbonate pump, is a critical component of the global carbon cycle that exerts a major influence on Earth's climate (Westbroek et al. 1993).

Coccolithophores are arguably the most productive group of calcifying organisms in today's oceans.

In particular, the morpho-species *E. huxleyi* accounts for 20%–50% of the total coccolithophore community in most areas and close to 100% in subpolar waters (Winter et al. 1994, Mohan et al. 2008). In contrast to most other coccolithophore species, it can form massive blooms, often related to the annual spring succession. While the initiation of *E. huxleyi* blooms appears to be controlled in a bottom-up manner (e.g., by nutrient availability, irradiance, or stratification), their termination by viruses is a clear example of top-down regulation in plankton ecology (Bratbak et al. 1996, Schroeder et al. 2003). Frada et al. (2008) suggested that virus-mediated termination of diploid populations induces a meiotic transition in some individuals followed by the growth of a new haploid population. This transition was termed the ''Cheshire Cat'' escape strategy, by which *E. huxleyi* seeks refuge in its haploid, apparently virus-resistant life-cycle stage.

Coccolithophores in general are known to follow a haplo-diplontic life cycle, with individuals of both stages being able to propagate independently by mitosis (Billard 1994). *E. huxleyi* can exist in a coccolith-bearing form, which is diploid (2N, i.e., possessing the double set of chromosomes) and in a noncalcifying flagellated form with organic scales that is haploid (1N, i.e., possessing the reduced, single set of chromosomes). A third form, known to be diploid, nonmotile, and uncalcified, may be a culture artifact (Klaveness 1972, Green et al. 1996). Until recently, coccolithophore research has largely ignored the haploid life-cycle stage of *E. huxleyi* due to the absence of calcification and assumed limited biogeochemical impact. The haploid cells, however, apparently immune to viral attacks, are not obliged to undergo sexual fusion. Thus, they may persist independently in nature for long periods of time and form new inocula for diploid offspring populations after spatial and/or temporal dispersion (Frada et al. 2008). Regarding this important ecological role, the two stages are likely to represent differentiated entities that are evolutionarily shaped to fulfill their ecological purpose in the contrasting environments they typically occupy. Furthermore, the obvious morphological differences between the two stages (flagellae in 1N, calcification in 2N) suggest significantly divergent physiologies a priori, for example, regarding carbon/nutrient uptake mechanisms, energy budgeting, and/or trophic modes of biomass acquisition (i.e., phagotrophy).

Phagotrophy involves endocytosis, a main constitutive function of the endomembraneous system (EMS). EMS-derived organelles can be selectively equipped with protein/enzymatic machinery, enabling cells to establish a variety of chemical microenvironments within, for example, for digestion or calcification (Corstjens and Gonzáles 2004). Anterograde (outward) traffic lines of the EMS deliver membrane material, receptors, and enzymes to the plasma membrane or the extracellular space by fusing vesicles to the plasma membrane (exocytosis). Vice versa, the retrograde traffic lines retrieve recyclable protein material and membrane material by internalization and constriction (endocytosis) and can also serve to take up material from the extracellular space for trophic purposes (i.e., phagotrophy). Especially in protists, phagotrophy plays a key role, as it provided (and still provides) a prerequisite for heterotrophic feeding and the evolution of photoautotrophy in eukaryotes (Raven 1997). Mixotrophy, for example, has been observed in numerous haptophytes (Jones et al. 1994) and was also suspected for *E. huxleyi* (Houdan et al. 2005).

Furthermore, the difference in DNA content between the life-cycle stages necessitates regulatory activities to control stage-specific expression of genes. Cellular gene regulation is versatile and can be applied on the levels of DNA (e.g., condensation or decondensation of chromosomes), RNA (e.g., posttranscriptional and translational regulation), or protein (e.g., posttranslational modifications). Hence, the level the regulation is applied on has different implications regarding the cell's energetic effort and ecological benefits (e.g., response times to external stimuli). To understand the differences between the life-cycle stages, a deeper understanding of the regulation of gene expression (i.e., the usage of the respective genomes) is crucial.

In this study, the differential gene expression patterns between high- and low-light-acclimated haploid (uncalcified) and diploid (coccolith bearing) life-cycle stages of *E. huxleyi* (RCC 1217 and RCC 1216) were assessed. As analyses yielded evidence for increased endocytotic and proteolytic activity in silico, preliminary follow-up feeding experiments were performed with both life-cycle stages.

MATERIALS AND METHODS

Culture conditions. Axenic haploid and diploid cells (strains RCC 1217 and RCC 1216, respectively, obtained from the Roscoff culture collection) of *E. huxleyi* were grown as dilute-batch cultures at 15°C in 0.2 μm filtered modified F/2 medium, consisting of North Sea water (salinity 32.2 psu), enriched with vitamins and trace metals (Guillard and Ryther 1962). Nitrate and phosphate were added to concentrations of 100 and 6.25 μM, respectively. Cultures were exposed to light intensities of 50 and 300 μmol photons $\cdot$ m^{-2} $\cdot$ s^{-1} provided by Biolux 965 daylight lamps (Osram, München, Germany) at a 16:8 light:dark cycle. Light intensities were adjusted using a LI-1400 datalogger (Li-Cor, Lincoln, NE, USA) with a 4π-sensor (Walz, Effeltrich, Germany). Cells were acclimated to culture conditions for at least 2 weeks prior to sampling. Cylindrical flasks of 900 mL were continuously bubbled through a frit with humidified ambient air (130 ± 10 mL $\cdot$ min^{-1}) to avoid cell sedimentation. Cell concentrations were monitored using a Multisizer III hemocytometer (Beckman-Coulter, Fullerton, CA, USA). The pH was monitored daily using a pH3000 microprocessor pH-meter (WTW, Weilheim, Germany), which was calibrated using National Institute of Standards and Technology–certified buffer systems (therefore referred to as pH$_{NBS}$). Culture pH$_{NBS}$ did not deviate more than 0.05 units from cell-free medium.

TABLE 1. Carbonate chemistry, growth rates, and cellular quotas of particulate organic carbon/inorganic carbon (POC, PIC).

Culture	pH$_{NBS}$	Dissolved inorganic carbon ($\mu mol \cdot kg^{-1}$)	Total alkalinity ($\mu mol \cdot kg^{-1}$)	pCO$_2$ (μatm)	Growth (μ) (d^{-1})	POC ($pg \cdot cell^{-1}$)	PIC ($pg \cdot cell^{-1}$)
1N LL	8.176 ± 0.005	2,111 ± 19	2,393 ± 24	351 ± 7	0.87 ± 0.12	7.7 ± 0.7	0.6 ± 0.1
1N HL	8.177 ± 0.019	2,096 ± 24	2,380 ± 10	350 ± 4	1.18 ± 0.20	9.7 ± 1.9	0.6 ± 0.4
2N LL	8.112 ± 0.014	1,997 ± 44	2,254 ± 20	399 ± 4	0.63 ± 0.14	7.5 ± 0.5	10.4 ± 0.6
2N HL	8.083 ± 0.004	2,018 ± 15	2,273 ± 5	430 ± 2	1.02 ± 0.15	10.8 ± 1.4	8.8 ± 2.3
Reference	8.134 ± 0.010	2,134 ± 25	2,411 ± 13	404 ± 12	–	–	–

HL, high light; LL, low light.

Cells were harvested during the exponential growth phase, at average cell concentrations of 90,000 cells $\cdot$ mL^{-1}, to avoid effects of shifted carbonate chemistry (Table 1). Calculations of the carbonate system were based on measurements of pH$_{NBS}$, total alkalinity, temperature, and salinity and were performed with the program CO$_2$sys (Lewis and Wallace 1998). For the calculations, average phosphate concentrations of 4 μM were assumed. Dissociation constants of carbonic acid (Mehrbach et al. 1973 refit by Dickson and Millero 1987) and the dissociation constants of sulfuric acid (Dickson 1990) were used. Results are reported for 15°C. Samples were taken between 4 and 8 h after the start of the light period.

RNA sampling. Samples of $\sim 1.5 \times 10^7$ cells were concentrated by filtration (1.2 μm polycarbonate filters; Millipore, Billerica, MA, USA) and pelleted by 5 min centrifugation at 5,000g in a table centrifuge (Hettich, Bäch, Switzerland). Cell disruption was performed with a beadmill (Qiagen, Hilden, Germany) after adding 100 μL glassbeads (0.1 mm). Lysate was homogenized using QIAshredder spin-columns (Qiagen). RNA extraction was performed using a silica-column-based guanidinium thiocyanate method (RNeasy mini; Qiagen). To digest DNA in the isolate, 7 Kunitz units of bovine DNase I (Qiagen) were applied to the silica matrix following incubation for 20 min at room temperature. After elution, MicroCon YM 30 ultrafiltration columns (Millipore) were used to further enrich RNA. Concentration and purity were measured photometrically with a Nanodrop ND1000 (PeqLab, Erlangen, Germany), and integrity of the isolate was assessed using a BioAnalyzer 2100 (Agilent, Santa Clara, CA, USA) running an RNA 6000 Nano LabChip (Agilent).

Microarray hybridizations. RNA Spike-In Mix (Agilent, p/n 5188-5279) was added to the RNA samples prior to the labeling reactions serving as internal standard and benchmark for hybridization performance (Agilent RNA Spike-In Kit protocol). Two hundred nanograms total RNA was reversely transcribed, amplified, and labeled using the two-color low RNA Input fluorescent linear amplification kit (Agilent, p/n 5184-3523). Incorporation of Cy-3 and Cy-5 labeled cytidine 5′-triphosphate (Perkin Elmer, Waltham, MA, USA) was verified photometrically using the NanoDrop ND1000 (PeqLab). Labeling efficiencies were calculated as pmol dye $\cdot$ (ng cRNA)$^{-1}$ from the results of photometry and were in the range of 0.013–0.018 pmol dye $\cdot$ (ng cRNA)$^{-1}$. Individual microarray hybridizations were carried out in biological triplicates according to the scheme presented in Figure 1 using SureHyb hybridization chambers (Agilent, p/n G2534A). Seven hundred fifty nanograms of each Cy-3 and Cy-5 labeled cRNA was hybridized to 4×44K *E. huxleyi* custom-built microarrays (Agilent), containing 60mer oligonucleotide probes. Microarray probes were derived from computer-predicted "best gene models" compiled from the *E. huxleyi* CCMP1516 genome project, conducted by the U.S. Department of Energy Joint Genome Institute (JGI; http://www.jgi.doe.gov) in collaboration with the user community. Probe design was done using Agilent's eArray online platform. Following the Two-Color
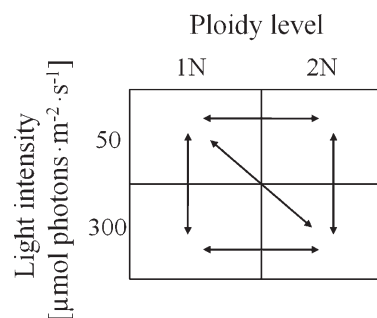
Ploidy level

FIG. 1. Hybridization scheme of microarray experiments to test the effect of acclimation light intensity and ploidy levels on *Emiliania huxleyi*; vertical hybridizations report irradiance effects on either haploid or diploid gene expression. Horizontal hybridizations reveal ploidy-level effects on low- and high-light-acclimated cultures. The diagonal cross hybridization reports cumulative ploidy- and irradiance-related effects. These can be superimposed on the acquired data set and reduce the significant features to a more feasible number.

Microarray-based Gene Expression Analysis protocol (Agilent, p/n 5188-5242), hybridization was performed in a hybridization oven at 65°C for 17 h at an agitation of 6 rpm. After hybridization, microarrays were disassembled in Wash Buffer 1 (Agilent, p/n 5188-5325), washed with Wash Buffer 1, Wash Buffer 2 (Agilent, p/n 5188-5326), acetonitrile (VWR, Darmstadt, Germany), and Stabilization and Drying Solution (Agilent, p/n 5185-5979) according to manufacturer's instructions. Stabilization and Drying Solution, an ozone scavenger, protects the Cy-dye signal from degradation. Arrays were scanned with a G2565BA microarray scanner (Agilent) using standard photomultiplier tube settings and 5 μm scan resolution.

Microarray data evaluation. Raw data were extracted with Feature Extraction Software version 9.0 (Agilent), incorporating the GE2_105_Dec08 protocol. Array quality was monitored using the QC Tool v1.0 (Agilent) with the metric set GE2_QCMT_Feb07. Spots that had been flagged "outliers," "not known," or "bad" based on background median analysis were excluded from further processing. The data set was automatically normalized by the Feature Extraction Software using the locally weighted scatterplot smoothing (LOWESS) algorithm. Normalized data were submitted to the MIAMExpress database hosted by the European Bioinformatics Institute (EBI; http://www.ebi.ac.uk/arrayexpress; accession code E-MEXP-2896). Gene expression analysis was performed using the MultiExperiment Viewer 4.2 (MEV), which is part of the TM4 Software suite (Saeed et al. 2003). Triplicate experiments were statistically evaluated in single class tests using the "significance analysis of microarrays" (SAM) algorithm introduced by Tusher et al. (2001). Data sets were permuted 500 times each, and differential gene expression was called significant when gene-specific q-values, which represent a statistically estimated

false discovery rate (Storey 2003), were ≤0.1%. Significant array features were assigned to "best gene model" predictions using available classifications of eukaryotic orthologous genes (KOG), provided by the JGI. Acquired KOG-based data sets were visually inspected toward key enzymes or expression patterns that may give hints to underlying metabolic pathways or cytobiological processes being more prominent in either the haploid or diploid stage. In the following, exemplary transcripts will be notated with their associated JGI Protein ID#.

Quantitative real-time polymerase chain reaction (qRT-PCR) validation. Primer sets for qRT-PCR were designed with PrimerExpress software 2.0.0 (Applied Biosystems, Darmstadt, Germany) for seven genes of interest after the visual inspection of the microarray data set (Table S1 in the supplementary material). Total RNA (250 ng) of haploid and diploid cultures was spiked with known concentrations of transcripts of the "nitrile-specifier protein" (NSP; 10 pg) and "major allergen" (MA; 10 ng) genes from the cabbage butterfly *Pieris rapae*. These "alien spikes" were used for the relative quantification using the $2^{-\Delta\Delta Ct}$ method (Livak and Schmittgen 2001) and served as a control for pipetting error as well as performance and linearity of cDNA synthesis (Krell et al. 2007). Spiked RNA was submitted to linear reverse transcription using SuperScript III reverse transcriptase (Invitrogen, Carlsbad, CA, USA) and anchored poly-dT Primers (Invitrogen). Resulting first strand cDNA was diluted and 2.5 ng of cDNA were amplified in a quantitative reverse transcription using Sybr Green I reporter dye master mix (Applied Biosystems, Foster City, CA, USA) and a Prism 7000 qRT-PCR cycler (Applied Biosystems) to measure relative expression of transcripts. Efficiencies of qRT-PCR primer sets were assessed by amplifying serial dilutions of generated cDNA. Curves were used to calculate the fold change of transcript expression relative to the haploid stage grown under low light (1N LL). Absolute target-copy-number calibrations for AP2B1 and ATPVa were performed by amplifying dilution series of known concentrations of DNA amplicons generated by PCR. The PCR primers for these quantifications were generated with Primer3 (Rozen and Skaletsky 2000; Table S1).

Microbead cell treatment. To test for endocytotic capacities, 1N and 2N cultures were grown under 40 µmol photons · $m^{-2} \cdot s^{-1}$ in 50 mL culture flasks. Ten milliliter subsamples were taken at different time points during the phases of culture growth and incubated with sulfate-coated fluorescent beads (Sigma-Aldrich, Hamburg, Germany) of 0.5 µm diameter with a final concentration of 15–20 beads · $cell^{-1}$. Cultures were spiked with 100 µL of dissolved organic matter 16 h prior to incubation with the fluorescent microspheres because additions of organic compounds have been shown to stimulate possible phagotrophic activity in phytoplankton (Legrand and Carlsson 1998). The added dissolved organic matter consisted of sterile-filtered (0.2 µm) beadmill-lysate of ~2.5×10^7 *E. huxleyi* cells resuspended in 2 mL medium. After 60 min of incubation with the beads, cells were fixed with formaldehyde to an effective concentration of 5% (v/v). Cells were then scanned using a confocal laser-scanning microscope (Leica TCS, Wetzlar, Germany) that allowed separate detection of both the microspheres (excitation at 488 nm; detection at 500–560 nm) and chl *a* (excitation at 488 nm; detection at 610–670 nm) from single cells. Fluorescent scans were combined with bright field images to locate the chloroplasts and the microspheres within the cells.

RESULTS

Gene expression analysis. Hybridization data reported no significant transcriptomic differences between high-light and low-light acclimations in either haploid or diploid cultures (Fig. 2a). Cross-hybridizations (Fig. 1, diagonal arrow; 2a, dashed circle), representing expression patterns in response to different light acclimations and ploidy stages, indicated strong expression regulation (>6,700 significant features), but only very few of them (<10) were differentially expressed as a response originating from different acclimation light intensities.

In contrast, 1,840 and 2,449 features were determined to be expressed significantly higher and lower in diploid individuals (i.e., correspondingly lower and higher expressed in haploid individuals) under both light intensities, indicating distinct patterns of gene expression originating from different life-cycle stages (Fig. 2b). Cross-hybridizations (Fig. 2b, dashed circle) strongly supported this
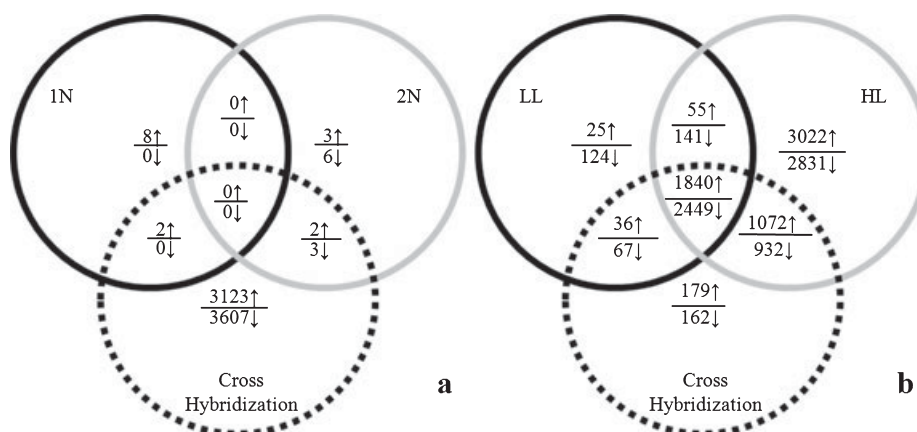

FIG. 2. (a) *Emiliania huxleyi* transcriptomic responses to different acclimation light intensities of the haploid (1N, black circle) and diploid (2N, gray circle) cells. Dashed circle represents cross hybridization; ↑ = up-regulated in high light, ↓ = down-regulated in high light. Central intersection holds the transcriptomic effects which are exclusively related to acclimation light intensity. (b) Transcriptomic responses to changes in ploidy level in low-light-acclimated (LL, black circle) and high-light-acclimated (HL, gray circle) cells. Dashed circle represents cross hybridization; ↑ = up-regulated in the diploid transcriptome, ↓ = down-regulated in diploid transcriptome. Central intersection holds the transcriptomic effect exclusively linked to differences in ploidy level.

conclusion, as they shared 95.6% of the significant features within the common intersection of ploidy responses in both light treatments. After assigning significant features to KOG annotations derived from gene models, a de visu evaluation of the obtained data set confirmed differential expression of various cellular functions between the two life-cycle stages (Table 2; and see Table S2 in the supplementary material for details).

In the following section, increased relative abundances of gene transcripts in the different stages are reported, meaning that these transcripts contribute to a higher extent to the respective stage-specific transcriptome. As expression ratios were assessed, it is important to note that presence of respective transcripts in the other stage is not excluded. However, the relative compositions of the transcriptomes differ clearly between stages.

Haplont-specific transcriptome features. In the haploid stage of *E. huxleyi*, increased relative expression

TABLE 2. Significantly up-regulated transcriptome features in diploid (2N) and haploid (1N) *Emiliania huxleyi*, classified by eukaryotic gene orthologies (KOG).

KOG classification of models	2N ↑	1N ↑
1. Amino acid transport and metabolism	19	28
2. Carbohydrate transport and metabolism	23	24
3. Cell cycle control, cell division, chromosome partitioning	4	8
4. Cell wall/membrane/envelope biogenesis	7	8
5. Chromatin structure and dynamics	18	6
6. Coenzyme transport and metabolism	0	8
7. Cytoskeleton and cell motility	40	101
8. Defense mechanisms	3	3
9. Energy production and conversion	20	27
10. Extracellular structures	23	18
11. Function unknown	30	43
12. General function prediction only	114	82
13. Inorganic ion transport and metabolism	28	20
14. Intracellular trafficking, secretion, and vesicular transport	10	17
15. Lipid transport and metabolism	9	20
16. Nuclear structure	1	5
17. Nucleotide transport and metabolism	0	6
18. Posttranslational modification, protein turnover, chaperones	35	47
19. Replication, recombination, and repair	5	14
20. RNA processing and modification	28	10
21. Secondary metabolite biosynthesis, transport, and catabolism	7	13
22. Signal transduction mechanisms	77	72
23. Transcription	48	44
24. Translation, ribosomal structure, and biogenesis	20	9
25. No functional annotation data available	1,273	1,816
Total	1,840	2,449

of nitrogen-distributing enzymes, such as aspartate aminotransferase (JGI# 413787), glutamine synthetase (JGI# 69253), glutaminase (JGI# 68199), threonine/serine dehydratase (JGI# 417175), and urea transporters (JGI# 194219), was observed (amino acid transport and metabolism; KOG class 1).

The relative expression levels of genes related to coenzyme transport and metabolism (KOG class 6) were also significantly higher in the haploid stage. Detected features include enzymes involved in synthesis of cobalamin derivatives (cobalamin-synthesis protein; JGI# 456427) and folic acid (methylenetetrahydrofolate dehydrogenase; JGI# 448747).

The haploid stage further intensively expressed cytoskeletal intermediary filaments like tubulins α (JGI# 445562) and β (TubB; JGI# 464996) and associated motor machinery, that is, subunits of dyneins (DynH, JGI# 75572) and kinesins (Kin, JGI# 101580; KOG class 7).

Higher relative abundances of transcripts coding for genes involved in carbon metabolism (isocitrate lyase; JGI# 436528), the tricarboxylic acid cycle (malate dehydrogenase; JGI# 414497), and general energy metabolism (pyruvate carboxylase, JGI# 456927; F_OF_1-ATP-Synthase subunits, JGI# 441432) were detected (KOG class 9).

The Ca^{2+}-binding protein GPA (JGI# 431830), which is usually attributed to calcification (Corstjens et al. 1998, Schroeder et al. 2005), was found to be more prominently expressed in the haploid stage (KOG class 12).

Finally, features related to posttranslational modifications (KOG class 18) were also more strongly expressed in haploid *E. huxleyi*: Higher abundances of transcripts related to ubiquitin-mediated proteasomal degradation (e.g., E3 ubiquitin ligase, E3UL, JGI# 106507) as well as 26S proteasome compounds and the associated regulatory proteins (e.g., JGI# 449934) were observed.

Diplont-specific transcriptome features. The diploid stage exhibited increased expression of machinery involved in chromatin structuring and dynamics (KOG class 5). Numerous transcripts of genes participating in nucleosome remodeling (POB3 homologs, JGI# 451523), gene activation (histone-acetyltransferase, JGI# 365731), and gene silencing (histone H3 [Lysine-9] methyltransferase; JGI# 450763) were detected to be prominently expressed.

Transcripts of polyketide synthases (PKSs; JGI# 631889 and 631892; KOG class 8) were found in the diploid data set.

Features related to energy production and conversion (KOG class 9) indicated prominent expression of various subunits of a vacuolar H^+-ATPase (V-ATPase, e.g., subunit α, JGI# 439538).

Regarding the transport of inorganic ions (KOG class 13), the Ca^{2+}/H^+ antiporter CAX3 (JGI# 416800) and a Na^+-independent Cl^-/HCO_3^- exchanger (AE, JGI# 99943) were expressed in the calcifying diploid stage.

Furthermore, transcript abundances related to vesicular traffic (KOG class 14) were generally higher in the diploid stage, the data set revealing prominent presence of clathrin-coated vesicle-related machinery (adaptor protein 2 subunit β_1, AP2B1, JGI# 558382) and vacuolar protein sorting factors of the SNARE-type (JGI# 465386).

Increased expression of genes related to post-translational modifications (KOG class 18) was also found. A set of various vacuolar peptidases, for example, subtilisin-related vacuolar protease B (SVP1, JGI# 436633) and aspartyl-, asparaginyl-, and metallopeptidases (JGI# 112299, 455379, 451158) was prominently expressed in the diploid stage.

Features relevant for RNA processing and modification (KOG class 20) indicated elevated abundance of splicing coactivators of the so-called SR family (JGI# 427170), which are components of small nuclear ribonucleoproteins (snRNPs) and also of proteins acting in pretranslational RNA processing (RNA helicase, JGI# 418728) in the diploid cells.

qRT-PCR validation. To validate the microarray results, the expression levels of seven genes of interest were assessed by means of qRT-PCR (Table 3). Results were normalized to the abundance levels detected in haploid, low-light-acclimated cultures (1N LL) and are given in relative fold change. The assessed abundances agree with the outcome of the statistical microarray evaluation.

Two transcripts important for clathrin-mediated endocytosis (AP2B1, JGI# 558382) as well as for vacuolar acidification (ATPVa, JGI# 439538) were quantified absolutely (Fig. 3), showing that AP2B1 transcripts were expressed in the haploid stage of *E. huxleyi* (0.71–1.06×10^5 copies · [ng cDNA]$^{-1}$), but their abundance in the diploid stage (3.5–5.3×10^5 copies · [ng cDNA]$^{-1}$) was 3- to 5-fold higher. With respect to light intensities, obtained means of transcript copy numbers were proved not significantly different in both life-cycle stages (*t*-test, $P = 0.05$). Transcript abundances of the V-ATPase alpha subunit were >1,000-fold higher in the diploid cells (11.8–13.0×10^6 copies · [ng cDNA]$^{-1}$) compared to the haploid cells (4.7–11.1×10^3 copies · [ng cDNA]$^{-1}$). Effects of light intensity on expression levels could not be confirmed, the means of the light treatments were only insignificantly different (*t*-test, $P = 0.05$) in both stages.

Microbead cell treatment. The presence of gene transcripts related to clathrin-coated vesicles and degradative machinery was shown by both microarray (Table 2; Table S2) and qRT-PCR (Table 3).

Preliminary feeding experiments indicated that both life-cycle stages are capable of endocytotic uptake of particles: While no bead ingestion could be detected during exponential and initial stationary growth phase, endocytosed particles could be observed in the last sampling, 2–3 d after entering stationary phase (Fig. 4). Fluorescence microscopy observations revealed that within an incubation time of 1 h up to 8 beads · cell^{-1} were taken up in both haploid and diploid individuals. Beads were typically observed to reside in the center of the cells, between the two chloroplasts (Fig. 5).

DISCUSSION

Microarray analyses revealed that overall *E. huxleyi* expression patterns, as obtained with the applied test sharpness, were not detectably altered by the different acclimation light intensities. The KOG database used contained only few genes related to photosynthesis, but this cannot account for the small absolute amount of significant features (Fig. 2a). Alterations in light intensity of this order of magnitude (50–300 μmol photons · m^{-2} · s^{-1}) resemble short-term variations typically imposed in nature (e.g., by cloud shading or vertical mixing). Hence, the transcriptomic indifference may be attributed to the ability of *E. huxleyi* to cope with such variability in irradiances at the photophysiological or posttranslational level rather than on the transcriptional level. In contrast, clear ploidy-dependent regulation patterns were observed (cf. Table 2; Table S1).

Haplont-specific transcriptome. A prominent relative increase in the expression of genes involved in nitrogen metabolism was detected in haploid *E. huxleyi*, including glutamine synthetase, the entry enzyme for ammonia into the metabolism. Furthermore, increased expression of multispecific aminotransferases as well as serine/threonine dehydratase suggests a close connection between the amino acid and carboxylic acid metabolism.

Transcripts of vitamin-synthesizing enzymes were prominent in the haploid stage of *E. huxleyi*. The diploid stage of at least one strain of *Emiliania* was determined to lack the ability to synthesize thiamine and cobalamin (Provasoli and Carlucci 1974). Consequently, as the organism obviously possesses the

TABLE 3. Quantitative real-time polymerase chain reaction (qRT-PCR) validations of seven transcripts.

	AP2B1	ATPVa	DynH	Kin	TubB	E3UL	SVP1
1N LL	1.0 ± 0.2	1.0 ± 0.3	1.0 ± 0.3	1.0 ± 0.1	1.0 ± 0.2	1.0 ± 0.2	1.3 ± 1.2
1N HL	0.7 ± 0.1	2.6 ± 2.2	1.1 ± 0.5	0.8 ± 0.1	1.0 ± 0.3	1.7 ± 0.6	4.3 ± 2.1
2N LL	4.4 ± 1.7	4,052 ± 1,094	0.25 ± 0.1	0.003 ± 0.001	0.1 ± 0.1	0.1 ± 0.04	773.0 ± 293
2N HL	2.8 ± 0.8	3,624 ± 896	0.14 ± 0.04	0.004 ± 0.001	0.1 ± 0.04	0.1 ± 0.04	632.4 ± 502

HL, high light; LL, low light.
Values indicate fold change in relation to haploid low-light-acclimated cells (1N LL).
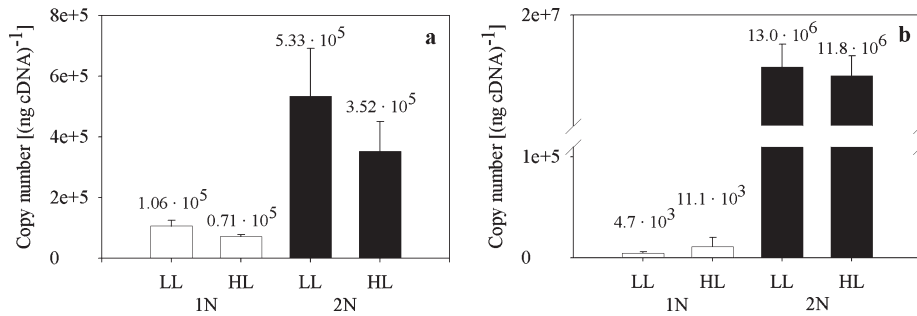
Fɪɢ. 3. Abundances of transcript copies of genes AP2B1 (a) and ATPVa (b) in haploid (1N) and diploid (2N) *Emiliania huxleyi* cells acclimated to low light (LL) and high light (HL) intensities.
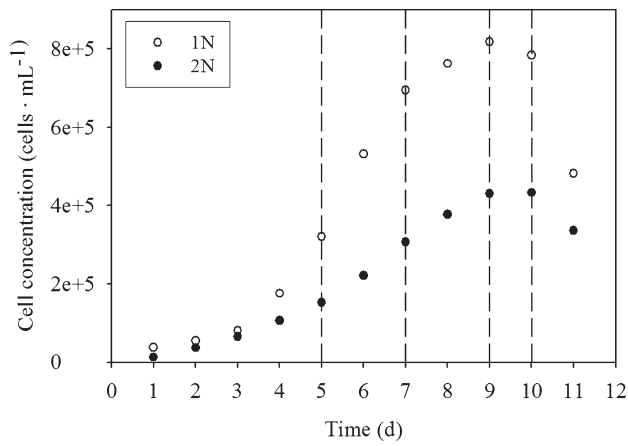

Fɪɢ. 4. Time course of culture growth for microbead treatment; dashed lines indicate samplings.

necessary genes, absence of the phenotypic ability must be attributed to suppression of gene transcription in the diplont. The presence of these pathways in the haploid stage, however, may indicate a stage-specific constitutive expression.

Higher expression of cytoskeleton-related genes in the haploid stage must be attributed to the fact that this stage is flagellated (von Dassow et al. 2009). Tubulins and their associated motors are crucial for cell motility, a trait specific to the haploid stage. Diploid cells may only express the amounts of transcripts needed for maintenance of intracellular microtubular structures.

The haploid *E. huxleyi* stage exhibits a pronounced carboxylic acid and energy metabolism (malate dehydrogenase, pyruvate carboxylase, and F_OF_1-ATP-Synthase subunits). The expression of isocitrate lyase was increased. This enzyme, catalyzing
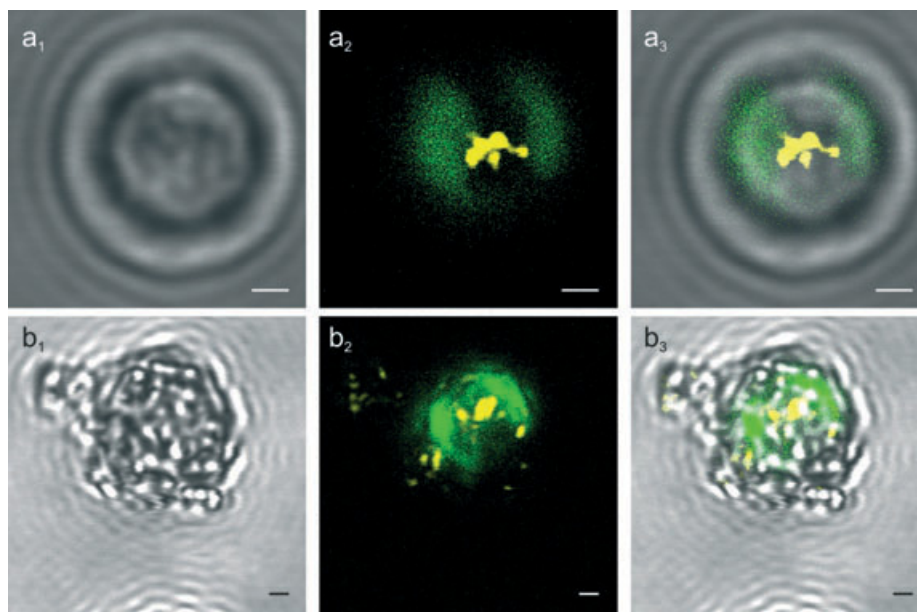
Fɪɢ. 5. Ingested fluorescent beads in haploid (a) and diploid (b) individuals of *Emiliania huxleyi*: 1, transmission image of single cells; 2, combined fluorescent scans indicating the respective cellular localization of the beads (yellow, emission 500–560 nm) and the chloroplasts (green, emission 610–670 nm); 3, confocal scans superimposed on transmission image (1 + 2). Scale bar = 1 μm.

the conversion of isocitrate into succinate and glyoxylate and vice versa, is able to convey catabolically produced C_2 products (e.g., from digestion of lipids) into anabolic C_3/C_4 carboxylic acid metabolism. This finding suggests a broad flexibility with respect to regulation of co-occurring anabolic and catabolic activities and resource management.

The elevated expression of GPA is in agreement with the findings of von Dassow et al. (2009). This protein was hypothesized to assist in the nucleation of calcium carbonate crystals (Corstjens et al. 1998). The increased expression indicates that GPA obviously fulfills cell-biological tasks in the noncalcifying life-cycle stage as well. As it was discussed to be associated with secretory polysaccharides, von Dassow et al. (2009) argued that it might also be involved in the formation of the extracellular organic scales observed in this life-cycle stage.

DNA sequence variations within the GPA gene were successfully used as a molecular marker within the species *E. huxleyi* (Schroeder et al. 2005), being able to tell apart A and B coccolith morphotypes. The detection of the mRNA of the strain used in this study (R morphotype) must therefore be attributed to the unspecificity of the oligonucleotide probe used toward minor sequence differences. Sequencing of the GPA transcript of strain 1216/1217 may be performed to validate the functionality of this genetic marker and possibly extend its usage to this and other R morphotype strains.

The haploid-specific transcriptome further displays a prominent increase in features related to ubiquitin-mediated proteasomal degradation, the process in which proteins are selectively disassembled into amino acids. As argued by Klaveness (1972), mechanical stress (e.g., by aerating the culture) may rupture the flagellae and impair the cells' physiology. In microscopic examinations, however, cells were intact and actively swimming, and growth rates were consistently high. The increased expression of ubiquitin-related machinery may rather be linked to the relatively intense catabolic activity and nitrogen metabolism discussed above and might therefore indicate higher relative protein turnover, which could increase the flexibility of the proteome to respond more quickly to short-term cellular demands.

Diplont-specific transcriptome. In the diplont, increased expression of genes involved in chromatin structuring, like Pob3 homologs (Formosa et al. 2001) and DNA methyl- and acetyltransferases (Bird 2002), must be linked to the epigenetic management of the double set of chromosomes. As in all diploid organisms, cells need to suppress transcription of double alleles to avoid futility and possibly adverse gene-dosage effects (Papp et al. 2003). Apparent absence of vitamin-synthesizing gene products in the diploid stages of some *E. huxleyi* strains may be attributed to such selective gene-silencing. Diploid cells also strongly express machinery related

to pre-mRNA modifications, that is, differential splicing (Blencowe et al. 2000), which might increase the versatility of the proteome on a post-transcriptional basis.

Transcripts related to PKSs were detected in higher amounts in diploid *E. huxleyi*. These evolutionary deep-branching enzymes synthesize a broad range of long-chained secondary metabolites, which can be relevant in species interactions such as defense or hunting (John et al. 2008 and references therein). Given the modular structure of PKSs, the observed transcripts cannot be attributed to any particular chemical and thus their function in *E. huxleyi* requires further investigations. These enzymes might, however, potentially be related to polyunsaturated long-chain (C_{37-39}) alkenones, alkenoates, and alkenes (Eltgroth et al. 2005), which have been extensively studied as biomarkers and paleo-proxies (Beltran et al. 2007).

The prominent expression of V-ATPase subunits in diploid cells indicates a higher activity of the EMS, in particular the maintenance of vacuolar membrane potentials and proton gradients. Acidification of vacuolar compartments plays a key role in multiple cellular processes including endocytosis, macromolecular processing and degradation, as well as coupled transport of small molecules (Stevens and Forgac 1997). In the coccolithophore *Pleurochrysis carterae*, a dedicated V-ATPase, mediating H^+-transport in a Ca^{2+}-dependent manner, was found in coccolith vesicles (Corstjens and Gonzáles 2004). Thus, high relative expression of V-ATPase, which was also confirmed in the diplont by qRT-PCR (>1,000-fold expression relative to the noncalcifying haploid stage), is likely to be linked to coccolithogenesis. Although seemingly counterintuitive, an inward proton pumping is suspected to play a major role in the complex acid-base chemistry of coccolith-producing vesicles (Mackinder et al. 2010). Vacuolar H^+-ATPases that energize transporter-mediated alkalization of the extracellular space have been observed, and mechanistic models have been proposed by which pH-coupled ion-transport may achieve this (Harvey 2009).

Furthermore, increased expression levels of the CAX3 Ca^{2+}/H^+ antiporter and of a Cl^-/HCO_3^- exchanger of the SLC4 family were observed. These gene products have been observed to be expressed specifically in the diplont (von Dassow et al. 2009) and were postulated to play active roles in coccolithophore biomineralization (Mackinder et al. 2010). With respect to the EMS, diploid *E. huxleyi* are significantly richer in gene transcripts related to formation and traffic of endocytotic clathrin-coated vesicles, especially AP2-related subunits. The coexpression of machinery involved in endocytosis and endosomal vesicle sorting, like SNARE type sorting factors (von Dassow et al. 2009) suggests higher endocytotic activity in the diploid stage. Increased retrograde membrane traffic is a cell-biological

necessity in this stage, as the continuous export of coccoliths by exocytosis would otherwise eventually diminish the EMS. Interestingly, a versatile set of proteases, many of which are putative zymogen-activating enzymes, were also observed to be up-regulated in the diploid transcriptome. These vesicular proteases are known to cleave enzyme precursors to enable their activity, often for degradative purposes. This finding might be interpreted as a sign of increased secretion of degrading enzymes to vesicles or the extracellular space. Yet, a significant fraction of these proteases cannot be assigned to pro-protein conversion due to their exopeptidase character. These enzymes participate in proteolytic degradation within digestive compartments. They might serve the recycling of retrieved membrane proteins but also represent the basic machinery needed for the digestion of endocytosed extracellular matter.

Data indicate that haploid cells drive a flexible conventional primary metabolism involving classical anabolic and catabolic key pathways and increased protein turnover. The smaller genome of the haploid stage and hence the more parsimonious and basic transcriptome simplify the processes of gene expression and thereby minimize cellular energetic and material efforts. As the haploid stage is thought to occur mainly as an ''ecological backup'' of the terminated diploid population, its higher initial numbers and the streamlined metabolism may lead to high competitiveness and enable it to thrive in postbloom waters.

The diploid stage, in turn, strongly expresses machinery related to epigenetic management of chromosomes and pretranslational processing of mRNA. Together with pronounced expression of transcriptional regulation machinery, these findings indicate that the versatility of the diploid proteome is controlled more on a pretranslational basis, rather than by posttranslational modifications and increased protein turnover as observed in the haploid stage.

E. huxleyi: *a mixotrophic phytoplankton species?* Most haptophytes possess chloroplasts and are therefore considered photoautotrophs. Some species (e.g., *Prymnesium parvum*) have, however, been shown to be capable of ingesting dissolved or particulate organic material (Jones et al. 1994, Tillmann 2003). The motility and reduction of calcification in the haploid stage of *E. huxleyi* have been hypothetically linked to mixotrophic behavior (Houdan et al. 2005).

The transcriptome analyses indicated endocytotic activity in the exponential growth phase, whereas the microscopy observations revealed phagocytotic particle uptake only in late stationary phase. This emphasizes the critical difference between constitutive endocytotic activity as a vital cellular function and an inducible phagocytotic particle uptake. It further indicates that phagocytotic behavior is induced only under certain environmental conditions, for example (post-) bloom settings with depleted macro- and/or micronutrients. Yet, the particular triggers and purposes of phagotrophy in *E. huxleyi* remain elusive.

Recent research indicates, however, that endocytotic vesicles might be the vehicle exploited in viral infection of diploid *E. huxleyi* cells (Mackinder et al. 2009). It may therefore be hypothesized that under limiting (i.e., bloom-) conditions, the virus hitchhikes the induced phagocytotic machinery to intrude cells and induce bloom termination. Clearly, more research is necessary to elucidate the interconnections between environmental conditions, ecological succession scenarios, and life cycling in *E. huxleyi*, in which the reasons for the high competitiveness of this species in contemporary oceans might lie.

Beltran, C., de Rafélis, M., Minoletti, F., Renard, M., Sicra, M. A. & Ezat, U. 2007. Coccolith δ18O and alkenone records in middle Pliocene orbitally controlled deposits: high-frequency temperature and salinity variations of sea surface water. *Geochem. Geophys. Geosyst.* 8:Q05003. DOI: 10.1029/2006GC001483.

Billard, C. 1994. Life cycles. *In* Green, J. C. & Leadbeater, B. S. C. [Eds.] *The Haptophyte Algae.* Clarendon Press, Oxford, UK, pp. 167–86.

Bird, A. 2002. DNA methylation patterns and epigenetic memory. *Genes Dev.* 16:6–21.

Blencowe, B. J., Baurén, G., Eldridge, A. G., Issner, R., Nickerson, J. A., Rosonina, E. & Sharp, P. A. 2000. The SRm160/300 splicing coactivator subunits. *RNA* 6:111–20.

Bratbak, G., Wilson, W. & Heldal, M. 1996. Viral control of *Emiliania huxleyi* blooms? *J. Mar. Syst.* 9:75–81.

Corstjens, P. L. A. M. & Gonzáles, E. L. 2004. Effects of nitrogen and phosphorus availability on the expression of the coccolith-vesicle V-ATPase (subunit c) of *Pleurochrysis* (Haptophyta). *J. Phycol.* 40:82–7.

Corstjens, P. L. A. M., van der Kooij, A., Linschooten, C., Brouwers, G. J., Westbroek, P. & deVrind-de Jong, E. 1998. GPA, a calcium-binding protein in the coccolithophorid *Emiliania huxleyi* (Prymnesiophyceae). *J. Phycol.* 34:622–30.

von Dassow, P., Ogata, H., Probert, I., Wincker, P., Da Silva, C., Audic, S., Claverie, J. M. & de Vargas, C. 2009. Transcriptome analysis of functional differentiation between haploid and diploid cells of *Emiliania huxleyi*, a globally significant photosynthetic calcifying cell. *Gen. Biol.* 10:R114. DOI: 10.1186/gb-2009-10-10-r114.

Dickson, A. G. 1990. Standard potential of the reaction: AgCl(s) + ½ H_2(g) = Ag(s) + HCl(aq), and the standard acidity constant of the ion HSO_4^- in synthetic seawater from 273.15 to 318.15 K. *J. Chem. Thermodynamics* 22:113–27.

Dickson, A. G. & Millero, F. J. 1987. A comparison of the equilibrium constants for the dissociation of carbonic acid in seawater media. *Deep-Sea Res.* 34:1733–43.

Eltgroth, M. L., Watwood, R. L. & Wolfe, G. V. 2005. Production and cellular localization of neutral long-chain lipids in the haptophyte algae *Isochrysis galbana* and *Emiliania huxleyi*. *J. Phycol.* 41:1000–9.

Falkowski, P. G. & Raven, J. A. 2007. *Aquatic Photosynthesis*, 2nd ed. Princeton University press, Princeton, New Jersey, pp. 1–3.

Formosa, T., Eriksson, P., Wittmeyer, J., Ginn, J., Yu, Y. & Stillman, D. J. 2001. Spt16-Pob3 and the HMG protein Nhp6 combine to form the nucleosome-binding factor SPN. *EMBO J.* 20:3506–17.

Frada, M., Probert, I., Allen, M. J., Wilson, W. H. & De Vargas, C. 2008. The ''Cheshire Cat'' escape strategy of the coccolithophore *Emiliania huxleyi* in response to viral infection. *Proc. Natl. Acad. Sci. U. S. A.* 105:15944–9.

Green, J. C., Course, P. A. & Tarran, G. A. 1996. The life-cycle of *Emiliania huxleyi*: a brief review and a study of relative ploidy levels using flow cytometry. *J. Mar. Syst.* 9:33–44.

Guillard, R. R. L. & Ryther, J. H. 1962. Studies of marine planktonic diatoms. *Can. J. Microbiol.* 8:229–39.

Harvey, W. R. 2009. Voltage coupling of primary H^+ V-ATPases to secondary Na^+- or K^+-dependent transporters. *J. Exp. Biol.* 212:1620–9.

Houdan, A., Véron, B., Claquin, P., Lefebvre, S. & Poncet, J. M. 2005. Cryopreservation of the coccolithophore *Emiliania huxleyi* (Haptophyta, Prymnesiophyceae). *J. Appl. Phycol.* 17:413–22.

John, U., Beszteri, B., Derelle, E., de Peer, Y. V., Read, B., Moreau, H. & Cembella, A. 2008. Novel insights into evolution of protistan polyketide synthases through phylogenomic analysis. *Protist* 159:21–30.

Jones, H. L. J., Leadbeater, B. S. C. & Green, J. C. 1994. Mixotrophy in haptophytes. *In* Green, J. C. & Leadbeater, B. S. C. [Eds.] *The Haptophyte Algae.* Clarendon Press, Oxford, UK, pp. 167–86.

Klaveness, D. 1972. *Coccolithus huxleyi* (Lohm.) Kamptn. II. The flagellate cell, aberrant cell types, vegetative propagation and life cycles. *Br. Phycol. J.* 7:309–18.

Krell, A., Funck, D., Plettner, I., John, U. & Dieckmann, G. 2007. Regulation of proline metabolism under salt stress in the psychrophilic diatom *Fragilariopsis cylindrus* (Bacillariophyceae). *J. Phycol.* 43:753–62.

Legrand, C. & Carlsson, P. 1998. Uptake of high molecular weight dextran by the dinoflagellate *Alexandrium catenella*. *Aquat. Microb. Ecol.* 16:81–6.

Lewis, E. & Wallace, D. W. R. 1998. *Program Developed for CO_2 System Calculations.* Carbon Dioxide Information Analysis Centre, Oak Ridge National Laboratory, U.S. Department of Energy, Oak Ridge, Tennessee.

Livak, K. J. & Schmittgen, T. D. 2001. Analysis of relative gene expression data using real-time quantitative PCR and the 2-[Delta][Delta]CT method. *Methods* 25:402–8.

Mackinder, L. C. M., Wheeler, G. L., Schroeder, D. C., Riebesell, U. & Brownlee, C. 2010. Molecular mechanisms underlying calcification in coccolithophores. *Geomicrobiol. J.* 27:585–95.

Mackinder, L. C. M., Worthy, C. A., Biggi, G., Hall, M., Ryan, K. P., Varsani, A., Harper, G. M., Wilson, W. H., Brownlee, C. & Schroeder, D. C. 2009. A unicellular algal virus, *Emiliania huxleyi* virus 86, exploits an animal-like infection strategy. *J. Gen. Virol.* 90:2306–16.

Mehrbach, C., Culberson, C. H., Hawley, J. E. & Pytkowicz, R. M. 1973. Measurement of the apparent dissociation constants of carbonic acid in seawater at atmospheric pressure. *Limnol. Oceanogr.* 18:897–907.

Mohan, R., Mergulhao, L. P., Guptha, M. V. S., Rajakumar, A., Thamban, M., Anil-Kumar, N., Sudhakar, M. & Ravindra, R. 2008. Ecology of coccolithophores in the Indian sector of the Southern Ocean. *Mar. Micropaleontol.* 67:30–45.

Papp, B., Pal, C. & Hurst, L. D. 2003. Dosage sensitivity and the evolution of gene families in yeast. *Nature* 424:194–7.

Provasoli, L. & Carlucci, A. F. 1974. Vitamins and growth regulators. *In* Stewart, W. D. P. & Pierce, C. E. [Eds.] *Algal Physiology and Biochemistry.* Blackwell, Malden, Massachusetts, 741 pp.

Raven, J. A. 1997. Phagotrophy in phototrophs. *Limnol. Oceanogr.* 42:198–205.

Rost, B. & Riebesell, U. 2004. Coccolithophores and the biological pump: responses to environmental changes. *In* Thierstein, R. & Young, J. R. [Eds.] *Coccolithophores: From Molecular Processes to Global Impact.* Springer-Verlag, Berlin, pp. 99–125.

Rozen, S. & Skaletsky, H. J. 2000. Primer3 on the WWW for general users and for biologist programmers. *In* Krawetz, S. & Misener, S. [Eds.] *Bioinformatics Methods and Protocols: Methods in Molecular Biology.* Humana Press, Totowa, New Jersey, pp. 365–86.

Saeed, A. I., Sharov, V., White, J., Li, J., Liang, W., Bhagabati, N., Braisted, J., Klapa, M., Currier, T. & Thiagarajan, M. 2003. TM4: a free, open source system for microarray data management and analysis. *BioTechniques* 34:374–8.

Schroeder, D. C., Biggi, G. F., Hall, M., Davy, J., Martínez, J., Richardson, A. J., Malin, G. & Wilson, W. H. 2005. A genetic marker to separate *Emiliania huxleyi* (Prymnesiophyceae) morphotypes. *J. Phycol.* 41:874–9.

Schroeder, D. C., Oke, J., Hall, M., Malin, G. & Wilson, W. 2003. Virus succession observed during an *Emiliania huxleyi* bloom. *Appl. Environ. Microbiol.* 69:367–79.

Stevens, T. H. & Forgac, M. 1997. Structure, function and regulation of the vacuolar (H^+)-ATPase. *Annu. Rev. Cell Dev. Biol.* 13:779–808.

Storey, J. D. 2003. The positive false discovery rate: a Bayesian interpretation and the q-value. *Ann. Stat.* 31:2013–35.

Tillmann, U. 2003. Kill and eat your predator: a winning strategy of the planktonic flagellate *Prymnesium parvum*. *Aquat. Microb. Ecol.* 32:73–84.

Tusher, V. G., Tibshirani, R. & Chu, G. 2001. Significance analysis of microarrays applied to the ionizing radiation response. *Proc. Natl. Acad. Sci. U. S. A.* 98:5116–21.

Westbroek, P., Brown, C. W., Van Bleijswijk, J., Brownlee, C., Brummer, G. J., Conte, M., Egge, J. et al. 1993. A model system approach to biological climate forcing: the example of *Emiliania huxleyi*. *Glob. Planet. Change* 8:27–46.

Winter, A., Jordan, R. W. & Roth, P. H. 1994. Biogeography of living coccolithophores in ocean waters. *In* Winter, A. & Siesser, W. G. [Eds.] *Coccolithophores.* Cambridge University Press, Cambridge, UK, pp. 161–77.

Supplementary Material

The following supplementary material is available for this article:

Table S1. Quantitative real-time polymerase chain reaction (qRT-PCR) primer sets for validated transcripts and the respective amplification efficiencies; MA and NSP data taken from Krell et al. (2007).

Table S2. Microarray data set of genes that are significantly up-regulated preferentially in the haploid (1N) and diploid (2N) stage.

This material is available as part of the online article.

Please note: Wiley-Blackwell are not responsible for the content or functionality of any supplementary materials supplied by the authors. Any queries (other than missing material) should be directed to the corresponding author for the article.

Publication II: Effects of CO_2 and their modulation by light in the life-cycle stages of the coccolithophore *Emiliania huxleyi*

Effects of CO_2 and their modulation by light in the life-cycle stages of the coccolithophore *Emiliania huxleyi*

Sebastian D. Rokitta* and Björn Rost

Alfred Wegener Institute for Polar and Marine Research, Bremerhaven, Germany

Abstract

The effects of ocean acidification on the life-cycle stages of the coccolithophore *Emiliania huxleyi* and their modulation by light were examined. Calcifying diploid and noncalcifying haploid cells (Roscoff culture collection strains 1216 and 1217) were acclimated to present-day and elevated CO_2 partial pressures (P_{CO_2}; 38.5 vs. 101.3 Pa, i.e., 380 vs. 1000 μatm) under low and high light (50 vs. 300 μmol photons m^{-2} s^{-1}). Growth rates as well as cellular quotas and production rates of C and N were measured. Sources of inorganic C for biomass buildup were determined using a ^{14}C disequilibrium assay. Photosynthetic O_2 evolution was measured as a function of dissolved inorganic C and light by means of membrane-inlet mass spectrometry. The diploid stage responded to elevated P_{CO_2} by shunting resources from the production of particulate inorganic C toward organic C yet keeping the production of total particulate C constant. As the effect of ocean acidification was stronger under low light, the diploid stage might be less affected by increased acidity when energy availability is high. The haploid stage maintained elemental composition and production rates under elevated P_{CO_2}. Although both life-cycle stages involve different ways of dealing with elevated P_{CO_2}, the responses were generally modulated by energy availability, being typically most pronounced under low light. Additionally, P_{CO_2} responses resembled those induced by high irradiances, indicating that ocean acidification affects the interplay between energy-generating processes (photosynthetic light reactions) and processes competing for energy (biomass buildup and calcification). A conceptual model is put forward explaining why the magnitude of single responses is determined by energy availability.

The uptake of anthropogenic carbon dioxide (CO_2) by the oceans is causing a significant chemical shift toward higher acidity and P_{CO_2}, a phenomenon known as ocean acidification (OA). As the saturation state for calcium carbonate ($CaCO_3$) concomitantly decreases, calcifying organisms like corals, foraminifers, and coccolithophores have caught the attention of oceanographers, physiologists, and ecologists. Over the past decade, numerous studies have investigated the potential effects of OA on marine calcifiers, especially the coccolithophore *Emiliania huxleyi*. By the formation and export of organic carbon and $CaCO_3$, these bloom-forming unicellular algae sustain vertical gradients of dissolved inorganic C (DIC) and alkalinity (Rost and Riebesell 2004). Furthermore, the $CaCO_3$ can enhance export of aggregated particulate organic matter by ballasting (Klaas and Archer 2002; Lam et al. 2011). As these processes affect the CO_2 exchange with the atmosphere, an influence of OA on these organisms may alter the biogeochemical cycling of C and thereby climate (Zondervan et al. 2001; Rost and Riebesell 2004; Ridgwell et al. 2007).

Riebesell et al. (2000) found that calcification rates decreased with increasing P_{CO_2} in *E. huxleyi* (strain PLYB92/11). Based on these observations, they proposed "reduced marine planktonic calcification" and a rather grim future for calcifiers. Langer et al. (2006), in turn, found nonlinear response patterns or insensitivity in other coccolithophore genera (*Calcidiscus* sp. and *Coccolithus* sp.). Iglesias-Rodriguez et al. (2008) observed increased calcification rates in *E. huxleyi* (strain NZEH) with

increasing P_{CO_2}. In a more recent study, Langer et al. (2009) could show that response patterns diverge even between strains, illustrating the difficulties in generalizing OA responses within the *E. huxleyi* morphospecies complex.

Until recently, global change research largely ignored that *E. huxleyi* pursues a haplo-diplontic life cycling, which seems to play a crucial role in its ecology: haploid individuals, for instance, can survive attacks of stage-specific viruses that diminish blooms of diploid individuals. Thus, meiosis is believed to function as an escape strategy (Frada et al. 2008). The haploid stage was found to drive a clearly differentiated metabolism, possibly because of its distinct ecological functionality (Rokitta et al. 2011). It is therefore of interest whether and to which degree the flagellated, noncalcifying life-cycle stage is prone to OA.

Several mechanisms have been put forward in attempt to explain the responses to OA. An increased proton (H^+) concentration may impair transport processes, such as the uptake of inorganic carbon (C_i) or calcium ions (Ca^{2+}), being dependent on electrochemical membrane potentials (Mackinder et al. 2010; Taylor et al. 2011). Increased [CO_2] might directly benefit biomass production either by enhancing the carboxylation reaction at RubisCO (Raven et al. 2005), by reducing CO_2 leakage (Rost et al. 2006), or by allowing a down-regulation of activity of the energy-intensive carbon concentrating mechanism (CCM; Kranz et al. 2010). It has also been indicated that responses to OA are often modulated by light intensities (Kranz et al. 2010; Lefebvre et al. 2010). Investigating the underlying processes as well as the modulating effects of energy availability will therefore improve the understanding of the origins of measured responses.

---

* Corresponding author: Sebastian.Rokitta@awi.de

In the present study, diploid and haploid cells of *Emiliania huxleyi* (strains 1216 and 1217 from the Roscoff culture collection, RCC) were acclimated to an experimental matrix of present-day vs. elevated P_{CO_2} (38.5 vs. 101.3 Pa) under low vs. high light intensities (50 vs. 300 μmol photons m^{-2} s^{-1}). Besides the assessment of growth rates, cellular quotas of particulate inorganic and organic C (PIC, POC), and particulate organic N (PON), different in vivo assays were conducted to investigate the underlying processes. ^{14}C disequilibrium assays were used to determine the preferential C_i source used for biomass production (CO_2 or HCO_3^-). Photosynthetic O_2 evolution was assessed as a function of [DIC] and light intensities by means of membrane-inlet mass spectrometry (MIMS).

Methods

Culture conditions—Diploid and haploid *Emiliania huxleyi* (strains RCC 1216 and 1217, also known as TQ26 2N and 1N) were obtained from the Roscoff culture collection (www.sb-roscoff.fr/Phyto/RCC). Cells were grown at 15°C in 0.2 μm filtered North Sea seawater (salinity 32), enriched with vitamins and trace metals (Guillard and Ryther 1962). Nitrate and phosphate were added in concentrations of 100 and 6.25 μmol L^{-1}, respectively. Cultures were irradiated with 50 and 300 μmol photons m^{-2} s^{-1} provided by Biolux 965 daylight lamps (Osram) under a 16:8-h light:dark (LD) cycle. Light intensities were adjusted using a Li-1400 data logger (Li-Cor) with a 4π sensor (Walz). Cells were preacclimated to the culture conditions for two weeks in medium that was preconditioned by purging with either ambient air (38.5 Pa CO_2) or CO_2-enriched air (101.3 Pa CO_2). CO_2-free air ($<$ 0.1 Pa CO_2; Dominick Hunter) was mixed with pure CO_2 (Air Liquide) by a CGM 2000 mass flow controller system (MCZ Umwelttechnik). The P_{CO_2} was regularly controlled with a nondispersive infrared analyzer system Li-6252 (Li-Cor) that was calibrated with CO_2-free air and purchased air mixtures of 15.2 $\pm$ 0.1 and 101.3 $\pm$ 2.0 Pa CO_2 (Air Liquide). After inoculation, the 900-mL cylindrical flasks were continuously purged with these humidified P_{CO_2}-adjusted gas mixtures to avoid cell sedimentation (flow-rate 130 $\pm$ 10 mL min^{-1}).

Seawater chemistry—To ensure quasi-constant seawater carbonate chemistry (Table 1), only cultures were used for measurements in which the pH did not deviate more than 0.05 units from a cell-free medium (pH measured with pH3000 microprocessor pH-meter; Wissenschaftlich-Technische Werkstätten). The pH electrode was daily calibrated using buffers certified by the U.S. National Bureau of Standards (NBS); obtained values are therefore reported on the NBS scale (pH_{NBS}). DIC was measured colorimetrically according to Stoll et al. (2001), using a TRAACS CS800 autoanalyzer (Seal Analytical). Total alkalinity (TA) was inferred from linear Gran-titration plots (Dickson 1981), which were produced using an automated TitroLine burette system (Schott). Calculations on carbonate chemistry were performed using CO$_2$SYS (Pierrot et al. 2006) and were based on measurements of pH_{NBS}, TA, temperature, and

Table 1. Carbonate chemistry in the experiment; Attained P_{CO_2}, DIC, HCO_3^-, CO_3^{2-}, and $\Omega_{calcite}$ are calculated based on pH_{NBS} and TA using CO$_2$Sys (Pierrot et al. 2006). Results are reported for 15°C ($n \geq 3$; $\pm$ SD).

Strain, ploidy	Photon flux (μmol m^{-2} s^{-1})	Treatment P_{CO_2} (Pa)	Attained P_{CO_2} (Pa)	pH_{NBS}	TA (μmol kg^{-1})	DIC (μmol kg^{-1})	HCO_3^- (μmol kg^{-1})	CO_3^{2-} (μmol kg^{-1})	$\Omega_{calcite}$
RCC 1216, 2N	50	Low, 38.5	40.4±0.4	8.112±0.014	2254±20	1997±44	1910±17	140.1±2.1	3.47±0.05
		High, 101.3	97.3±11.1	7.808±0.012	2385±7	2232±22	2186±1	80.0±2.8	1.94±0.07
	300	Low, 38.5	43.5±0.2	8.083±0.040	2273±5	2018±15	1942±4	134.6±0.6	3.33±0.01
		High, 101.3	110.6±14.6	7.741±0.002	2322±35	2174±32	2149±36	68.8±1.9	1.67±0.05
RCC 1217, 1N	50	Low, 38.5	35.6±0.4	8.176±0.005	2393±24	2111±19	1978±21	170.8±2.8	4.23±0.07
		High, 101.3	95.7±1.9	7.823±0.022	2398±3	2249±23	2190±4	83.5±1.5	2.03±0.04
	300	Low, 38.5	35.5±0.4	8.177±0.019	2380±10	2096±24	1967±18	169.5±3.4	4.20±0.08
		High, 101.3	95.2±5.9	7.818±0.038	2402±21	2296±34	2199±14	81.7±7.1	1.98±0.17
Reference	—	Low, 38.5	40.9±1.2	8.134±0.010	2411±13	2134±25	2030±3	156.7±4.9	3.88±0.12
		High, 101.3	100.9±10.4	7.770±0.025	2396±17	2269±45	2171±4	78.2±7.7	1.90±0.19

salinity. For the calculations, phosphate concentrations of 4 μmol L^{-1} were assumed. Dissociation constants of carbonic acid (Mehrbach et al. 1973, refit by Dickson and Millero 1987) and sulfuric acid (Dickson 1990) were used.

Cell growth—In all treatments ($n \geq 3$), cells were harvested in midexponential growth phase 4–6 d after inoculation at densities of 50,000–90,000 cells mL^{-1}. To avoid biases arising from diurnal changes, sampling was done 4–8 h after the beginning of the light period. Cell concentrations were assessed daily using a Multisizer III hemocytometer (Beckman-Coulter), and specific growth rates (μ) were calculated from the daily increments:

$$\mu = (\ln_{c_1} - \ln_{c_0}) \times \Delta t^{-1} \qquad (1)$$

where c_0 and c_1 are the initial and final cell concentrations and Δt is the time interval in days.

Elemental composition—For elemental analysis, cells were filtered onto precombusted (12 h, 500°C) GF/F filters (1.2 μm; Whatman) by applying a suction pressure of -20 kPa. To determine cellular POC quotas, respective filters were soaked with 200 μL 0.2 mol L^{-1} HCl (Merck) to remove calcite. Cellular PIC quotas were assessed as the difference in carbon content between the HCl-treated (POC) and untreated filters (total particulate C, TPC). PON measurements were performed on all filters. Analysis was carried out using an automated N and C analyzer SL 20-20 mass spectrometer (SerCon). The multiplication of cellular elemental quotas (POC, PIC, TPC, and PON) with respective specific growth rates yielded daily production rates. Note that these calculated rates are based on estimates of cell density and elemental quotas, which were assessed in a strict time window (Zondervan et al. 2002). Chlorophyll *a* (Chl *a*) quotas were determined fluorometrically after extraction in 90% acetone (Sigma), following the method described by Holm-Hansen and Riemann (1978). The TD-700 fluorometer (Turner Designs) was calibrated with standardized solutions of Chl *a* (Sigma) in 90% acetone.

C$_i$ source—To assess the relative contribution of CO$_2$ and HCO$_3^-$ to biomass production, the ^{14}C disequilibrium assay (Espie and Colman 1986; Elzenga et al. 2000) was used. Cells were concentrated by gentle filtration (polycarbonate filters, 3 μm; Millipore), and culture medium was successively exchanged with ^{14}C assay medium that was buffered with 50 mmol L^{-1} N,N-Bis(2-hydroxyethyl)glycine (BICINE), having a pH$_{NBS}$ of 8.50 at 15°C. ^{14}C spikes were prepared by adding 10 μL of NaH^{14}CO$_3$ solution (GE Healthcare) to 190 μL deionized water buffered with 20 mmol L^{-1} 4-(2-hydroxyethyl)-1-piperazineethanesulfonic acid (HEPES) having a pH$_{NBS}$ of 7.00 at 20°C, yielding an activity of $\sim$ 740 kBq. Prior to the addition of the ^{14}C spike, 4 mL of stirred cell suspension were irradiated in a temperature-controlled cuvette (15°C) with the respective acclimation light intensity for 6 min to reach steady-state photosynthesis. After the addition of the ^{14}C spike, 200-μL

subsamples were taken in short time intervals and dispensed into 2 mL 6 mol L^{-1} HCl to stop vital processes and dissolve calcite. DI^{14}C was removed by degassing. After addition of 10 mL scintillation cocktail (Ultima Gold AB; PerkinElmer), samples were measured with a Tri-Carb liquid scintillation counter (PerkinElmer). Blank measurements were produced using cell-free aliquots of spiked assay medium. Experiments were performed in the presence of 50 μmol L^{-1} dextrane-bound sulfonamide (Ramidus), inhibiting possible external carbonic anhydrase. Time courses of ^{14}C incorporation were used to assess the relative contribution of CO$_2$ and HCO$_3^-$ to biomass production (Rost et al. 2007).

DIC dependence of photosynthesis—To assess the DIC dependence of photosynthetic O$_2$ evolution, cells were concentrated by gentle filtration (polycarbonate filters, 3 μm; Millipore), and culture medium was successively exchanged with 50 mmol L^{-1} HEPES-buffered, DIC-free medium (pH$_{NBS}$ 8.20 at 15°C) that was prepared by purging with humidified CO$_2$-free air for at least 18 h. Eight mL of concentrated cell suspension was transferred to a temperature-controlled cuvette (15°C) that was coupled to a sector-field multicollector mass spectrometer (Isoprime; MicroMass) via a gas-permeable membrane (Polytetrafluorethylen, 0.01 mm) inlet system. In LD intervals with the respective acclimation light intensity, known amounts of DIC were consecutively added in form of NaHCO$_3$ solution during darkness. Net rates of photosynthesis were measured as the change in [O$_2$] over time. [O$_2$] signals were two-point calibrated between 0% (after addition of sodium dithionite, an O$_2$ scavenger) and 21% (as measured in air-equilibrated medium using the solubility coefficient obtained by Weiss 1970). Measured rates of O$_2$ evolution were corrected for machine-inherent O$_2$ consumption. The CO$_2$ baseline was determined by adding NaOH (45 mmol L^{-1} final concentration) into DIC-free assay medium. CO$_2$ concentrations were calibrated by adding standardized amounts of DIC in form of NaHCO$_3$ solution into 0.2 mol L^{-1} HCl. By adding known amounts of DIC to buffered assay medium, the pH-dependent ratio of [DIC]:[CO$_2$] was determined. By the addition of carbonic anhydrase (1 μg; Sigma) to the assay, rapid equilibration of the carbonate system was assured, allowing the calculation of [DIC] from the recorded CO$_2$ signals. Obtained kinetic curves were fit with the Michaelis–Menten equation:

$$P = \frac{V_{max} \times [S]}{K_{1/2} + [S]} \qquad (2)$$

where P is the net rate of photosynthesis, V_{max} is the DIC-saturated net rate of photosynthesis, [S] is the substrate concentration (i.e., [DIC]), and $K_{1/2}$ is the half-saturation concentration for the substrate.

Light dependence of photosynthesis—To assess the light dependence of photosynthetic O$_2$ evolution, cells were concentrated as described above and medium was exchanged with air-equilibrated 50 mmol L^{-1} HEPES-buffered assay

Rokitta and Rost

medium (pH_{NBS} 8.20 at 15°C). Net rates of photosynthesis were measured as described above. Photosynthesis vs. irradiance curves were fit using the following equation:

$$P = V_{max} \times \left(1 - e^{(-b \times (I-c))}\right) \qquad (3)$$

where P is the net photosynthetic rate, V_{max} is the light-saturated net rate of photosynthesis, and I is the irradiance. The light intensity at which the photosynthesis starts to enter saturation (i.e., light acclimation index, I_k) and the initial light-limited slope of the curve (i.e., maximum light-use efficiency, α) were calculated according to the following:

$$I_k = b^{-1} + c \qquad (4)$$

$$\alpha = V_{max} \times b \qquad (5)$$

Statistics—For parameters that were calculated by multiplication from error-afflicted values (i.e., production rates, Chl a : POC), error propagation was taken into account: relative propagated standard deviations ($SD_{rel;prop}$) were calculated as the square root of the sum of the squared relative standard deviations ($SD_{rel;1,2}$):

$$SD_{rel;prop} = \sqrt[2]{\left(SD_{rel;1}{}^2\right) + \left(SD_{rel;2}{}^2\right)} \qquad (6)$$

Statistical significances of data were obtained by applying two-way ANOVAs to the full data matrix of P_{CO_2} vs. light vs. ploidy. The null hypothesis was withdrawn when the ANOVA p-values were < 0.05. To obtain significances between means, Tukey's honestly significant difference statistic was applied for post hoc testing. If not stated otherwise, results were called significant at a 95% confidence level, that is, when p-values were ≤ 0.05. In all measurements, the sample size of biological replicates n was ≥ 3.

Results

Because of the chosen matrix approach, results of the treatments can be viewed from two directions: the effects of P_{CO_2} can be modulated as a result of altered light intensity, and, vice versa, light-induced effects can be modulated by P_{CO_2}. To maintain scope and clarity of this study, the following sections exclusively focus on CO_2 effects and their modulation by light. Results are presented separately for each particular life-cycle stage.

The diploid life-cycle stage—Growth rates of the diplont were not significantly affected by elevated P_{CO_2} under both light conditions (Fig. 1a). In response to elevated P_{CO_2}, the POC quota increased significantly under high (+59%) and low light conditions (+40%; Table 2). The production rates of POC in the diploid cells reacted to elevated P_{CO_2} with a prominent increase under low light (+84%), whereas this effect was attenuated under high light (Fig. 1b). The PIC quota significantly decreased with elevated P_{CO_2} under low light (−77%) but not under high light (Table 2). Consequently, PIC production was strongly reduced under low light (−74%) but not under high light (Fig. 1c). The PIC : POC ratio of the diploid cells decreased under

elevated P_{CO_2} (Table 2). This effect is highly significant under low light (−85%) but attenuated under high light conditions. Regarding the production of TPC, however, no alterations were observed in response to elevated P_{CO_2} (Fig. 1d). Under elevated P_{CO_2}, PON quotas of the diploid stage increased significantly under low (+84%) and high light conditions (+51%; p = 0.051, significant at a 90% confidence level; Table 2). As these quotas closely followed the trends of the respective POC quotas, no effects of P_{CO_2} on the POC : PON ratio (Table 2) were observed. Cellular Chl a quotas were not affected by P_{CO_2} (Fig. 1e). When normalized to POC, however, Chl a contents (Chl a : POC) decreased notably in response to elevated P_{CO_2} under low light (−29%), whereas this decrease was less pronounced under high light (Fig. 1f).

Regarding the source of inorganic carbon, ^{14}C disequilibrium assays revealed that in the diploid stage, HCO_3^- contribution (75–90%) was not altered by P_{CO_2} under low light but decreased slightly under high light (−11%; Fig. 2a). MIMS-based affinity assays could not show any alterations of half-saturation concentrations for DIC ($K_{1/2}$;DIC) in response to elevated P_{CO_2} (Fig. 2b). Regarding the light dependence of O_2 evolution, Chl a-normalized maximum photosynthetic rates ($V_{max;Chl}$) decreased in response to elevated P_{CO_2}, an effect that was significant under low light (−45%) but not under high light (Fig. 2c). Cell-normalized maximum rates ($V_{max;cell}$) under elevated P_{CO_2} decreased significantly under low light (−59%) but not under high light (Fig. 2d). The I_k values and Chl a-normalized maximum light-use efficiencies (α_{Chl}) of the diploid stage were not affected by P_{CO_2} (Table 2). Cell-normalized maximum light-use efficiencies (α_{cell}), however, decreased significantly under low light (−40%), whereas this effect was insignificant under high light (Table 2). Under in situ light intensities, cell-normalized net rates of photosynthesis of the diploid stage ($V_{in\ situ;cell}$) significantly decreased in response to elevated P_{CO_2} under low light (−48%), but not under high light (Fig. 2f). After normalization to Chl a, however, $V_{in\ situ;Chl}$ is not affected by P_{CO_2} in any of the light treatments (Fig. 2e).

The haploid life-cycle stage—In the haplont, elevated P_{CO_2} leads to significant decreases in growth rates under both low light (−14%; p = 0.06, i.e., significant at a 90% confidence level) and high light (−28%; Fig. 1a). Quotas of POC were not significantly affected by elevated P_{CO_2} under both light conditions (Table 2). Likewise, POC productions were not significantly altered by P_{CO_2} (Fig. 1b). PIC quotas measured in the haploid stage were < 1 pg cell^{-1} in all treatments, reflecting the absence of calcification (Fig. 1c). Also, the PON quotas were not significantly altered by elevated P_{CO_2} (Table 2). Consequently, POC : PON ratios were unaffected by elevated P_{CO_2} (Table 2). Chl a quotas of the haplont decreased significantly in response to elevated P_{CO_2} under low light (−31%), whereas the effect was attenuated under high light (Fig. 1e). Chl a : POC decreased prominently in response to elevated P_{CO_2} under low light (−47%) but not under high light (Fig. 1f).

Regarding C_i acquisition, the contribution of HCO_3^- to C fixation (83–90%) was not influenced by P_{CO_2} (Fig. 2a).
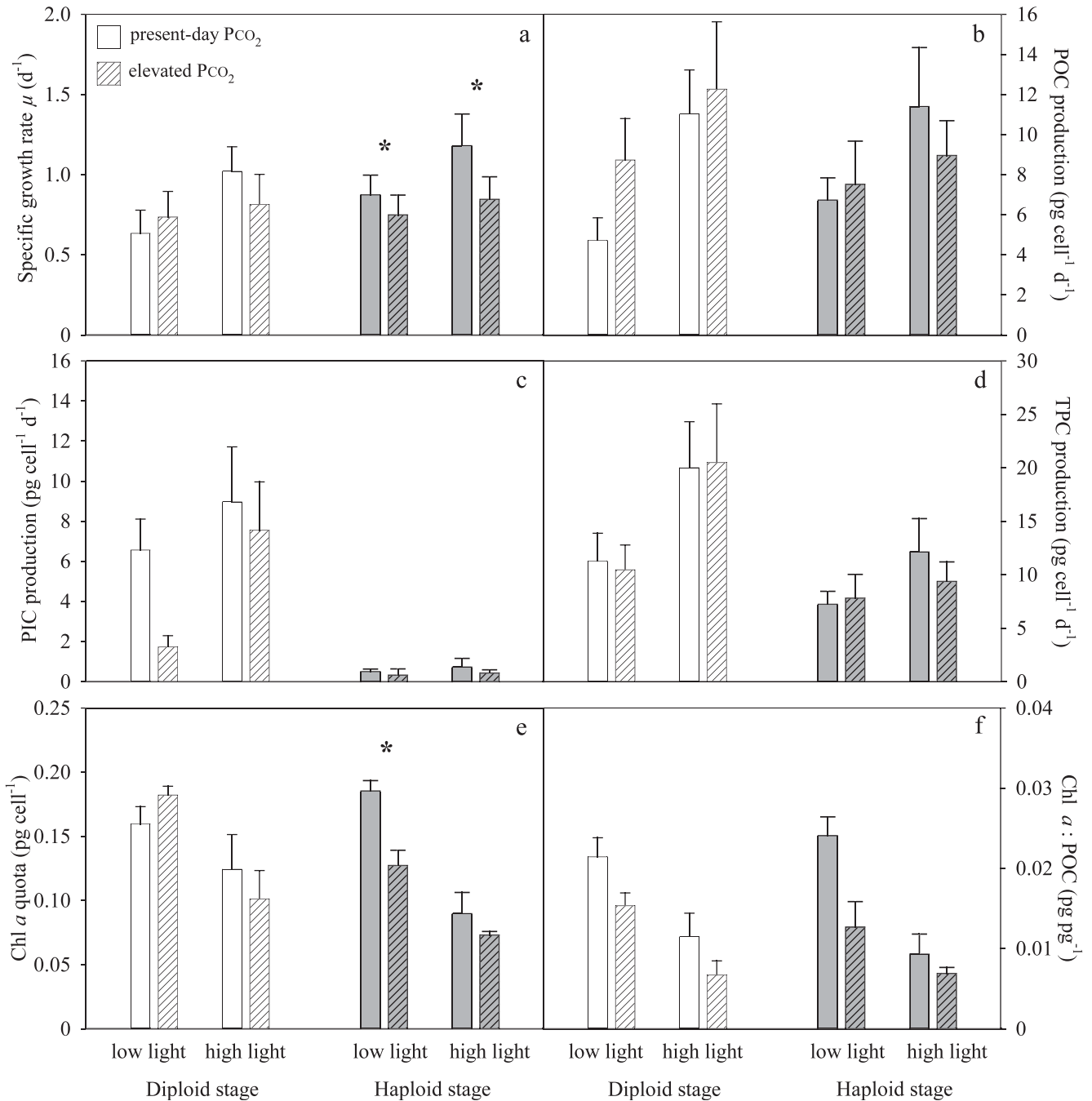
Fig. 1.   Phenomenological responses of diploid (white) and haploid (gray) *Emiliania huxleyi* (RCC1216 and 1217) to present-day P_{CO_2} (filled; 38.5 Pa) and elevated P_{CO_2} (shaded, 101 Pa) under low (50 μmol photons m^{-2} s^{-1}) and high (300 μmol photons m^{-2} s^{-1}) light intensity. Error bars denote 1 SD ($n \geq 3$).

Yet, in response to elevated P_{CO_2}, $K_{1/2}$ (DIC) increased significantly under low light (+409%), an effect that was attenuated under high light (Fig. 2b). No significant effects on $V_{max;Chl}$ were observed in response to P_{CO_2} under both light conditions (Fig. 2c). Values of $V_{max;cell}$, however, decreased significantly in response to elevated P_{CO_2} under both, low (−52%) and high light conditions (−40%; Fig. 2d). I_k values decreased significantly as an effect of elevated P_{CO_2} under low (−51%; $p = 0.06$, i.e., significant at

a 90% confidence level) and high light conditions (−58%; Table 2). Elevated P_{CO_2} caused significant increases in α_{Chl} under low light (+84%) and high light (+187%; Table 2) conditions. Cell-normalized light-use efficiencies (α_{cell}) were, however, insensitive to P_{CO_2} (Table 2). Values of $V_{in\ situ;Chl}$ increased significantly in response to elevated P_{CO_2} under high (+74%; $p = 0.06$, i.e., significant at a 90% confidence level) but not under low light (Fig. 2e). Values of $V_{in\ situ;cell}$ were, however, not affected by P_{CO_2} (Fig. 2f).

Table 2. Responses of diploid and haploid *Emiliania huxleyi* (RCC 1216 and 1217; 2N and 1N) grown under low P_{CO_2} (38.5 Pa) and elevated P_{CO_2} (101.3 Pa) under low (50 μmol photons m^{-2} s^{-1}) and high (300 μmol photons m^{-2} s^{-1}) light intensity. Errors denote 1 SD ($n \geq 3$). Light intensity (μmol photons m^{-2} s^{-1}); specific growth rate (d^{-1}); quotas (pg cell^{-1}); productions (pg cell^{-1} d^{-1}); PIC:POC, POC, PON, POC:PON, HCO$_3^-$ uptake:net fixation (mol mol^{-1}); Chl a:POC (pg pg^{-1}); K$_{1/2}$ (DIC) (μmol kg^{-1}); V$_{max;Chl}$, V$_{in\ situ;Chl}$ (μmol O$_2$ [mg Chl a]$^{-1}$ h^{-1}); V$_{max;cell}$, V$_{in\ situ;cell}$ (fmol O$_2$ cell^{-1} h^{-1}); I$_k$ (μmol photons m^{-2} s^{-1}); α_{Chl} (μmol O$_2$ [mg Chl a]$^{-1}$ h^{-1} [μmol photons m^{-2} s^{-1}]$^{-1}$); α_{cell} (fmol O$_2$ cell^{-1} h^{-1} [μmol photons m^{-2} s^{-1}]$^{-1}$).

Strain, ploidy	RCC 1216, 2N				RCC 1217, 1N			
Light intensity	50		300		50		300	
P$_{CO_2}$ treatment	38.5	101.3	38.5	101.3	38.5	101.3	38.5	101.3
Specific growth rate	0.63±0.14	0.74±0.16	1.02±0.15	0.81±0.19	0.87±0.12	0.75±0.12	1.18±0.20	0.85±0.14
POC quota	7.45±0.54	11.87±1.14	10.81±1.41	15.08±2.20	7.70±0.67	10.04±2.34	9.65±1.90	10.58±1.05
PIC quota	10.35±0.63	2.35±0.58	8.78±2.34	9.29±2.03	0.58±0.12	0.43±0.41	0.61±0.35	0.51±0.16
PON quota	1.25±0.08	2.31±0.29	1.52±0.37	2.29±0.39	1.49±0.15	2.07±0.56	1.63±0.35	1.93±0.20
PIC:POC	1.40±0.16	0.20±0.07	0.82±0.22	0.65±0.19	0.07±0.01	0.06±0.03	0.06±0.04	0.05±0.02
POC:PON	6.97±0.31	5.95±0.91	7.48±0.26	7.75±0.63	6.00±0.13	5.84±0.56	6.92±0.33	6.71±0.30
POC production	4.72±1.13	8.73±2.07	11.03±2.19	12.27±3.36	6.73±1.11	7.52±2.15	11.40±2.94	8.96±1.74
PIC production	6.56±1.55	1.73±0.57	8.96±2.74	7.55±2.41	0.51±0.12	0.32±0.31	0.73±0.43	0.43±0.15
TPC production	11.29±2.59	10.46±2.31	20.00±4.32	20.49±5.49	7.24±1.21	7.81±2.21	12.12±3.11	9.37±1.83
PON production	0.79±0.19	1.70±0.42	1.55±0.44	1.87±0.54	1.30±0.23	1.55±0.49	1.93±0.53	1.63±0.32
Chl a quota	0.16±0.01	0.18±0.01	0.12±0.03	0.10±0.02	0.19±0.01	0.13±0.01	0.09±0.02	0.07±0.00
Chl a:POC	0.02±0.00	0.02±0.00	0.01±0.00	0.01±0.00	0.02±0.00	0.01±0.00	0.01±0.00	0.01±0.00
HCO$_3^-$ uptake:net fixation	0.85±0.01	0.86±0.04	0.89±0.03	0.76±0.05	0.87±0.01	0.87±0.03	0.89±0.03	0.83±0.05
K$_{1/2}$ (DIC)	111±110	114±62	20±20	50±43	66±48	333±72	126±81	156±135
V$_{max;Chl}$	451±33	246±16	505±81	378±69	300±50	270±59	254±38	307±66
V$_{max;cell}$	49±3	20±5	36±4	26±6	39±7	19±5	21±4	13±2
V$_{in\ situ;Chl}$	116±17	81±25	445±55	348±57	66±31	113±21	167±48	290±64
V$_{in\ situ;cell}$	13±2	7±2	32±2	24±5	8±4	8±1	14±4	12±2
I$_k$	121±6	91±16	151±21	124±13	160±45	79±24	293±65	123±9
α_{Chl}	4.47±0.52	3.66±0.71	3.94±0.23	3.32±0.37	2.29±0.91	4.21±0.61	1.15±0.38	3.30±0.71
α_{cell}	0.49±0.05	0.29±0.04	0.29±0.02	0.23±0.04	0.29±0.11	0.29±0.03	0.10±0.04	0.14±0.03
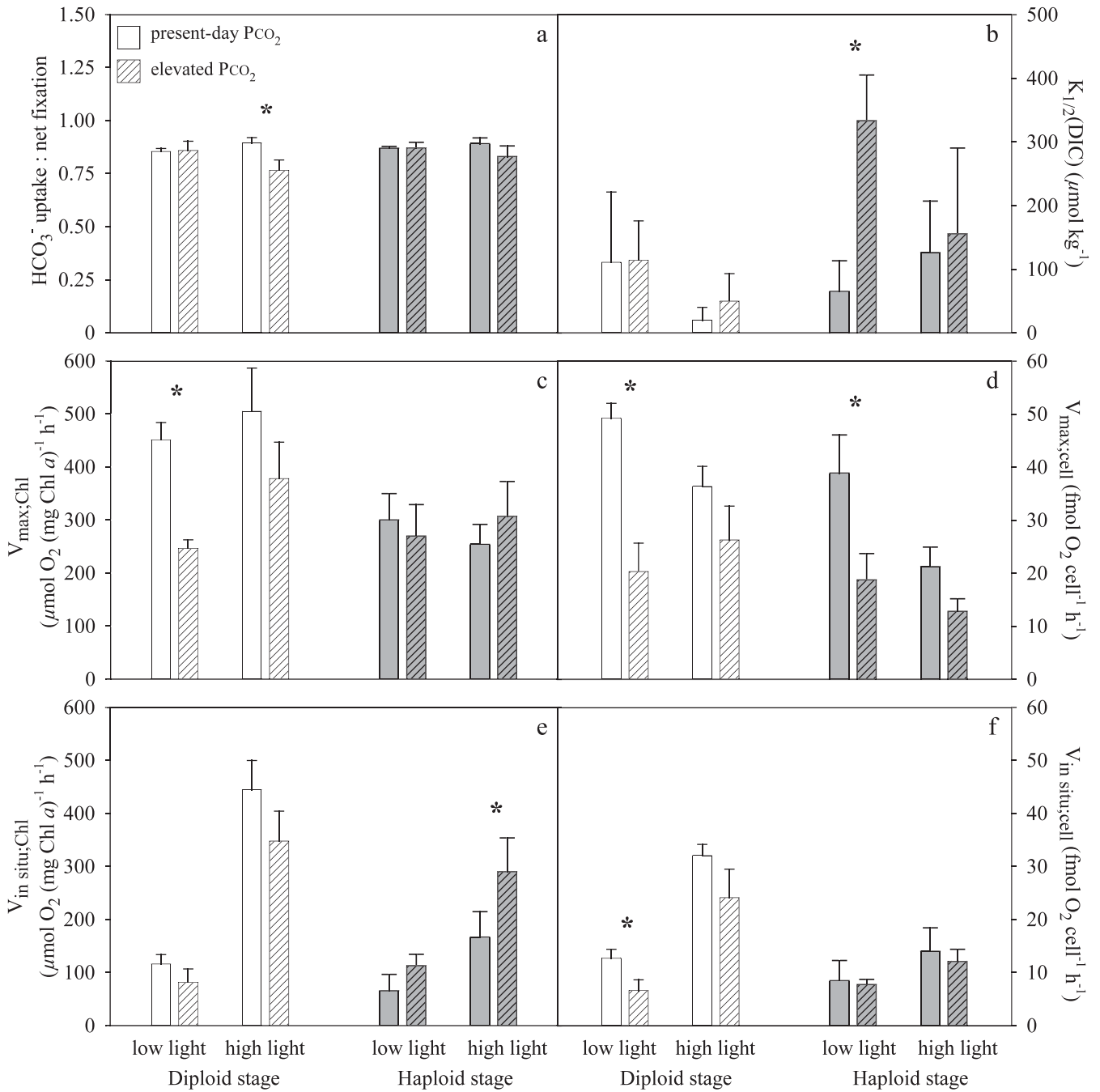
Fig. 2. Physiological responses of diploid (white) and haploid (gray) *Emiliania huxleyi* (RCC1216 and 1217) to present-day P_{CO_2} (filled; 38.5 Pa) and elevated P_{CO_2} (shaded, 101 Pa) under low (50 μmol photons m^{-2} s^{-1}) and high (300 μmol photons m^{-2} s^{-1}) light intensity. Error bars denote 1 SD ($n = 3$).

Discussion

The life-cycle stages of *E. huxleyi* represent independent entities with strikingly divergent features (Frada et al. 2008; Von Dassow et al. 2009; Rokitta et al. 2011). A direct comparison of measured parameters between them is therefore obsolete. For this reason, the effects of P_{CO_2} and their modulation by light are first evaluated separately for the diplont and haplont and, at a later stage, discussed synoptically.

The diploid life-cycle stage—Cellular quotas and production rates of POC and PIC were affected by P_{CO_2} (Fig. 1b,c; Table 2). Elevated P_{CO_2} stimulated POC production, while production rates of PIC were reduced (Fig. 1b,c). Similar response patterns were observed in the

strain PLYB92/11 (Riebesell et al. 2000; Zondervan et al. 2002): Under 150 μmol photons m^{-2} s^{-1}, for instance, POC production increased from 9.0 to 9.8 pg cell^{-1} d^{-1}, while PIC production decreased from 9.2 to 7.6 pg cell^{-1} d^{-1} over a P_{CO_2} range of about 15.2 to 81.1 Pa. The findings of the present study are also in line with Langer et al. (2009), who found comparable responses in strain RCC1216 grown under 400 μmol photons m^{-2} s^{-1}. Richier et al. (2011) found small yet insignificant increases in POC and PIC production under OA in this same strain, which may originate from different culture conditions (e.g., smaller P_{CO_2} range of 44.6 vs. 78.0 Pa). Although the comparable studies differ in terms of absolute values and trends, POC and PIC production typically exhibited opposing trends. This anticorrelation, reflected by decreasing PIC:POC ratios in response to elevated P_{CO_2} is widely observed in strains of the *E. huxleyi* morphospecies complex (Riebesell et al. 2000; Langer et al. 2009; Feng et al. 2008) and has often been used to demonstrate the exceptionally high sensitivity of coccolithophores to OA.

TPC production was not affected by P_{CO_2} (Fig. 1d). Although not explicitly stated, quasi-constant TPC productions were reported in a number of other studies. In Zondervan et al. (2002), TPC productions (as calculated from averaged growth rates and PIC and POC quotas) were independent of P_{CO_2} over a range 15.2 to 81.1 Pa (20.7 $\pm$ 1.3 and 18.3 $\pm$ 0.9 pg TPC cell^{-1} under light intensities of 80 and 150 μmol photons m^{-2} s^{-1}, respectively). Likewise, Langer et al. (2009) found unaltered rates of TPC production in strain RCC1216 (24.0 $\pm$ 1.6 pg TPC cell^{-1}) over a P_{CO_2} range of 22.3 to 121.6 Pa. In the study of Feng et al. (2008), clear effects of P_{CO_2} on TPC productions are also lacking in most treatments. Only at high temperature (24°C), a slight P_{CO_2}-related effect can be recognized. The apparent insensitivity in TPC production toward changes in P_{CO_2} suggests that the overall acquisition of inorganic carbon is not generally hampered yet that carbon is differently allocated among cellular processes under OA.

To explore the origins of these phenomena, in vivo assays were conducted to assess properties of carbon acquisition. ^{14}C disequilibrium assays demonstrated that HCO_3^- is the major source of inorganic carbon for photosynthetic C fixation in all P_{CO_2} treatments (75–90%; Fig. 2a). This corresponds to earlier studies on *E. huxleyi*, showing that diploid cells operate a CCM based mainly on HCO_3^- uptake (Trimborn et al. 2007), for which now also preliminary molecular evidence exists (Von Dassow et al. 2009; Rokitta et al. 2011). Regarding the affinities for inorganic carbon, $K_{1/2}$ (DIC) values were low and not significantly altered in response to P_{CO_2} (Fig. 2b), indicating C_i saturation of transporters under in situ conditions. Affinities were similar to previously obtained values for diploid cells grown under comparable conditions (36.5 Pa CO_2; 180 μmol photons m^{-2} s^{-1}; 16:8-h LD cycle; Rost et al. 2006). The slightly lower $K_{1/2}$ (DIC) values under high light may be attributed to a higher energization of the C_i uptake system (Beardall 1991) or a generally higher C_i demand (Rost et al. 2006), as also indicated by higher TPC productions (Fig. 1d).

Parameters of light-dependent photosynthesis, that is, maximum as well as in situ rates of O_2 evolution (Fig. 2c–f) and maximum light-use efficiencies (Table 2), decreased in response to elevated P_{CO_2}. Such responses are typically observed in the context of light acclimations, indicating decreased energy generation under high light (MacIntyre et al. 2002). A large part of this photoacclimation usually originates from a lowered Chl a:POC ratio, which is also the case under elevated P_{CO_2} (Fig. 1f). The observed similarities between effects of high light and elevated P_{CO_2} indicate that the throttling of energy generation is a common mechanism not only to cope with a high energy supply but also to adjust to a decreased energy demand. Feng et al. (2008) observed an apparently opposing trend, that is, an increase in photosynthesis under elevated P_{CO_2}. However, while Feng and coworkers assessed net ^{14}C incorporation into biomass over 24 h, in this study net rates of O_2 evolution were measured over several minutes during midday. Note that comparability between methods is given only when measurements use similar units and time frames. When considering the more comparable data on biomass production, that is, the increased buildup of POC under elevated P_{CO_2} (Fig. 1b), both studies in fact show consistent trends.

To sum up, the diploid cells maintain their TPC production rates under elevated P_{CO_2} by reallocating acquired resources from PIC toward POC production (Fig. 1b–d). As C_i acquisition appears unaltered in the assays, the shunting of resources likely originates from processes that occur downstream of the C_i accumulation. Also, these processes might be responsive to [H$^+$] rather than C_i concentrations (Taylor et al. 2010; Lefebvre et al. 2012). Suffrian et al. (2011) have shown that external pH perturbations translate linearly into cytoplasmic pH changes. An impairment of transport processes (e.g., for DIC and Ca^{2+}) due to low internal pH might weaken the process of biomineralization. In any case, the anticorrelation between PIC and POC production once more stresses that calcification is neither a prerequisite nor a means for supporting C fixation (Trimborn et al. 2007).

Despite lowered photosynthetic energy generation under elevated P_{CO_2} (Fig. 2e,f), the diploid cells maintain and even increase production rates of TPC and POC, respectively (Fig. 1b,d). One reason for these P_{CO_2}-dependent changes in energy efficiency might be a downregulation of CCM activity. For example, decreased leakage of actively accumulated CO_2 may supersede part of the CCM activity under elevated P_{CO_2}. A down-regulation might therefore liberate significant amounts of energy (Kranz et al. 2010). Although assay results that are obtained under constant pH do not indicate significant alterations in C_i source and affinities (Fig. 2a,b), the CCM activity may in fact be altered under in situ carbonate chemistry. Especially in the ^{14}C-disequilibrium assay, the high pH of 8.5 deviates strongly from in situ pH values being lower than 7.9 in the high P_{CO_2} treatments (Table 1). Consequently, the assay results might be biased because C_i transporters are reacting not only to CO_2 and HCO_3^- availability but also to [H$^+$]. In view of these shortcomings, assay conditions should be modified to resemble in situ pH values.

Light strongly modulated the magnitude of the P_{CO_2} responses (Figs. 1, 2). Under energetic constraints, that is, low light, the effect of elevated P_{CO_2} was typically most pronounced. As discussed above, an altered energetic status of the cells may originate from down-regulation of CCM activity. The impairment of calcification under elevated P_{CO_2} may reduce the ability of this process to compete with POC production for resources like C_i and energy. This detrimental effect of OA can apparently be compensated by higher energy supply; that is, PIC production is partially reestablished when light intensity is high (Fig. 1c).

The haploid life-cycle stage—Neither the quotas of POC and PON nor the respective production rates were significantly altered by elevated P_{CO_2} (Table 2; Fig. 1b), suggesting that overall productivity of haploid *E. huxleyi* cells is only marginally affected by OA. Also, the POC : PON ratios were independent from P_{CO_2} but increased slightly with light (Table 2), emphasizing that the processes of carbon fixation and nitrogen acquisition are tightly coupled (under N-replete conditions) and depend on energy availability rather than carbonate chemistry. In vivo assays resolved that the described maintenance of elemental composition and the absence of clear macroscopic effects can be attributed to adjustments within C_i acquisition and photophysiology.

[14]C disequilibrium assays could show that HCO_3^- is the major C_i source ($\sim$ 80–90%) and that the fractional contribution to biomass buildup is not altered by elevated P_{CO_2} (Fig. 2a). MIMS-based assays could resolve that elevated P_{CO_2} leads to decreased C_i uptake affinities under low light but not under high light (Fig. 2b). Decreased C_i affinities in response to elevated P_{CO_2} have been reported for diploid *E. huxleyi* (strain PLYB92/11; Rost et al. 2003), a number of diatoms (Trimborn et al. 2008), and also cyanobacteria (Sültemeyer et al. 1998). The latter study suggests posttranslational modification being responsible for decreased affinities under elevated P_{CO_2}.

Regarding the light dependence of O_2 evolution, the Chl *a*–normalized maximum net rates of photosynthesis ($V_{max;Chl}$) are not affected by elevated P_{CO_2} (Fig. 2c), indicating that the photosystems can in principle deliver the same energetic output when light saturated. Photosystems do, however, not perform equally well at acclimation light intensities, which is indicated by higher Chl *a*–normalized in situ rates under elevated P_{CO_2} ($V_{in\ situ;Chl}$; Fig. 2e). As cellular Chl *a* quotas are, however, themselves affected by the treatments, cell normalization yields more meaningful measures: accounting for this, cellular in situ rates of photosynthesis were not affected by elevated P_{CO_2} ($V_{in\ situ;cell}$; Fig. 2f); that is, cells generate the same amount of photosynthetic energy. The down-regulation in Chl *a* content and $V_{max;cell}$ under elevated P_{CO_2} resembles responses typically observed in high light acclimations (McIntyre et al. 2002).

To sum up, haploid cells adjust their metabolism to elevated P_{CO_2}, resulting in constant productivity, elemental composition, and cellular energy budget. The unaltered cellular in situ rates of photosynthesis despite lowered Chl *a* : POC indicate improved energy efficiency under elevated P_{CO_2}. As suggested for the diploid stage, improved CO_2 supply might in part supersede CCM activity and reduce the costs associated with active C_i acquisition. The fact that the haploid cells down-scale light harvesting instead of enhancing biomass production under elevated P_{CO_2} is in line with the parsimonious lifestyle that was proposed from transcriptomic analyses (Von Dassow et al. 2009; Rokitta et al. 2011).

Synopsis and conceptual model—A common trait of both life-cycle stages is the quasi-constant TPC production under elevated P_{CO_2}, which is also in line with the P_{CO_2} insensitivity in POC : PON ratios observed (Table 2). This unaltered "productivity" might originate from cell-physiological constraints, such as surface : volume ratio, transporter density, or macromolecular composition. Regarding the P_{CO_2} effects on pigment contents, the haplont keeps its POC quotas constant but decreases its Chl *a* quota, whereas the diploid stage increases POC quotas and maintains its Chl *a* quota. The result in both stages, however, is a reduction of Chl *a* : POC, indicating decreased light harvesting under elevated P_{CO_2}.

Despite this down-regulation in light harvesting, cells of both stages were able to maintain or increase TPC or POC productions, suggesting improved energy efficiency under elevated P_{CO_2}. Furthermore, observed CO_2 responses were typically pronounced under low light and minimized under high light. This can be explained when considering applied conditions, such as elevated P_{CO_2}, as energetically beneficial or adverse for any defined metabolic process that follows a typical saturation kinetic (Fig. 3). While the energetic status of the cell is governed primarily by light, secondary treatments may further increase or decrease the amount of energy that is available to the process. The saturation behavior explains why the same absolute energetic benefit or detriment (here induced by elevated P_{CO_2}) causes responses of different magnitudes, depending on the light levels. In the case of POC production, elevated P_{CO_2} increases the available energy and thereby stimulates biomass production in the diplont. In the case of PIC production, elevated P_{CO_2} apparently increases the costs, thereby lowering available energy and reducing calcification. In other words, the overall energetic status of the cell (governed by environmental parameters, primarily light) determines whether responses to energetically relevant environmental changes are large or small. This conceptual model might explain some of the apparent variability in OA responses observed within the *E. huxleyi* morphospecies complex (Langer et al. 2009; Hoppe et al. 2011) and even within a single strain (Langer et al. 2009; Richier et al. 2011; this study).

This interdependence of responses toward changing environmental conditions emphasizes the multidimensionality of physiological processes. Studies have shown that changes in energetically relevant environmental parameters, especially P_{CO_2} and light, are mutually influencing (Smith 1936; this study). In addition to the assessment of modulated effects, the application of such multifactorial matrices and the ceteris paribus principle further allows the identification of causal relationships. Clearly, these
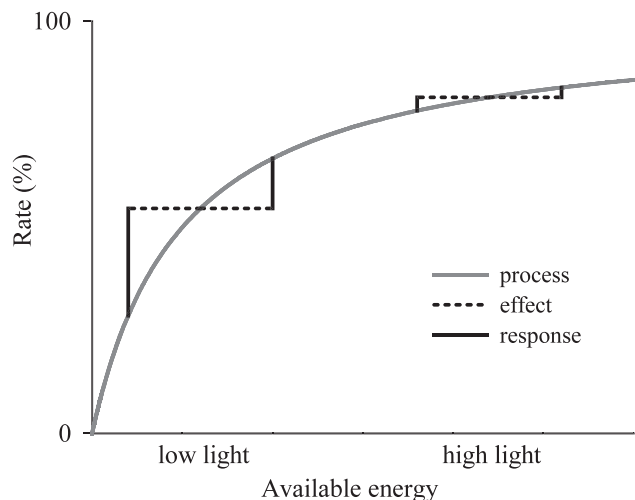
Fig. 3. Energy-dependent modulation of physiological responses to an environmental parameter. The rate of a physiological process (gray line) is governed primarily by energy supply (i.e., irradiance). Changes in other environmental parameters (e.g., P_{CO_2}) cause additional, adverse or beneficial effects (dotted black lines) on the overall energy availability. Although these effects are of the same magnitude, the responses (solid black lines), that is, the changes in process rates, are notably stronger under low energy availability.

approaches deepen the understanding of cellular mechanisms that underlie the observed phenomena. It is therefore to be appreciated that experiments are increasingly conducted using different combinations of relevant environmental conditions (Feng et al. 2008; Kranz et al. 2010; Shi et al. 2010).

Ecological and biogeochemical implications—Our findings show that the responses to OA are strongly modulated by light. In the natural environment, the vertical motion of water masses causes the phytoplankton to experience a broad range of light intensities. As OA effects were diminished at higher light intensities, that is, at the surface ocean, the rise in P_{CO_2} will mostly affect specimens residing at lower irradiances, that is, at the lower photic zone. Blooms of *E. huxleyi*, however, tend to develop under highly stratified conditions (Tyrrell and Merico 2004), and thus the concomitant high mean irradiances may partially attenuate OA effects. Even though OA effects on physiology appear small at times, such as under high light, they may translate into large ecological consequences in the real world, where competition and grazing play a crucial role. Floristic shifts due to OA have been observed within the group of coccolithophores, lightly calcified strains being favored over heavily calcified ones (Beaufort et al. 2011). Investigations on combined effects of abiotic and biotic factors, conducted in monoclonal as well as in field populations, are needed to understand and predict the fate of coccolithophore calcification in the framework of global change.

In terms of consequences for elemental cycling, the effects of OA on the haploid life-cycle stage are not likely to translate into biogeochemically significant effects. In the diploid stage, which probably constitutes the primal part of the life cycle, the alterations in PIC and POC productions may have implications for the depth export not only of alkalinity but also of organic material. The likely lowered vertical flux of alkalinity in the future may increase the uptake capacity of surface waters for anthropogenic CO_2 (Zondervan et al. 2001). A lowered degree of calcification could, however, also hamper the vertical export of organic carbon due to lowered ballasting (Klaas and Archer 2002), in turn leading to decreased C drawdown from surface waters (Lam et al. 2011). Further assessment of the relative strengths of the biological carbon pumps and their interdependence is needed for thorough predictions of carbon cycling in contemporary and future oceans.

References

BEARDALL, J. 1991. Effects of photon flux density on the "CO_2 concentrating mechanism" of the cyanobacterium *Anabaena variabilis*. J. Plankton Res. **13:** 133–141.

BEAUFORT, L., AND OTHERS. 2011. Sensitivity of coccolithophores to carbonate chemistry and ocean acidification. Nature **476:** 80–83, doi:10.1038/nature10295

DICKSON, A. G. 1981. An exact definition of total alkalinity and a procedure for the estimation of alkalinity and total inorganic carbon from titration data. Deep-Sea Res. **28:** 609–623, doi:10.1016/0198-0149(81)90121-7

———. 1990. Standard potential of the reaction: AgCl(s) + ½ H_2(g) = Ag(s) + HCl(aq), and the standard acidity constant of the ion HSO_4^- in synthetic seawater from 273.15 to 318.15 K. J. Chem. Thermodyn. **22:** 113–127, doi:10.1016/0021-9614(90)90074-Z

———, AND F. J. MILLERO. 1987. A comparison of the equilibrium constants for the dissociation of carbonic acid in seawater media. Deep-Sea Res. **34:** 1733–1743, doi:10.1016/0198-0149(87)90021-5

ELZENGA, J. T. M., H. B. A. PRINS, AND J. STEFELS. 2000. The role of extracellular carbonic anhydrase activity in inorganic carbon utilization of *Phaeocystis globosa* (Prymnesiophyceae): A comparison with other marine algae using the isotopic disequilibrium technique. Limnol. Oceanogr. **45:** 372, doi:10.4319/lo.2000.45.2.0372

ESPIE, G. S., AND B. COLMAN. 1986. Inorganic carbon uptake during photosynthesis—a theoretical analysis using the isotopic disequilibrium technique. Plant Physiol. **80:** 863–869, doi:10.1104/pp.80.4.863

FENG, Y., M. E. WARNER, Y. ZHANG, J. SUN, F. X. FU, J. M. ROSE, AND D. A. HUTCHINS. 2008. Interactive effects of increased P_{CO_2}, temperature and irradiance on the marine coccolithophore *Emiliania huxleyi* (Prymnesiophyceae). Eur. J. Phycol. **43:** 78–98, doi:10.1080/09670260701664674

FRADA, M., I. PROBERT, M. J. ALLEN, W. H. WILSON, AND C. DE VARGAS. 2008. The "Cheshire Cat" escape strategy of the coccolithophore *Emiliania huxleyi* in response to viral infection. PNAS **105:** 15944–15949, doi:10.1073/pnas.0807707105

GUILLARD, R. R. L., AND J. H. RYTHER. 1962. Studies of marine planktonic diatoms. Can. J. Microbiol. **8:** 229–239, doi:10.1139/m62-029

HOLM-HANSEN, O., AND B. RIEMANN. 1978. Chlorophyll *a* determination: Improvements in methodology. Oikos **30:** 438–447, doi:10.2307/3543338

HOPPE, C. J. M., G. LANGER, AND B. ROST. 2011. *Emiliania huxleyi* shows identical responses to elevated P$_{CO_2}$ in TA and DIC manipulations. JEMBE **406:** 54–62, doi:10.1016/j.jembe.2011.06.008

IGLESIAS-RODRIGUEZ, M. D., AND OTHERS. 2008. Phytoplankton calcification in a high-CO$_2$ world. Science **320:** 336–340, doi:10.1126/science.1154122

KLAAS, C., AND D. E. ARCHER. 2002. Association of sinking organic matter with various types of mineral ballast in the deep sea: Implications for the rain ratio. Glob. Biogeochem. Cycles **16:** 1116, doi:10.1029/2001GB001765

KRANZ, S. A., O. LEVITAN, K.-U. RICHTER, O. PRASIL, I. BERMAN-FRANK, AND B. ROST. 2010. Combined effects of CO$_2$ and light on the N$_2$-fixing cyanobacterium *Trichodesmium* IMS101: Physiological responses. Plant Physiol. **154:** 334–345, doi:10.1104/pp.110.159145

LAM, P. J., S. C. DONEY, AND J. K. B. BISHOP. 2011. The dynamic ocean biological pump: Insights from a global compilation of particulate organic carbon, CaCO$_3$, and opal concentration profiles from the mesopelagic. Glob. Biogeochem. Cycles **25:** 1–14, doi:10.1029/2010GB003868

LANGER, G., M. GEISEN, K. H. BAUMANN, J. KLÄS, U. RIEBESELL, S. THOMS, AND J. R. YOUNG. 2006. Species-specific responses of calcifying algae to changing seawater carbonate chemistry. Geochem. Geophys. Geosyst. **7:** 1–12, doi:10.1029/2005GC001227

———, G. NEHRKE, I. PROBERT, J. LY, AND P. ZIVERI. 2009. Strain-specific responses of *Emiliania huxleyi* to changing seawater carbonate chemistry. Biogeosciences **6:** 2637–2646, doi:10.5194/bg-6-2637-2009

LEFEBVRE, S. C., G. HARRIS, R. WEBSTER, N. LEONARDOS, R. J. GEIDER, AND C. A. RAINES. 2010. Characterization and expression analysis of the *Lhcf* gene family in *Emiliania huxleyi* (Haptophyta) reveals differential responses to light and CO$_2$. J. Phycol. **46:** 123–134, doi:10.1111/j.1529-8817.2009.00793.x

———, AND OTHERS. 2012. Nitrogen source and P$_{CO_2}$ synergistically affect carbon allocation, growth and morphology of the coccolithophore *Emiliania huxleyi*: potential implications of ocean acidification for the carbon cycle. Glob. Change Biol. **18:** 493–503, doi:10.1111/j.1365-2486.2011.02575.x

MACINTYRE, H. L., T. M. KANA, T. ANNING, AND R. J. GEIDER. 2002. Photoacclimation of photosynthesis irradiance response curves and photosynthetic pigments in microalgae and cyanobacteria. J. Phycol. **38:** 17–38, doi:10.1046/j.1529-8817.2002.00094.x

MACKINDER, L., G. WHEELER, D. SCHROEDER, U. RIEBESELL, AND C. BROWNLEE. 2010. Molecular mechanisms underlying calcification in coccolithophores. Geomicrobiol. J. **27:** 585–595, doi:10.1080/01490451003703014

MEHRBACH, C., C. H. CULBERSON, J. E. HAWLEY, AND R. M. PYTKOWICZ. 1973. Measurement of the apparent dissociation constants of carbonic acid in seawater at atmospheric pressure. Limnol. Oceanogr. **18:** 897–907, doi:10.4319/lo.1973.18.6.0897

PIERROT, D. E., E. LEWIS, AND D. W. R. WALLACE. 2006. MS Excel program developed for CO$_2$ system calculations. Carbon Dioxide Information Analysis Center, Oak Ridge National Laboratory, U.S. Department of Energy, Available from http://cdiac.ornl.gov/ftp/co2sys

RAVEN, J. A., L. A. BALL, J. BEARDALL, M. GIORDANO, AND S. C. MABERLY. 2005. Algae lacking carbon concentrating mechanisms. Can. J. Bot. **83:** 879–890, doi:10.1139/b05-074

RICHIER, S., S. FIORINI, M.-E. KERROS, P. VON DASSOW, AND J.-P. GATTUSO. 2011. Response of the calcifying coccolithophore *Emiliania huxleyi* to low pH/high P$_{CO_2}$: From physiology to molecular level. Mar. Biol. **158:** 551–560, doi:10.1007/s00227-010-1580-8

RIDGWELL, A. J., I. ZONDERVAN, J. C. HARGREAVES, J. BIJMA, AND T. M. LENTON. 2007. Assessing the potential long-term increase of oceanic fossil fuel CO$_2$ uptake due to CO$_2$-calcification feedback. Biogeosciences **4:** 481–492, doi:10.5194/bg-4-481-2007

RIEBESELL, U., I. ZONDERVAN, B. ROST, P. D. TORTELL, E. ZEEBE, AND F. M. M. MOREL. 2000. Reduced calcification in marine plankton in response to increased atmospheric CO$_2$. Nature **407:** 634–637, doi:10.1038/35030078

ROKITTA, S. D., L. J. DE NOOIJER, S. TRIMBORN, C. DE VARGAS, B. ROST, AND U. JOHN. 2011. Transcriptome analyses reveal differential gene expression patterns between life-cycle stages of *Emiliania huxleyi* (Haptophyta) and reflect specialization to different ecological niches. J. Phycol. **47:** 829–838, doi:10.1111/j.1529-8817.2011.01014.x

ROST, B., S. A. KRANZ, K.-U. RICHTER, AND P. D. TORTELL. 2007. Isotope disequilibrium and mass spectrometric studies of inorganic carbon acquisition by phytoplankton. Limnol. Oceanogr.: Methods **5:** 328–337, doi:10.4319/lom.2007.5.328

———, U. RIEBESELL, S. BURKHARDT, AND D. SÜLTEMEYER. 2003. Carbon acquisition of bloom-forming marine phytoplankton. Limnol. Oceanogr. **48:** 55–67, doi:10.4319/lo.2003.48.1.0055

———, AND U. RIEBESELL. 2004. Coccolithophores and the biological pump: Responses to environmental changes, p. 76–99. *In* H. R. Thierstein and E. B. Young [eds.], Coccolithophores—from molecular processes to global impact. Springer.

———, ———, AND D. SÜLTEMEYER. 2006. Carbon acquisition of marine phytoplankton: Effect of photoperiod length. Limnol. Oceanogr. **51:** 12–20, doi:10.4319/lo.2006.51.1.0012

SHI, D., Y. XU, B. M. HOPKINSON, AND F. M. M. MOREL. 2010. Effect of ocean acidification on iron availability to marine phytoplankton. Science **327:** 676–679, doi:10.1126/science.1183517

SMITH, E. L. 1936. Photosynthesis in relation to light and carbon dioxide. PNAS **22:** 504–511, doi:10.1073/pnas.22.8.504

STOLL, M. H. C., K. BAKKER, G. H. NOBBE, AND R. R. HAESE. 2001. Continuous-flow analysis of dissolved inorganic carbon content in seawater. Anal. Chem. **73:** 4111–4116, doi:10.1021/ac010303r

SUFFRIAN, K., K. G. SCHULZ, M. A. GUTOWSKA, U. RIEBESELL, AND M. BLEICH. 2011. Cellular pH measurements in *Emiliania huxleyi* reveal pronounced membrane proton permeability. New Phytol. **190:** 595–608, doi:10.1111/j.1469-8137.2010.03633.x

SÜLTEMEYER, D., B. KLUGHAMMER, M. R. BADGER, AND G. D. PRICE. 1998. Fast induction of high-affinity HCO$_3^-$ transport in cyanobacteria. Plant Physiol. **116:** 183–192, doi:10.1104/pp.116.1.183

TAYLOR, A. R., A. CHRACHI, G. WHEELER, H. GODDARD, AND C. BROWNLEE. 2011. A voltage-gated H$^+$ channel underlying pH homeostasis in calcifying coccolithophores. PLoS Biol. **9:** e1001085, 1–14, doi:10.1371/journal.pbio.1001085

TRIMBORN, S., G. LANGER, AND B. ROST. 2007. Effect of varying calcium concentrations and light intensities on calcification and photosynthesis in *Emiliania huxleyi*. Limnol. Oceanogr. **52:** 2285–2293, doi:10.4319/lo.2007.52.5.2285

———, N. LUNDHOLM, S. A. THOMS, K.-U. RICHTER, B. KROCK, P. J. HANSEN, AND B. ROST. 2008. Inorganic carbon acquisition in potentially toxic and non-toxic diatoms: The effect of pH-induced changes in seawater carbonate chemistry. Physiol. Plant. **133:** 92–105, doi:10.1111/j.1399-3054.2007.01038.x

TYRRELL, T., AND A. MERICO. 2004. *Emiliania huxleyi*: Bloom observations and the conditions that induce them, p. 75–97. *In*: H. R. Thierstein and J. R. Young [eds.], Coccolithophores: From molecular processes to global impact. Springer.

VON DASSOW, P., H. OGATA, I. PROBERT, P. WINCKER, C. DA SILVA, S. AUDIC, J.-M. CLAVERIE, AND C. DE VARGAS. 2009. Transcriptome analysis of functional differentiation between haploid and diploid cells of *Emiliania huxleyi*, a globally significant photosynthetic calcifying cell. Genome Biol. **10:** R114, doi:10.1186/gb-2009-10-10-r114

WEISS, R. F. 1970. The solubility of nitrogen, oxygen and argon in water and seawater. Deep-Sea Res. **17:** 721–735, doi:10.1016/0011-7471(70)90037-9

ZONDERVAN, I., B. ROST, AND U. RIEBESELL. 2002. Effect of CO_2 concentration on the PIC:POC ratio in the coccolithophore *Emiliania huxleyi* grown under light-limiting conditions and different daylengths. JEMBE **272:** 55–70, doi:10.1016/S0022-0981(02)00037-0

———, R. E. ZEEBE, B. ROST, AND U. RIEBESELL. 2001. Decreasing marine biogenic calcification: A negative feedback on rising atmospheric P_{CO_2}. Glob. Biogeochem. Cycles **15:** 507–516.

Publication III: Ocean Acidification affects carbon allocation and ion-homeostasis at the transcriptomic level in the life-cycle stages of *Emiliania huxleyi*

PLOS | ONE

Ocean Acidification Affects Redox-Balance and Ion-Homeostasis in the Life-Cycle Stages of *Emiliania huxleyi*

Sebastian D. Rokitta*, Uwe John, Björn Rost

Alfred Wegener Institute for Polar and Marine Research, Bremerhaven, Germany

Abstract

Ocean Acidification (OA) has been shown to affect photosynthesis and calcification in the coccolithophore *Emiliania huxleyi*, a cosmopolitan calcifier that significantly contributes to the regulation of the biological carbon pumps. Its non-calcifying, haploid life-cycle stage was found to be relatively unaffected by OA with respect to biomass production. Deeper insights into physiological key processes and their dependence on environmental factors are lacking, but are required to understand and possibly estimate the dynamics of carbon cycling in present and future oceans. Therefore, calcifying diploid and non-calcifying haploid cells were acclimated to present and future CO_2 partial pressures (pCO_2; 38.5 Pa vs. 101.3 Pa CO_2) under low and high light (50 vs. 300 µmol photons m^{-2} s^{-1}). Comparative microarray-based transcriptome profiling was used to screen for the underlying cellular processes and allowed to follow up interpretations derived from physiological data. In the diplont, the observed increases in biomass production under OA are likely caused by stimulated production of glycoconjugates and lipids. The observed lowered calcification under OA can be attributed to impaired signal-transduction and ion-transport. The haplont utilizes distinct genes and metabolic pathways, reflecting the stage-specific usage of certain portions of the genome. With respect to functionality and energy-dependence, however, the transcriptomic OA-responses resemble those of the diplont. In both life-cycle stages, OA affects the cellular redox-state as a master regulator and thereby causes a metabolic shift from oxidative towards reductive pathways, which involves a reconstellation of carbon flux networks within and across compartments. Whereas signal transduction and ion-homeostasis appear equally OA-sensitive under both light intensities, the effects on carbon metabolism and light physiology are clearly modulated by light availability. These interactive effects can be attributed to the influence of OA and light on the redox equilibria of NAD and NADP, which function as major sensors for energization and stress. This generic mode of action of OA may therefore provoke similar cell-physiological responses in other protists.

Introduction

The dissolution of carbon dioxide (CO_2) in the oceans and the resulting formation of carbonic acid are causing a chemical shift towards higher [CO_2] and acidity ([H$^+$]), a phenomenon known as ocean acidification (OA) [1]. OA has been demonstrated to affect metabolic processes and especially calcification in numerous marine organisms [2], including coccolithophores. Like other phytoplankton, these bloom-forming unicellular algae sustain vertical gradients of dissolved inorganic carbon (DIC) by the formation of particulate organic carbon (POC, i.e., biomass) and its subsequent depth-export (organic carbon pump) [3]. Additionally, calcification and the export of particulate inorganic carbon (PIC, i.e., CaCO$_3$) maintain vertical gradients of alkalinity in the oceans (inorganic carbon pump) [3]. The CaCO$_3$ mineral furthermore ballasts organic matter aggregates and enhances their export [4,5], thereby influencing the oceans capacity to sequester carbon [6–8]. Insights into the cell-biology of biomass production and calcification and their dependence on environmental factors are required to understand and possibly estimate the dynamics of carbon cycling in present and future oceans.

For more than a decade, *Emiliania huxleyi*, the most abundant coccolithophore, has been intensively investigated towards its susceptibility to OA [9,10] and the functioning of its carbon concentrating mechanism (CCM) [11–13]. In experiments, cells were usually acclimated to a range of different OA-scenarios with controlled carbonate chemistry before assessing elemental composition and physiological parameters. Although partly contradictive results were obtained between species and strains [14], most *E. huxleyi* datasets showed an overarching pattern of increased or unaltered production of POC accompanied by a reduced or unaltered PIC production, typically reflected by a decreased PIC:POC ratio [9,15,16]. Bach et al. [17] observed that PIC and POC production possess different [CO_2] optima, the lower boundary being defined by limitation of inorganic carbon (C_i) whereas the upper boundary is restricted by detrimental [H$^+$]. This adds support to the idea that both processes operate largely independent and consequently are in competition for energy and C_i in the cell.

In recent studies, so-called matrix approaches were used, in which the effects of OA were investigated in combination with other, independently varied parameters like light, temperature, or

nutrients [18–21]. These studies revealed that the effects of OA on different physiological parameters vary significantly, depending on the constellation of framing environmental parameters, which directly or indirectly relate to cellular energy state (Fig. 3 in [16]). Also, the often neglected haploid life-cycle stage has attracted interest as it appears to play an intriguing role in this species ecology. For instance, haplonts are resistant to attacks of stage-specific viruses that diminish blooms of diploid individuals, so that meiosis is believed to be an ecological escape strategy [22]. Besides this, the haplo-diplontic life-cycle provides a unique model system in which calcification can be studied in two functionally different stages that share the same genetic material. To characterize the energy dependence of OA-effects in the haploid and diploid life-cycle stages of *E. huxleyi* (RCC 1216 and RCC 1217, respectively), cells were acclimated to an experimental matrix of present-day vs. elevated [CO_2] (38.5 Pa vs. 101.3 Pa CO_2, corresponding to ~380 vs. ~1000 µatm and yielding [CO_2] of ~14 vs. ~39 µmol kg^{-1}) under low and high light intensities (50 vs. 300 µmol photons m^{-2} s^{-1}) [16]. This study found that the diploid stage shunted resources from PIC towards POC production under OA, yet keeping the production of total particulate carbon constant. In the haploid stage, major physiological rearrangements, like changes in the photosynthetic apparatus, were evident but resulting elemental composition and production rates were more or less unaffected by OA. Both life-cycle stages appear to pursue distinct strategies to deal with altered carbonate chemistry. As a general pattern, OA-responses were strongly modulated by energy availability and typically most pronounced under low light [16].

In the present study, microarray-based gene expression data are presented that originate from RNA samples from that very experiment. This comparative approach not only enables the investigation of OA-responses and their energy-dependent modulation on a transcriptomic level, but also the advancement of functional interpretations derived from existing physiological data [16]: As OA affected the allocation of carbon and enhanced cellular energy efficiency, the presented analyses focused on genes related to carbon metabolism and light physiology. In addition, since increased acidity under OA affects membrane potentials [23,24], genes related to signal transduction and ion fluxes were examined. Lastly, the responses of the life-cycle stages were compared to elaborate on commonalities and peculiarities of their OA-responses.

Results and Discussion

The responses to OA and their modulation by light intensity were examined in the calcifying and non-calcifying life-cycle stages of *Emiliania huxleyi*. Transcriptomic data was mined for indicative cellular functions. Findings were discussed in the context of previously obtained physiological data to resolve the effects of OA on the sub-cellular interplay between processes that generate energy (photosynthetic light reactions) and those that compete for it (biomass buildup and calcification). In the following, mentioned up- or down-regulation (in response to OA and/or high light) is always related to the respective opposite treatment (i.e., present-day pCO_2$ and/or low light). For scope and clarity, more emphasis was put on the effects of OA rather than on the effects of high light intensity.

The Diploid Stage

In low-light acclimated cultures, OA significantly altered the expression of 2033 genes (1172 up-regulated ($\uparrow$) and 861 down-regulated ($\downarrow$), respectively; Fig. 1A). In the high-light acclimated cultures, 1896 genes were significantly regulated in response to OA (1082 $\uparrow$ and 814 $\downarrow$; Fig. 1B). The intersection of sets A and B yielded the diplont-specific 'core OA-response' with 1350 significantly CO_2-regulated genes (725 $\uparrow$ and 625 $\downarrow$; Fig. 1C). The visual inspection of this subset revealed 158 genes (115 $\uparrow$ and 43 $\downarrow$) that could be assigned to the predefined categories 'carbon metabolism', 'light physiology', 'signaling' and 'ion fluxes' (Fig. 2A; Table S1C).

General OA-responses. Expression of genes of the primary carbon metabolism was prominently stimulated under OA (Fig. 2A; Table S1C), including trehalose-6-phosphate synthase/phosphatase (GJ27270) and genes relevant in glycolysis (GL), e.g., glucose-6-phosphate isomerase (GJ06821), phosphoglyceratkinase (GJ28540) and phosphoglycerate mutase (GJ25367). Also, expression of genes of the pentose phosphate pathway (PPP) was stimulated by OA, e.g., glucose-6-phosphate dehydrogenase (GJ12738), 6-phosphogluconolactonase (GJ20503) or ribulose-5-phosphate epimerase (GJ03996). The induction of trehalosephosphate synthase/phosphatase points towards a decreased activity of glycolysis (GL), as this enzyme is considered an important pacemaker of cytoplasmic carbohydrate breakdown [25]. Furthermore, the up-regulation of several other regulatory enzymes involved in GL ([26], [27]) and the PPP ([28], [29]) under OA suggests altered fluxes of carbon through the metabolism: GL and PPP are the main pathways competing for cytoplasmic glucose-6-phosphate. GL and subsequent oxidative reactions of the mitochondrial tricarboxylic acid cycle generate NADH mostly destined for respiration. The PPP, in contrast, can operate within several flux modes to satisfy different demands, especially for NADPH required in anabolic, reductive processes like storage-compound synthesis [30]. Under OA, cells obviously increase the relative activity of the PPP and thereby redirect the metabolic carbon fluxes.

Numerous genes involved in the turnover of polysaccharides were up-regulated in response to OA, e.g., callose synthase (GJ16141) and glucan beta-1-3 glucosidase (GJ14154). Genes related to intra- and extracellular glycosylation, e.g., N-acetylglucosamine transferase (GJ14803) or N-acetylneuraminate transferase (GJ03189) were found to be differentially expressed. Lipid-synthesizing machinery was induced under OA, e.g., 3-oxoacyl-(ACP) synthases (GJ00191, GJ09435). Production of carbohydrates, especially chrysolaminaran-like β-1,3-glucans (Table S1C), provides a means of storing excess energy and carbon in situations of high photosynthate production, e.g., high light [31] and also under OA [32]. Especially the induction of lipid synthesis together with the observed up-regulation of the PPP advocates increased accumulation of storage compounds under OA, which is in line with the observed increased POC quotas [16].

Regarding light reactions, a prominent up-regulation of fucoxanthin-chlorophyll a/c binding proteins (FCPs), i.e., light harvesting antennae (GJ16045, GJ03834, GJ04497, GJ06058) and genes related to carotenoid biosynthesis, e.g., phytoene desaturases (GJ07905, GJ10400) was observed (Fig. 2A, Table S1C). This indicates higher turnover of light-harvesting antennae and intensified xanthophyll cycling. The latter serves to dissipate excess light energy and reductive pressure [33], which is in line with the observation that *E. huxleyi* downscales light harvesting under OA [16;34]. The absence of this regulation pattern from the light-response (i.e., Fig. 1J) indicates a clear causal relationship between the observed phenomena and OA. In line with this, intensified energy dissipation under OA was also observed in natural, diatom-dominated communities [35]. Enhanced dissipation of light energy under OA seems counterintuitive because an increased production of POC [16] as well as increased expression of lipid synthesizing
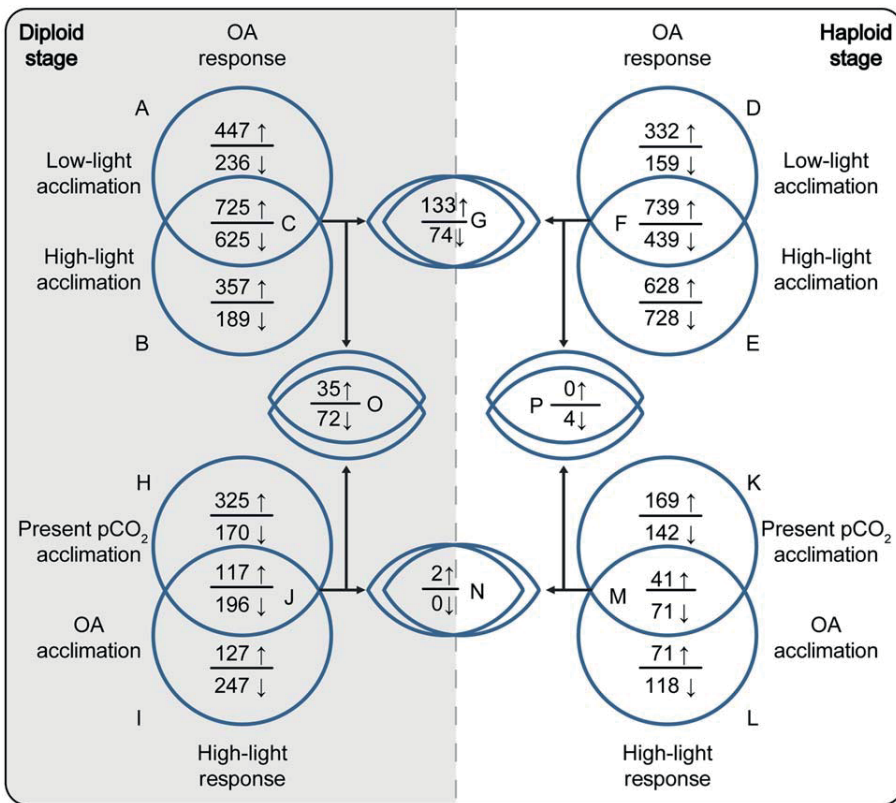
Figure 1. Sets and subsets of differential gene expression in *Emiliania huxleyi* in response to Ocean Acidification and high light intensity. Responses to Ocean Acidification (upper part) and high light intensity (lower part) are shown for the diploid (left part, shaded) and the haploid (right part) life-cycle stage. Numbers represent significantly regulated genes; arrows indicate up- or down-regulation (↑ or ↓).
doi:10.1371/journal.pone.0052212.g001

machinery (Table S1C) was observed, processes that should counteract the accumulation of NADPH. The down-regulation of light harvesting can, however, be explained by a decreased cellular demand for NADPH due to up-regulation of the also NADPH-generating PPP. These results show that OA causes a reconstellation of metabolic flux networks (especially GL and PPP) that

consequently affects the redox-equilibria of NAD and NADP. These equilibria are sensors of various environmental parameters, control organelle activity [28,36], and these compounds can be derivatized to function as second messengers in a number of viable cellular processes [37]. Apparently, OA affects this central sensory system and, possibly by increasing the concentrations of carbon
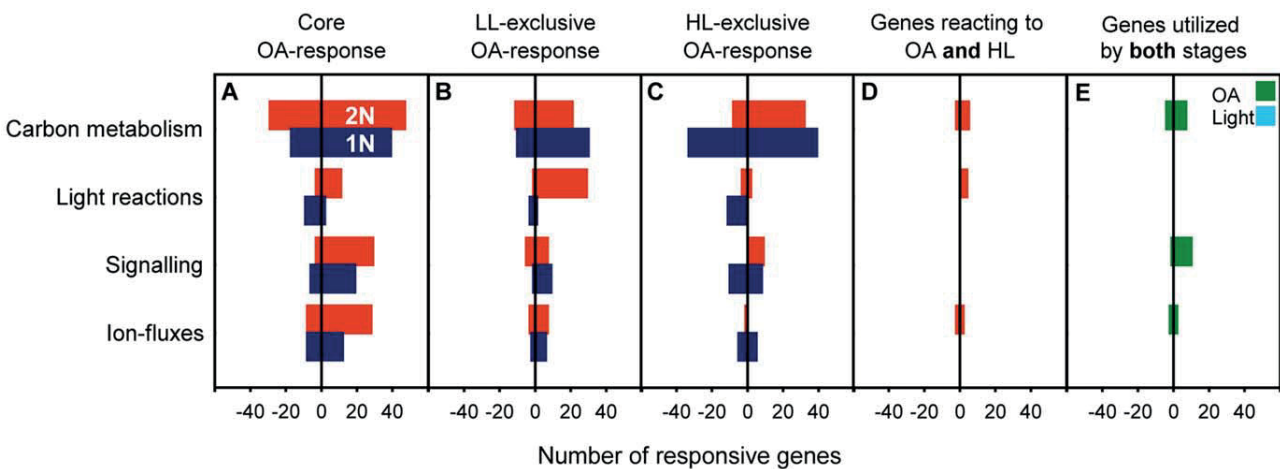
Figure 2. Numbers of responsive genes in the categories 'carbon metabolism', 'light reactions', 'signaling' and 'ion-fluxes'. Sign indicates up- or down-regulation (+ or −); LL and HL denote low-light and high-light specificity of responses.
doi:10.1371/journal.pone.0052212.g002
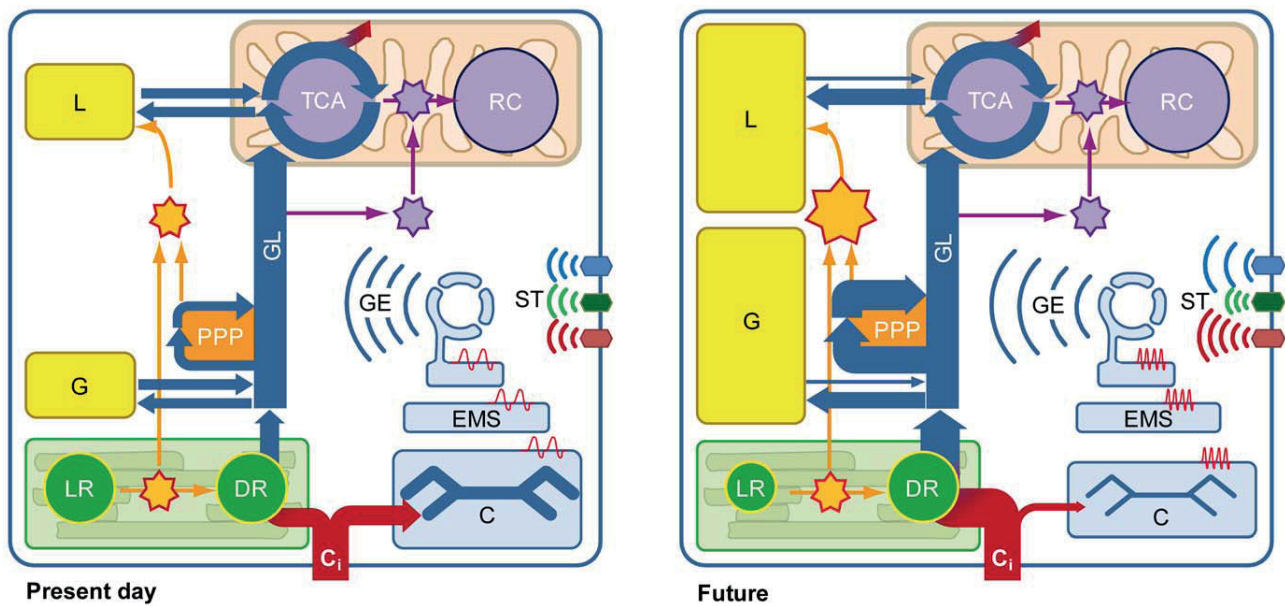
Figure 3. Proposed metabolic constellations of diploid *Emiliania huxleyi*. Under **present-day conditions** ($\sim$38.5 Pa CO_2), calcification (C) in the coccolith vesicle, and photosynthetic dark reaction (DR) occurring in the chloroplast compete for acquired inorganic carbon (C_i, red). DR fixes C_i into organic carbon (blue) that is channeled through glycolysis (GL) towards mitochondrial oxidation in the tricarboxylic acid cycle (TCA). NADH (purple star) produced in GL and TCA is used to drive mitochondrial ATP generation at the respiratory chain (RC). NADPH (orange star) created in the pentose phosphate pathway (PPP) and photosynthetic light reactions (LR) is used to produce reduced storage compounds like glucans (G) and lipids (L). Under **future conditions** ($\sim$101.3 Pa CO_2), gene expression (GE) is altered and calcification is reduced, probably in consequence of altered plasmalemmal signal transduction (ST) and action-potential signaling at the endomembrane system (EMS). Due to diminished calcification under Ocean Acidification, DR produces more organic carbon. In addition to the intense buildup of glucans, the stimulated activity of the PPP under Ocean Acidification provides more NADPH and promotes lipid synthesis. Enhanced cytosolic levels of NADPH, in turn, result in a down-regulation of NADPH production in the LR.
doi:10.1371/journal.pone.0052212.g003

precursors and NADPH, causes cells to shunt relatively more carbon into reduced storage compounds (Fig. 3). This mechanism explains the widely observed increase in POC production under OA [e.g., 9, 16, 38].

Genes related to cellular signaling, e.g., diverse phosphatidylinositolphosphate kinases (PIPKs; GJ04870, GJ03242, GJ22616, GJ02707), sphingosine-1-kinases (GJ24982, GJ10937) and associated downstream signaling kinases, so-called 'CBL-interacting proteins' (GJ14428, GJ00645, GJ01417, GJ01704) were prominently up-regulated (Fig. 2A, Table S1C). Apparently, OA alters signal transduction, affecting diverse actors in plasmalemma-situated signaling cascades that involve second messengers like inositolphosphates and sphingosine. These primarily control Ca^{2+} effluxes from the endoplasmic reticulum [39–41] and have been implicated in the response to ionic/osmotic stress [42] and apoptosis [43]. In line with this, cells were found to regulate the expression of ion transporters (Fig. 2A, Table S1C): OA induced up-regulation of diverse cellular ion exchangers, e.g., a Ca^{2+}/H^+ antiporter (GJ01185), a Ca^{2+}-transporting ATPase (GJ01493), a Na^+/H^+ exchanger (GJ10603) as well as a K^+-dependent Ca^{2+}/Na^+ exchanger (GJ00579). The dataset also showed that distinct HCO_3^- transporters were regulated in response to OA, two being up-regulated (GJ07173 and GJ00654), while one HCO_3^- transporter with an interspersed Ca^{2+}-binding EF-hand motif (GJ14380) was down-regulated. The Ca^{2+}/H^+ exchanger was examined earlier (CAX4; [44]) and was attributed to general ion-homeostasis rather than explicit coccolith production. The HCO_3^- transporters regulated under OA were earlier described as OA-insensitive [45]. In that study, however, the unaffected expression coincided with unaffected production rates of PIC and

POC. In the present experiment, the expression of HCO_3^- transporters as well as PIC:POC ratios were clearly affected by OA [16], which is in line with their hypothetical involvement in calcification. As these HCO_3^- transporters are situated in the plasma membrane as well as the plastid, it is yet not possible to relate all of them exclusively to the process of calcification. The regulation of energy-dependent ion-transporters clearly shows that altered ion fluxes are required under OA to establish sufficient membrane gradients and currents. In addition, a number of channels were regulated under OA that do work passively and react to transient action potentials. This suggests that the ultimately resulting signals are themselves modulated spatially, temporally as well as in amplitude, probably being a major reason for the impaired calcification commonly reported for diploid *E. huxleyi* under OA [9,15,18]. The prominent regulation patterns related to cellular signaling and ion-homeostasis did not occur in response to light intensity (i.e., Fig. 1H, 1I), proving that these effects are exclusively caused by OA. All in all, OA apparently not only affects the signaling networks that facilitate environmental sensing and control cellular ion-gradients but it also affects ion-transport itself (Fig. 3). Fluctuating or offset $[Ca^{2+}]$ or $[H^+]$ as well as possibly extensive glycosylation in the coccolith vesicle seem to be major reasons for the impaired PIC production typically observed in coccolithophores under OA [24,44].

Energy-modulation of OA-responses. To examine particularly the energy-modulation of OA-effects in the diploid stage, the subset C (i.e., the core response) was subtracted from sets A and B (termed 'A\C', 'B\C'). This subtraction yields only those OA-responses that occur exclusively under either low or high light levels (Fig. 1A and 1C, 1B and 1C; Table S1A and S1C, S1B and

S1C). These genes, being comprised only in either subset B or A (i.e., *low-light-specific* and *high-light-specific* OA-responses; Fig. 1), likely represent those cellular functions that underlie the observed light-modulation of OA-responses in the diploid stage [16].

The low-light specific OA-response showed significant regulation of 683 genes (447 ↑ and 236 ↓; Fig. 1A and 1C; Table S1A and S1C). Visual inspection of this group revealed 84 genes (64 ↑ and 20 ↓) that could be assigned to the categories of interest (Fig. 2B): Concerning carbon metabolism, there was up-regulation of cytoplasmic fructose-2,6-bisphosphatase (GJ04837) and plastidic fructose-1,6-bisphosphatase (GJ09341) especially under low-light conditions. Malate dehydrogenase (GJ02937) and cytoplasmic pyrophosphate-dependent fructose-1,6-bisphosphatase (GJ01131) were found down-regulated in response to OA under low light. These enzymes play catalytic and regulatory roles in GL and PPP and also control cellular levels of trioses, hexoses and inorganic phosphate [46,47]. The observed down-regulation of NAD-dependent malate dehydrogenase in response to OA, especially under low light, indicates reduced shuttling of reduction equivalents between cytoplasm and the mitochondrial matrix. This may be attributed to elevated [CO_2] affecting respiratory processes [36,48] and the overall reconstellation of the redox state. Genes related to light reactions, e.g., zeaxanthin epoxidases (GJ05220, GJ09052), violaxanthin de-epoxidase (GJ01361) as well as FCPs (GJ26033, GJ04236, GJ04295, GJ04849, GJ07716, GJ08463) were concertedly up-regulated under OA. This indicates a more intense xanthophyll cycling, i.e., energy-dissipation in response to OA, especially under low-light. No pronounced expression shifts could be recognized for genes related to 'signaling' or 'ion fluxes', besides one distinct HCO_3^- transporter (GJ15963), which was found up-regulated.

In the high-light specific OA-response, significant regulation of 546 genes (357 ↑ and 189 ↓; Fig. 1B and 1C; Table S1B and S1C) was observed. Visual inspection revealed 55 regulated genes (43 ↑ and 12 ↓) that could be assigned to the categories of interest (Fig. 2C). Several genes related to carbon metabolism were affected, namely there was up-regulation of a cytoplasmic fructose-2,6-bisphosphatase (GJ10649) and a number of organellar transporters for primary metabolites, e.g., mitochondrial tricarboxylate/dicarboxylate carriers (GJ03542, GJ20481) and putatively plastidic glucose-6-phosphate/phosphate and phosphoenolpyruvate/phosphate antiporters (GJ09586, GJ16251). These transporters not only connect the primary metabolic pathways of the organelles and the cytosol, but also shuttle reduction equivalents [49,50] and/or Acetyl-CoA, for instance in the context of the mitochondrial citrate-shuttle [51].

These results indicate that, when energy availability is low, cells under OA tightly regulate the allocation of organic carbon and hence organelle activity. Reduced expression of respiration-relevant genes, especially under low light, and the stimulated synthesis of storage compounds caused by OA, can therefore explain the relatively larger stimulation in POC production under these conditions (+84%; [16]). Increased OA-induced xanthophyll-cycling, especially under low light, can be explained by the NADPH surplus originating from increased PPP activity. Again, this surplus is relatively larger under low light, which agrees with the concept of energy-modulated responses (Fig. 3 in [16]). In turn, when energy availability is high, cells enhance fluxes of metabolites and energy between compartments by up-regulating corresponding transporters.

The Haploid Stage

In the low-light acclimated haploid cultures, OA significantly altered the expression of 1669 genes (1071 ↑ and 598 ↓; Fig. 1D;

Table S1D). Under high-light, 2534 genes were significantly regulated in response to OA (1367 ↑ and 1167 ↓; Fig. 1E, Table S1E). The intersection of sets D and E yielded the haplont-specific core OA-response with 1178 significantly regulated genes (739 ↑ and 439 ↓; Fig. 1F; Table S1F). The visual inspection of this subset revealed 112 genes (72 ↑ and 40 ↓) that could be assigned to the categories of interest (Fig. 2A).

General OA-responses. Concerning carbon metabolism, OA caused up-regulation of trehalose-6-phosphate synthase/phosphatase (GJ20366) as well as glycolytic enzymes, e.g., plastidic phosphoglucomutase (GJ12007), enolase (GJ01695) and lactate dehydrogenases (GJ12287, GJ17732). Genes of the PPP were found up-regulated, e.g., glucose-6-phosphate dehydrogenase (GJ04421) and 6-phosphogluconolactonase (GJ09221). Down-regulation was observed for plastidic fructose-1,6-bisphosphatase (GJ09341), plastidic phosphoribulokinase (GJ19188) and for functionally different forms of cytosolic glyceraldehyde-3-phosphate dehydrogenase (NADPH-producing, non-phosphorylating GJ03103; NADH-producing, phosphorylating GJ25044). These expression patterns indicate a redox-related reconstellation of carbon flux networks similar to the diplont. Down-regulation of plastidic phosphoribulokinase, the enzyme synthesizing ribulose-1,5-bisphosphate (substrate of RubisCO), indicates a throttling of photosynthetic dark reactions under OA. The up-regulation of lactate dehydrogenases shows that OA stimulates also fermentative reactions to regenerate cytosolic NAD^+. The NADPH-producing glyceraldehyde-3-phosphate dehydrogenase, which was found down-regulated (Table S1F), circumvents NADH- and ATP-producing steps of GL. The down-regulation shows that OA influences the redox-balance between plastids and the cytosol [52].

The down-regulation of callose synthase (GJ11230) and up-regulation of glucan beta-1,3-glucosidase (GJ14154) under OA indicates lowered buildup and enhanced degradation of chryso-laminaran-like glucans. OA also stimulated genes involved in catabolism of lipid compounds, e.g., the mitochondrial trifunctional enzyme (alpha subunit, GJ17682), a fatty acyl-CoA synthetase (GJ01107), but also a tentative polyketide synthase (GJ01666). In contrast to the diplont, mitochondrial beta-oxidation is induced indicating increased degradation of lipid storage compounds [53] under OA. While OA did not significantly affect cellular POC production on a phenomenological basis [16], which was interpreted as a physiological acclimation to maintain homeostasis, acquired transcriptomic data show that in particular the catabolic processes of carbon metabolism were strongly influenced by OA (Fig. 2A; Table S1F) and thereby counteracted stimulations in cellular POC production.

Regarding light reactions, a concerted down-regulation of genes related to chlorophyll synthesis, e.g., glutamate-1-semialdehyde aminomutase (GJ01010), porphobilinogen deaminase (GJ01909), uroporphyrinogen decarboxylases (GJ02406, GJ02644) and Mg-protoporphyrin O-methyltransferase (GJ14244) was observed in response to OA. Like in the diplont, this may be interpreted as a measure to decrease reductive pressure in photosynthetic light reactions. It is also in line with the lowered Chl *a*:POC ratios, i.e., the increased energy-efficiency observed under OA [16], and the hypothesis that cells need to reduce plastidic NADPH production to counteract the effects of OA-induced PPP activation. These findings show that also the haploid stage experiences a reconstellation of carbon fluxes between GL and PPP and consequently altered pool sizes and redox equilibria of NAD and NADP. The haploid cells, however, apply additional machinery to compensate for the alterations, namely by increasing catabolism of storage compounds, using unconventional fermentative pathways, and by lowering the rate of photosynthetic light and dark reactions. These

seem to be the causes for the stability of POC production in the haplont under OA [16].

Genes involved in plasmalemmal signaling, e.g., PIPKs (GJ04870, GJ03851 and GJ00119), sphingosine-1-kinase (GJ24982) and associated downstream signaling kinases (GJ14428, GJ01704) were prominently up-regulated under OA (Fig. 2A; Table S1F). This indicates that, also in the haploid stage, OA affects environmental sensing and thus the control over cellular Ca^{2+} fluxes. Regarding ion fluxes, OA induced up-regulation of ion exchangers, e.g., a Ca^{2+}/H^+ antiporter VCX1 (GJ04544), a Na^+/H^+ exchanger (GJ13239) and a voltage-dependent Na^+/Ca^{2+} channel VDC1 (GJ18307). The HCO_3^- transporter with the Ca^{2+} binding motif (GJ14380) was found down-regulated in response to OA also in the haplont. Similar to the situation in the diplont, the differential expression of transporters must be triggered by the altered membrane gradients under OA. Following the interpretation that diminished calcification benefits biomass buildup in the diplont [16], it can be argued that the absence of calcification in the haplont, i.e., the absence of a process competing for C_i, does not permit any stimulation of POC production under OA.

Energy-modulation of OA-responses. To examine the energy-modulation of OA-effects in the haplont, subset F was subtracted from subsets D and E, yielding only those OA-responses that occur exclusively under either low or high light levels. These subsets of genes responded to OA in an energy-dependent manner (i.e., *low-light-specific* and *high-light-specific* OA-responses; Fig. 1D and 1F, 1E and 1F; Fig. 2B, 2C), which likely underlies the observed light-dependent modulation of OA responses [16].

The low-light specific OA-response showed significant regulation of 491 genes (332 ↑ and 159 ↓; Fig. 1D and 1F; Table S1D and S1F). Visual inspection revealed 62 genes (46 ↑ and 16 ↓) that could be assigned to the categories of interest (Fig. 2B). Regarding carbon metabolism, three carbonic anhydrases (GJ19123, GJ04992, GJ1572) as well as cytoplasmic glyceraldehyde-3-phosphate dehydrogenase (GJ03426) and a lactate dehydrogenase (GJ11998) were up-regulated under OA when light intensity was low. A putative cytoplasmic fructose-2,6-bisphosphatase (GJ04538) and a plastidic glyceraldehyde-3-phosphate dehydrogenase (GJ26483) were found down-regulated. Such differential expression of key enzymes of the carbon metabolism suggests that haploid cells make use of unconventional pathways to control redox-balance (e.g., lactate fermentation, non-phosphorylating glyceraldehyde-3-phosphate dehydrogenases). Concerning light reactions, signaling and ion fluxes, no indicative regulation patterns could be interpreted in this low-light-specific OA-response.

In high-light acclimated haploid cells, OA caused additional expression of 1356 genes (628 ↑ and 728 ↓; Fig. 1E and 1F; Table S1E and S1F). Visual inspection revealed 111 significantly regulated genes (52 ↑ and 59 ↓) that could be assigned to the categories of interest (Fig. 2C). Regarding carbon metabolism, down-regulation of glycerol-3-phosphate dehydrogenase (GJ02661) was observed, indicating decreased activity of the glycerol-3-phosphate-shuttle system that conveys cytosolic NADH into the mitochondrial respiratory chain. Genes related to carboxylating enzymes were also OA-sensitive especially under high light, namely there was an up-regulation of two isoforms of phosphoenolpyruvate carboxykinase (GJ00405, GJ01561) and down-regulation of pyruvate carboxylase (GJ26507). These anaplerotically carbon-fixing enzymes are thought to primarily provide carbon skeletons for amino acids synthesis in the diploid stage [54]. Indeed, several genes of the amino acid metabolism

were prominently regulated in the high-light-specific OA response (Table S1E and S1F). Interestingly, genes related to fatty acid degradation, e.g., hydroxyacyl-CoA dehydrogenase (GJ00215), long-chain acyl-CoA synthetase (GJ22967) and 3-oxoacyl-CoA thiolase (GJ01189) were up-regulated under OA. In addition, expression of the glyoxylate pathway enzymes malate synthase G (GJ00164) and isocitrate lyase (GJ00349) was significantly increased. This pathway provides the tricarboxylic acid cycle with carbon skeletons derived from fatty acid beta-oxidation, strongly suggesting an increased utilization of lipid compounds in the haploid stage that was indicated previously [55]. Also, two beta-1,3-glucan hydrolases (GJ13343, GJ13856) were found up-regulated, indicating an enhanced OA-induced degradation of chrysolaminaran-like glucans. Regarding light reactions, uroporphyrinogen decarboxylase (GJ03150) and violaxanthin de-epoxidase (GJ02541) were down-regulated. Besides the down-regulation of two vacuolar pyrophosphate-dependent H^+-translocators (GJ03805, GJ18762), OA induced no further pronounced expression shifts in the categories 'signaling' or 'ion fluxes' under high light intensity.

Apparently, when haploid cells experience OA under scarce energy, tighter regulation of carbon fluxes and redox-balance is required. Under saturating light intensities, cells reduce the photosynthetic pressure of reduction equivalents and additionally intensify the breakdown of lipids and carbohydrates.

Stage-specific Utilization of Genetic Inventory

In view of the stage-specific core OA-responses discussed above, it becomes obvious that there are the certain functional responses to OA in both stages (e.g. affection of the PPP, signaling, ion-homeostasis). However, only few functions appear in the subset that contains the *stage-independent* responses: The stage-specific core responses to OA (Fig. 1C, 1F) were overlapped across stages, yielding those genes that react uniformly in both life-cycle stages (Fig. 1G; Table S1G). The stage-independent OA-response included 207 genes (133 ↑ and 74 ↓). Visual inspection revealed a significant regulation of 26 genes (19 ↑ and 7 ↓) that could be sorted into the categories of interest (Fig. 2E). Regarding carbon metabolism, both stages up-regulated a putative glucan beta-1,3-glucosidase (GJ14154) and a generic beta-galactosidase (GJ01691). Up-regulation of the PPP-enzyme 6-phosphoglucono-lactonase (GJ20503) and a 3-oxoacyl-(ACP) synthase involved in fatty acid synthesis (GJ00191) was observed. Regarding light reactions, no common OA-response could be found in the stages. With respect to signal transduction, OA induced up-regulation of a PIPK (GJ04870), a sphingosine-1-kinase (GJ24982), and downstream kinases, i.e., CBL-interacting protein kinases (GJ01704, GJ14428). Concerning ion fluxes, there was common up-regulation of a hyperpolarization-activated, cyclic nucleotide-gated K^+/Na^+ channel (GJ12789) as well as down-regulation of a voltage-gated Ca^{2+} channel (GJ05176). The putative HCO_3^- transporter with the Ca^{2+}-binding EF-hand motif (GJ14380) was found down-regulated in response to OA in both stages.

Apparently, although both stages regulate ~1200–1400 genes in response to OA, there are comparably few common genes used (~200; Fig. 1G, Table S1G). This strongly advocates the presence of a tripartite genome in *E. huxleyi*, of which one general part is constitutively expressed, while two parts are selectively expressed depending on the ploidy stage [56]. This stage-specific utilization of the genome is even more obvious when regarding the common response to high light intensities (Fig. 1N). These ploidy-specific genes products are most likely those that determine the distinct functionalities of the life-cycle stages and enable their evolutionary success in the contemporary oceans.

Treatment-specific Utilization of Genetic Inventory

It could be shown for both stages that the transcriptomic responses to OA (Fig. 1C, 1F) did not resemble the responses to high light intensity (Fig. 1J, 1M), as was previously hypothesized based on pigment contents and physiological data [16]. In fact, only a very limited number of genes was found uniformly regulated in response to both, OA and light (Fig. 1O, 1P; Fig. 2D; Table S1O, S1P), and those did not even reflect the functional responses discussed above. Apparently, OA and high light-intensities invoke regulation of *different* genes, which are, however, involved in the *same* pathways of the carbon metabolism (e.g., GL, PPP, lipid metabolism). Such mechanisms allow for the integration of qualitatively different environmental signals (e.g., $[CO_2]$, light) at the level of biochemical pathways. Thereby, the activity of the same physiological processes can be adjusted in response to multiple environmental variables. Such regulation schemes reflect the decentralized organization of metabolic networks, which is likely responsible for synergistic or compensatory effects of environmental stressors and may explain the similarity in phenomenological effects observed in response to high light and OA [16].

Carbon Concentrating Mechanisms

It was previously concluded that C_i acquisition in the diplont was insensitive to OA because the preferred carbon source ($\sim$80% HCO_3^-) and the high affinities for DIC were unaffected by the treatment [16]. Here, the observed regulation of uptake machinery in the diplont (i.e., 4 HCO_3^- transporters and 1 beta-carbonic anhydrase) shows, however, that an alteration of C_i acquisition indeed occurs, at least on the transcriptomic level. The apparent OA-insensitivity of HCO_3^- usage and uptake affinity observed previously may derive from instantaneous pH effects, as these measurements are performed under stabilized pH conditions that often do not mimic environmental situations. In the haplont, the major carbon source was also not influenced ($\sim$80% HCO_3^-) but uptake affinities were decreased, indicating altered CCM activity under OA [16]. Transcriptomic data show that a plastid-targeted HCO_3^- transporter is down-regulated under OA, together with energy-dependent regulation of four distinct carbonic anhydrases of the beta and delta-type (Table S1). Facing the large number of genes encoding HCO_3^- transporters and CAs (>12 and >7, respectively in CCMP1516; www.jgi.doe.gov) and their unknown cellular localization, it is challenging to derive conclusive statements about stage-specific CCM regulation in *E. huxleyi*. It can be concluded, however, that both stages apply distinct CCMs consisting of *different* modular components that complement the *same* plastidic Ca^{2+}-sensitive HCO_3^- transporter. Such coordinated expression and localization of active and passive CCM components may indeed represent differently cost-intensive modes of C_i acquisition.

Conclusion

In both stages, OA affected expression of genes involved in central carbon metabolism (GL, PPP, lipid and glucan turnover) as well as light physiology (light harvesting, xanthophyll cycling). This leads to altered fluxes of carbon and energy within and across compartments. The combined effects of OA and light on these fluxes originate from their feedback-interaction with the redox equilibria of NAD and NADP, which constitute a primal sensor- and control system in prokaryotic and eukaryotic cells [30]. In other words, OA affects cellular redox-state as a master regulator and thereby causes energy-dependent reconstellations of metabolic flux networks (Fig. 3). Another commonality of both life-cycle stages was the OA-sensitivity of signal-transduction mechanisms

and ion fluxes, processes being major controllers of the cellular Ca^{2+} messenger system. Regulation of these processes may compensate altered signal-processing and offset membrane gradients under OA. Interestingly, no energy-modulation of these OA-responses (Fig. 2B, 2C; Table S1) could be observed. In line with this, the absence of related genes from the light core-responses of both stages (Fig. 1J, 1M) emphasizes that OA, but not light, affects cellular signaling and ion fluxes. Obviously, these processes are independent of energy supply, most likely because signaling cascades and ion fluxes need to be shielded from fluctuations in light intensity, as easily imposed by mixing and clouding. While the OA-responses of the stages are functionally similar, the haplont utilizes a genetic repertoire distinct from the diplont, which emphasizes the genetic and ecological flexibility of this organism. Still, the functional similarity of OA-responses suggests a general 'mode of action' of OA that may well occur in other protists. Future research should target effects of multiple stressors on the interaction of redox-balance with carbon metabolism as well as the relations between signaling and calcification.

Materials and Methods

Culture Conditions

Diploid and haploid *Emiliania huxleyi* (strains RCC 1216 and 1217, also known as TQ26 2N and 1N) were grown at 15°C in 0.2 µm filtered North Sea seawater (salinity 32), enriched with vitamins and trace-metals (F/2 medium; [57]). Nitrate and phosphate were added in concentrations of 100 and 6.25 µmol L^{-1}, respectively. Cultures were grown under a 16:8 h light:dark cycle with light intensities of 50 and 300 µmol photons $m^{-2}s^{-1}$ (Biolux 965 daylight lamps, OSRAM, Germany), as measured with a datalogger (Li-Cor, Lincoln, USA) using a 4π-sensor (Walz, Effeltrich, Germany). Medium pCO_2 was set by purging with humidified pCO_2-adjusted gas mixtures (38.5 Pa and 101.3 Pa) for at least 16 h prior to inoculation. CO_2-free air (<1 ppm CO_2; Dominick Hunter, Willich, Germany) was mixed with pure CO_2 (Air Liquide Deutschland, Düsseldorf, Germany) by a mass flow controller based system (CGM 2000 MCZ Umwelttechnik, Bad Nauheim, Germany). The pCO_2 was regularly controlled with a non-dispersive infrared analyzer system (LI6252, Li-Cor) calibrated with CO_2-free air and purchased air mixtures of 150 ± 10 and 1000 ± 20 ppm CO_2 (Air Liquide, Düsseldorf, Germany). Prior to the experiment, cells were kept in exponential growth phase under experimental settings (light, pCO_2) for at least two weeks in dilute batch cultures to assure proper acclimation. This was done to assess steady-state effects instead of transient shock responses. After inoculation, the 900 mL cylindrical flasks were continuously purged with the humidified pCO_2-adjusted gas mixtures to avoid cell sedimentation and to minimize DIC depletion (flow-rate $\sim$130$\pm$10 mL min^{-1}).

Carbonate Chemistry

To ensure quasi-constant seawater carbonate chemistry (Table S2), only cultures in which the pH did not deviate more than 0.05 units from a cell-free medium were used for measurements (pH was measured with pH3000 microprocessor pH-meter; WTW, Weilheim, Germany; calibration was performed with NIST certified buffers). DIC was measured colorimetrically according to [58], using a TRAACS CS800 autoanalyzer (Seal Analytical, Norderstedt, Germany). Total alkalinity was calculated from linear Gran-titration plots [59], which were produced using an automated burette system (TitroLine alpha plus, Schott, Mainz, Germany). Calculations of carbonate chemistry were performed

using CO_2SYS [60] and were based on measurements of pH (NBS scale), total alkalinity, temperature and salinity. For the calculations, phosphate concentrations of 4 μmol L^{-1} were assumed. The carbonic acid dissociation constants obtained by Mehrbach et al. ([61] refit by [62]) and those of sulfuric acid obtained by Dickson [63] were used.

RNA Sampling

Acclimated cells were harvested between 4 and 8 h after the beginning of the light period at densities of 50.000–90.000 cells ml^{-1}, as assessed with a Multisizer III hemocytometer (Beckman-Coulter, Fullerton, USA). For sampling, ~1.5*10^7 cells were concentrated by filtration (1.2 μm polycarbonate filters, Millipore, Billerica, USA) and pelleted by 5 minute centrifugation at 5000 g in a table centrifuge (Hettich, Bäch, Switzerland). Cell disruption was performed with a beadmill (Qiagen, Hilden, Germany) after adding 100 μL glassbeads (0.1 mm). Lysate was homogenized using QIAshredder spin-columns (Qiagen). RNA extraction was performed using a silica-column based guanidinium thiocyanate method (RNeasy mini, Qiagen). To digest DNA in the isolate, 7 Kunitz units of bovine DNase I (Qiagen) were applied to the silica matrix for 20 minutes at room temperature. After elution, MicroCon YM 30 ultrafiltration columns (Millipore) were used to further enrich RNA. Concentration and purity of the RNA were measured photometrically with a Nanodrop ND1000 (PeqLab, Erlangen, Germany) and integrity of the isolate was verified using a Bioanalyzer 2100 (Agilent, Waldbronn, Germany) running an RNA 6000 Nano LabChip (Agilent).

Microarray Hybridizations

Microarrays were used as part of a standardized in-house working-pipeline. This assures reproducible sample processing and robust data analysis, not only between methods (e.g., in comparison with qRT-PCR; [55]) but also between experiments, which is not given with RNA-Sequencing approaches [64]. RNA Spike-In Mix (Agilent, p/n 5188–5279) was added to the RNA samples prior to the labeling reactions as an internal standard and benchmark for hybridization performance (Agilent RNA Spike-In Kit protocol). 200 ng total RNA from samples was reversely transcribed, and resulting cDNA was amplified as labeled cRNA (Two-color low RNA Input fluorescent linear amplification kit, Agilent, p/n 5184–3523). Incorporation of Cy-3 and Cy-5 labeled cytidine 5′-triphosphate (Perkin Elmer, Waltham, USA) into the cRNA and the control (pooled RNA from various treatments) was verified photometrically using the NanoDrop ND1000 (PeqLab). Labeling efficiencies were calculated as pmol dye (ng cRNA)$^{-1}$ from the results of photometry and were in the range of 0.013 - 0.018 pmol dye (ng cRNA)$^{-1}$. Microarray hybridizations were carried out in SureHyb hybridization chambers (Agilent, p/n G2534A). Every biological replicate was hybridized against a pooled, common control baseline to minimize hybridization biases. Treatment-vs.-treatment expression ratios were then calculated from the single treatment-vs.-control expression ratios. 750 ng of each Cy-3 and Cy-5 labeled cRNA was hybridized to 2×105K *Emiliania huxleyi* custom-built microarrays (Agilent). Three microarray probes were designed for each of 28670 transcript clusters (i.e. on-chip technical replication). The transcript clusters included sequences obtained by Sanger sequencing (Von Dassow et al. 2009) as well as ESTs compiled from the *E. huxleyi* CCMP1516 genome-project, conducted by the Joint Genome Institute (JGI; www.jgi.doe.gov). Probe design was done using Agilent's eArray online platform. Following the Two-Color Microarray-based Gene Expression Analysis protocol (Agilent, p/n 5188–5242), hybridization was performed in a hybridization

oven at 65°C for 17 hours at an agitation of 6 rpm. After hybridization, microarrays were disassembled in Wash Buffer 1 (Agilent, p/n 5188–5325), washed with Wash Buffer 1, Wash Buffer 2 (Agilent, p/n 5188–5326), acetonitrile (VWR, Darmstadt, Germany) and 'Stabilization and Drying Solution' (Agilent, p/n 5185–5979) according to manufacturer's instructions. Stabilization and Drying Solution, an ozone scavenger, protects the Cy-dye signal from degradation. Arrays were immediately scanned with a G2505C microarray scanner (Agilent) using standard photomultiplier tube settings and 5 μm scan resolution.

Data Generation

Raw data was extracted with Feature Extraction Software version 9.0 (Agilent), incorporating the GE2_105_Dec08 protocol. Array quality was monitored using the QC Tool v1.0 (Agilent) with the metric set GE2_QCMT_Feb07. Analysis was performed using GeneSpring 11 (Agilent). LOWESS-normalized data were submitted to the MIAMExpress database hosted by the European Bioinformatics Institute (EBI; www.ebi.ac.uk/arrayexpress; accession code E-MEXP-3624). Hybridization results of biological triplicates (i.e., treatment-vs.-treatment expression ratios) were evaluated in multiple comparison tests using ANOVA. Regulation was called significant when probe-specific p-values were $\leq$0.05. The dataset was then reduced to only those genes in which expression changed $\geq$1.5 fold in response to the treatment. When a divergent regulation was reported, i.e., one or more probes for the same transcript cluster indicating regulation in opposite directions, the respective probe set was as a whole excluded from further analyses ($<$12 probe sets per hybridization). In case that only one out of three probes reported significant differential expression but two probes reported unaltered expression, the respective probe sets were as well excluded from further analyses (300–700 probe sets per hybridization) to increase the confidence level of results. The remaining probe sets were merged and reported as one significantly regulated transcript cluster. For completeness, the number of hit probes and the averaged fold-change is reported for the transcript clusters (Table S1).

Gene Annotation

Significantly regulated transcripts were assigned to an annotation table. This table was generated by using BLASTn similarity searches, in which the ~28670 transcript clusters were aligned with the 'Emihu1_best_transcripts' database provided by the JGI. After excluding alignments with an e-value $>$10^{-5}, the two best aligning, but different transcript models were implemented into the annotation table. This allowed the assignment of ~21740 investigated transcript clusters to models existing in the JGI *E. huxleyi* gene catalog. Assigned JGI protein IDs were then aligned with 'best gene-model' predictions, based on similarity to eukaryotic orthologous genes (KOG; provided by the JGI). This KOG-database harbors functional information on ~11930 different *E. huxleyi* models in the JGI catalog. Additionally, generic gene information obtained by Blast2GO (B2G) queries of all clusters ([65]; e-value cutoff at $>$10^{-6}) was augmented to the annotation table. The final transcriptome screening involved ~10000 unique *E. huxleyi* gene models with a confidently predicted function.

Dataset Evaluation

Acquired datasets with significantly regulated clusters and their associated annotations were partitioned with Venn diagrams to compare the gene expression patterns occurring in response to the treatments. Subsets were manually inspected towards expression patterns that give information on metabolic pathways or processes

being regulated in response to the applied treatments. To overcome the problematic gap between crude gene expression patterns and enzyme activities [66,67] and to increase confidence in results, all findings were discussed in accordance with phenomenological and physiological observations obtained with independent methodologies [16]. Genes of interest were sorted into the *sensu-latu* categories 'carbon metabolism' (including turnover of hydrocarbons and carbohydrates), 'light reactions' (including pigment turnover), 'signaling', as well as 'inorganic ion transport'. After categorization, integrity and validity of the gene models of interest were reconfirmed by model inspection in the JGI draft genome database and by BLAST searches. In the text, exemplary transcripts are notated with their numerical cluster identifiers. JGI identifiers of the associated protein and complete expression datasets can be taken from supplementary spreadsheet file (Table S1).

Supporting Information

Table S1   Gene expression data on the effects of Ocean Acidifcation in diploid and haploid *Emiliania huxleyi* (RCC 1216/1217) under limiting and saturating light intensities. For completeness, the spreadsheet holds information on the quality of obtained BLAST and Blast2GO alignments.

References

1. Caldeira K, Wickett ME (2003) Anthropogenic carbon and ocean pH - The coming centuries may see more oceanic acidification than the past 300 million years. Nature 425(365): 365.
2. Kroeker KJ, Kordas RL, Crim RN, Singh GG (2010) Meta-analysis reveals negative yet variable effects of ocean acidification on marine organisms. Ecology Letters 13(11): 1419–1434.
3. Volk T, Hoffert MI (1985) Ocean carbon pumps: analysis of relative strengths and efficiencies in ocean-driven atmospheric CO_2 changes. In: Sunquist ET, Broecker WS, editors. The carbon cycle and atmospheric CO_2: natural variation archean to present. Washington, D.C.: American Geophysical Union, Geophysical Monographs. 99–110.
4. Klaas C, Archer DE (2002) Association of sinking organic matter with various types of mineral ballast in the deep sea: Implications for the rain ratio. Global Biogeochem Cycles 16(4): 1116–1130.
5. Lam PJ, Doney SC, Bishop JKB (2011) The dynamic ocean biological pump: Insights from a global compilation of particulate organic carbon, $CaCO_3$, and opal concentration profiles from the mesopelagic. Global Biogeochem Cycles 25: 1–14.
6. Rost B, Riebesell U (2004) Coccolithophores and the biological pump: responses to environmental changes. In: Thierstein HR, Young EB, editors. Coccolithophores–From Molecular Processes to Global Impact: Springer. 76–99.
7. Zondervan I (2007) The effects of light, macronutrients, trace metals and CO_2 on the production of calcium carbonate and organic carbon in coccolithophores - A review. Deep Sea Research Part II: Topical Studies in Oceanography 54(5–7): 521–537.
8. Ridgwell AJ, Zondervan I, Hargreaves JC, Bijma J, Lenton TM (2007) Assessing the potential long-term increase of oceanic fossil fuel CO_2 uptake due to CO_2-calcification feedback. Biogeosciences 4(4): 481–492.
9. Riebesell U, Zondervan I, Rost B, Tortell PD, Zeebe E, et al. (2000) Reduced calcification in marine plankton in response to increased atmospheric CO_2. Nature 407: 634–637.
10. Langer G, Nehrke G, Probert I, Ly J, Ziveri P (2009) Strain-specific responses of *Emiliania huxleyi* to changing seawater carbonate chemistry. Biogeosciences 6(11): 2637–2646.
11. Badger MR, Andrews TJ, Whitney SM, Ludwig M, Yellowlees DC (1998) The diversity and co-evolution of Rubisco, plastids, pyrenoids and chloroplast-based CO_2-concentrating mechanisms in the algae. Can J Bot 76: 1052.
12. Rost B, Riebesell U, Burkhardt S, Sueltemeyer D (2003) Carbon acquisition of bloom-forming marine phytoplankton. Limnol Oceanogr 48: 55.
13. Trimborn S, Langer G, Rost B (2007) Effect of varying calcium concentrations and light intensities on calcification and photosynthesis in Emiliania huxleyi. Limnol Oceanogr 52(5): 2285–2293.
14. Fabry VJ (2008) Marine Calcifiers in a High-CO_2 Ocean. Science 320(5879): 1020–1022.
15. Hoppe CJM, Langer G, Rost B (2011) *Emiliania huxleyi* shows identical responses to elevated pCO_2 in TA and DIC manipulations. JEMBE 406(1): 54–62.
16. Rokitta SD, Rost B (2012) Effects of CO_2 and their modulation by light in the life-cycle stages of the coccolithophore *Emiliania huxleyi*. Limnology and Oceanography 57(2): 607–618.
17. Bach LT, Riebesell U, Schulz KG (2011) Distinguishing between the effects of ocean acidification and ocean carbonation in the coccolithophore *Emiliania huxleyi*. Limnology and Oceanography 56(6): 2040–2050.
18. Feng Y, Warner ME, Zhang Y, Sun J, Fu FX, et al. (2008) Interactive effects of increased pCO_2, temperature and irradiance on the marine coccolithophore *Emiliania huxleyi* (Prymnesiophyceae). Eur J Phycol 43: 78–98.
19. De Bodt C, Van Oostende N, Harlay J, Sabbe K, Chou L (2010) Individual and interacting effects of pCO2 and temperature on *Emiliania huxleyi* calcification: study of the calcite production, the coccolith morphology and the coccosphere size. Biogeosciences 7: 1401–1412.
20. Fiorini S, Middelburg JJ, Gattuso JP (2011) Effects of elevated CO_2 partial pressure and temperature on the coccolithophore *Syracosphaera pulchra*. Aquatic Microbial Ecology 64(3): 221–232.
21. Fiorini S, Middelburg JJ, Gattuso JP (2011) Effects of elevated CO_2 partial pressure and temperature on the coccolithophore *Syracosphaera pulchra*. Aquatic Microbial Ecology 64(3): 221–232.
22. Frada M, Probert I, Allen MJ, Wilson WH, De Vargas C (2008) The "Cheshire Cat" escape strategy of the coccolithophore *Emiliania huxleyi* in response to viral infection. PNAS 105(41): 15944–15949.
23. Suffrian K, Schulz KG, Gutowska MA, Riebesell U, Bleich M (2011) Cellular pH measurements in *Emiliania huxleyi* reveal pronounced membrane proton permeability. New Phytologist 190(3): 595–608.
24. Taylor AR, Chrachri A, Wheeler G, Goddard H, Brownlee C (2011) A Voltage-Gated H^+ Channel Underlying pH Homeostasis in Calcifying Coccolithophores. PLoS Biol 9(6): 14pp.
25. Eastmond PJ, Graham IA (2003) Trehalose metabolism: a regulatory role for trehalose-6-phosphate? Current Opinion in Plant Biology 6(3): 231–235.
26. Cui I, Chai Y, Li J, Liu H, Zhang L, et al. (2010) Identification of a glucose-6-phosphate isomerase involved in adaptation to salt stress of *Dunaliella salina*. Journal of applied Phycology 22(5): 563–568.
27. Hallows WC, Yu W, Denu JM (2011) Regulation of Glycolytic Enzyme Phosphoglycerate Mutase-1 by Sirt1 Protein-mediated Deacetylation. Journal of Biological Chemistry 287(6): 3850–3858.
28. Krüger A, Grüning N-M, Wamelink MMC, Kerick M, Kirpy A, et al. (2011) The pentose phosphate pathway Is a metabolic redox sensor and regulates transcription during the antioxidant response. Antioxidants & Redox Signaling 15(2): 311–324.
29. Xiong Y, DeFraia C, Williams D, Zhang X, Mou Z (2009) Characterization of Arabidopsis 6-Phosphogluconolactonase T-DNA Insertion Mutants Reveals an Essential Role for the Oxidative Section of the Plastidic Pentose Phosphate Pathway in Plant Growth and Development. Plant and Cell Physiology 50(7): 1277–1291.
30. Kruger NJ, von Schaewen A (2003) The oxidative pentose phosphate pathway: structure and organisation. Current Opinion in Plant Biology 6(3): 236–246.
31. Staats N, Stal IJ, De Winder B, Mur LR (2000) Oxygenic photosynthesis as driving process in exopolysaccharide production of benthic diatoms. Marine Ecology Progress Series 193: 261–269.
32. Borchard C, Borges AV, Händel N, Engel A (2011) Biogeochemical response of *Emiliania huxleyi* (PML B92/11) to elevated CO_2 and temperature under

phosphorous limitation: A chemostat study. Journal of Experimental Marine Biology and Ecology 410: 61–71.

33. Goss R, Jakob T (2010) Regulation and function of xanthophyll cycle-dependent photoprotection in algae. Photosynthesis Research 106(1): 103–122.

34. McCarthy A, Rogers SP, Duffy SJ, Campbell DA (2012) Elevated carbon dioxide differentially alters the photophysiology of *Thalassiosira pseudonana* (Bacillariophyceae) and *Emiliania huxleyi* (Haptophyta). Journal of Phycology 48(3): 635–646.

35. Gao K, Xu J, Gao G, Li Y, Hutchins DA, et al. (2012) Rising CO$_2$ and increased light exposure synergistically reduce marine primary productivity. Nature Climate Change 2(7): 519–523.

36. Raghavendra AS, Padmasree K (2003) Beneficial interactions of mitochondrial metabolism with photosynthetic carbon assimilation. Trends in Plant Science 8(11): 546–553.

37. Pollak N, Dölle C, Ziegler M (2007) The power to reduce: pyridine nucleotides - small molecules with a multitude of functions. Biochem J 402(2): 205–218.

38. Shi D, Xu Y, Morel FMM (2009) Effetcs of the pH/pCO$_2$ control method on medium chemistry and phytoplankton growth. Biogeosciences 6: 1199–1207.

39. Berridge MJ, Lipp P, Bootman MD (2000) The versatility and universality of calcium signalling. Nature reviews Molecular cell biology 1(1): 11–21.

40. Hannun YA, Obeid LM (2008) Principles of bioactive lipid signalling: lessons from sphingolipids. Nat Rev Mol Cell Biol 9(2): 139–150.

41. Rosen H, Gonzalez-Cabrera PJ, Sanna MG, Brown S (2009) Sphingosine 1-Phosphate Receptor Signaling. Annual Review of Biochemistry 78(1): 743–768.

42. Amtmann A, Armengaud P (2007) The role of calcium sensor-interacting protein kinases in plant adaptation to potassium-deficiency: new answers to old questions. Cell Res 17(6): 483–485.

43. Vardi A, Van Mooy BAS, Fredricks HF, Popendorf KJ, Ossolinski JE, et al. (2009) Viral Glycosphingolipids Induce Lytic Infection and Cell Death in Marine Phytoplankton. Science 326(5954): 861–865.

44. Mackinder L, Wheeler G, Schroeder D, Von Dassow P, Riebesell U, et al. (2011) Expression of biomineralization-related ion transport genes in *Emiliania huxleyi*. Env Microbiol 16.

45. Richier S, Fiorini S, Kerros M-E, Von Dassow P, Gattuso J-P (2010) Response of the calcifying coccolithophore *Emiliania huxleyi* to low pH/high pCO$_2$: from physiology to molecular level. Mar Biol 158: 551–560.

46. Tamoi M, Hiramatsu Y, Nedachi S, Otori K, Tanabe N, et al. (2011) Increase in the activity of fructose-1,6-bisphosphatase in cytosol affects sugar partitioning and increases the lateral shoots in tobacco plants at elevated CO$_2$ levels. Photosynthesis Research 108(1): 15–23.

47. Fernie AR, Roscher A, Ratcliffe RG, Kruger NJ (2001) Fructose 2,6-bisphosphate activates pyrophosphate:fructose-6-phosphate 1-phosphotransferase and increases triose phosphate to hexose phosphate cycling in heterotrophic cells. Planta 212(2): 250–263.

48. Araújo WL, Nunes-Nesi A, Nikoloski Z, Sweetlove LJ, Fernie AR (2011) Metabolic control and regulation of the tricarboxylic acid cycle in photosynthetic and heterotrophic plant tissues. Plant, Cell & Environment 35(1): 1–21.

49. Weber APM, Linka N (2011) Connecting the Plastid: Transporters of the Plastid Envelope and Their Role in Linking Plastidial with Cytosolic Metabolism. Annual Review of Plant Biology 62(1): 53–77.

50. Eicks M, Maurino V, Knappe S, Flügge U-I, Fischer K (2002) The Plastidic Pentose Phosphate Translocator Represents a Link between the Cytosolic and the Plastidic Pentose Phosphate Pathways in Plants. Plant Physiology 128(2): 512–522.

51. Hanning I, Baumgarten K, Schott K, Heldt HW (1999) Oxaloacetate Transport into Plant Mitochondria. Plant Physiology 119(3): 1025–1032.

52. Bustos DM, Iglesias AA (2002) Non-phosphorylating glyceraldehyde-3-phosphate dehydrogenase is post-translationally phosphorylated in heterotrophic cells of wheat (*Triticum aestivum*). FEBS Letters 530(1–3): 169–173.

53. Graham IA, Eastmond PJ (2002) Pathways of straight and branched chain fatty acid catabolism in higher plants. Progress in Lipid Research 41(2): 156–181.

54. Tsuji Y, Suzuki I, Shiraiwa Y (2012) Enzymological Evidence for the Function of a Plastid-Located Pyruvate Carboxylase in the Haptophyte alga *Emiliania huxleyi*: A Novel Pathway for the Production of C4 Compounds. Plant and Cell Physiology 53(6): 1043–1052.

55. Rokitta SD, De Nooijer LJ, Trimborn S, De Vargas C, Rost B, et al. (2011) Transcriptome analyses reveal differential gene expression patterns between life-cycle stages of *Emiliania huxleyi* (Haptophyta) and reflect specialization to different ecological niches. J Phycol 47: 829–838.

56. Von Dassow P, Ogata H, Probert I, Wincker P, Da Silva C, et al. (2009) Transcriptome analysis of functional differentiation between haploid and diploid cells of *Emiliania huxleyi*, a globally significant photosynthetic calcifying cell. Genome Biol 10(10): R114.

57. Guillard RRL, Ryther JH (1962) Studies of marine planktonic diatoms. Can J Microbiol 8: 229–239.

58. Stoll MHC, Bakker K, Nobbe GH, Haese RR (2001) Continuous-Flow Analysis of Dissolved Inorganic Carbon Content in Seawater. Analytical Chemistry 73(17): 4111–4116.

59. Dickson AG (1981) An Exact Definition of Total Alkalinity and a Procedure for the Estimation of Alkalinity and Total Inorganic Carbon from Titration Data. Deep Sea Research Part I-Oceanographic Research Papers 28(6): 609–623.

60. Pierrot DE, Lewis E, Wallace DWR (2006) MS Excel program developed for CO$_2$ system calculations. Carbon Dioxide Information Analysis Center, Oak Ridge National Laboratory (ORNL). Oak Ridge, Tennessee, USA.

61. Mehrbach C, Culberson CH, Hawley JE, Pytkowicz RM (1973) Measurement of the Apparent Dissociation Constants of Carbonic Acid in Seawater at Atmospheric Pressure. Limnol Oceanogr 18(6): 897–907.

62. Dickson AG, Millero FJ (1987) A comparison of the equilibrium constants for the dissociation of carbonic acid in seawater media. Deep Sea Research Part I-Oceanographic Research Papers 34(10): 1733–1743.

63. Dickson AG (1990) Standard potential of the reaction: AgCl(s)+½ H$_2$(g) = Ag(s)+HCl(aq), and the standard acidity constant of the ion HSO$_4^-$ in synthetic seawater from 273.15 to 318.15 K. Journal of chemical Thermodynamics 22: 113–127.

64. Baginsky S, Hennig L, Zimmermann P, Gruissem W (2010) Gene Expression Analysis, Proteomics, and Network Discovery. Plant Physiology 152(2): 402–410.

65. Conesa A, Götz S, García-Gómez JM, Terol J, Talón M, et al. (2005) Blast2GO: a universal tool for annotation, visualization and analysis in functional genomics research. Bioinformatics 21(18): 3674–3676.

66. Feder ME, Walser JC (2005) The biological limitations of transcriptomics in elucidating stress and stress responses. Journal of Evolutionary Biology 18(4): 901–910.

67. Fernie AR, Stitt M (2012) On the Discordance of Metabolomics with Proteomics and Transcriptomics: Coping with Increasing Complexity in Logic, Chemistry, and Network Interactions Scientific Correspondence. Plant Physiology 158(3): 1139–1145.

DISCUSSION

The publications presented in this thesis have explored the general characteristics of the life-cycle stages of *E. huxleyi*, the stages′ respective sensitivities towards OA as well as the influence of energy on the manifestation of these responses. Data was acquired on the phenomenological, physiological and transcriptomic level. In this concluding discussion, the major findings from the publications will be elaborated to highlight novel views and perspectives on the life-cycle stages and their responses to OA. Subsequently, emerging response patterns are used to develop concepts of physiological responses that may not only explain the observations in *E. huxleyi*, but may also hold true for the physiological responses of other microbes to environmental perturbations.

Major findings for the diploid life cycle stage

In response to OA, the diploid stage shunted carbon from the production of PIC towards the production of POC, keeping the overall production of TPC constant (Publication II). The unaltered TPC production and the relatively unaffected C_i acquisition suggest that the effects of OA occur mainly inside the cells, i.e., downstream of the C_i acquisition processes. Interestingly, the increased biomass production under OA was achieved with reduced chlorophyll content and lowered rates of cellular *in-situ* O_2 evolution, strongly suggesting improved energy efficiency in biomass production. This may derive, for example, from decreased costs of C_i acquisition under elevated $[CO_2]$ or lowered energy demands caused by diminished calcification. The observed OA-responses were strongly light-modulated, the stimulation and reduction of POC and PIC production typically being most pronounced under low light-intensity. Apparently, when energy availability is high, PIC production can be maintained, so that neither C_i nor energy is re-allocated to benefit POC production (Publication II).

Subsequent transcriptome profilings could link these observations to biochemical functions (Publication III). OA affected signal-transduction mechanisms and ion homeostasis, which is most likely the cause for impaired PIC production. OA significantly altered carbon metabolism, most strikingly by increasing the intensity of the pentose phosphate pathway (PPP) relative to glycolysis (GL; Figure 10). This metabolic shift is likely to increase levels of reduced nicotinamide-adenine-dinucleotide-phosphate (NADPH) relative to nicotinamide-adenine-dinucleotide (NADH). Whereas the latter drives mitochondrial energy generation, the former is the primary electron donor in anabolic pathways. The thereby increased synthesis of sugars, lipids, or carotenoids likely causes the stimulation of biomass production under OA (Publication II). Increased cellular levels of NADPH under OA are likely also the reason for the downscaling of photosynthetic NADPH generation and the thus improved energy efficiency.

The energy modulation of OA-responses derives from the fact that both, OA and light affect the cellular redox sensing systems (Publication III): While OA apparently determines the flux-routes of carbon and energy among the reductive and oxidative pathways, light controls the relative intensity of physiological processes (e.g., POC and PIC production) within the determined flux-routes.
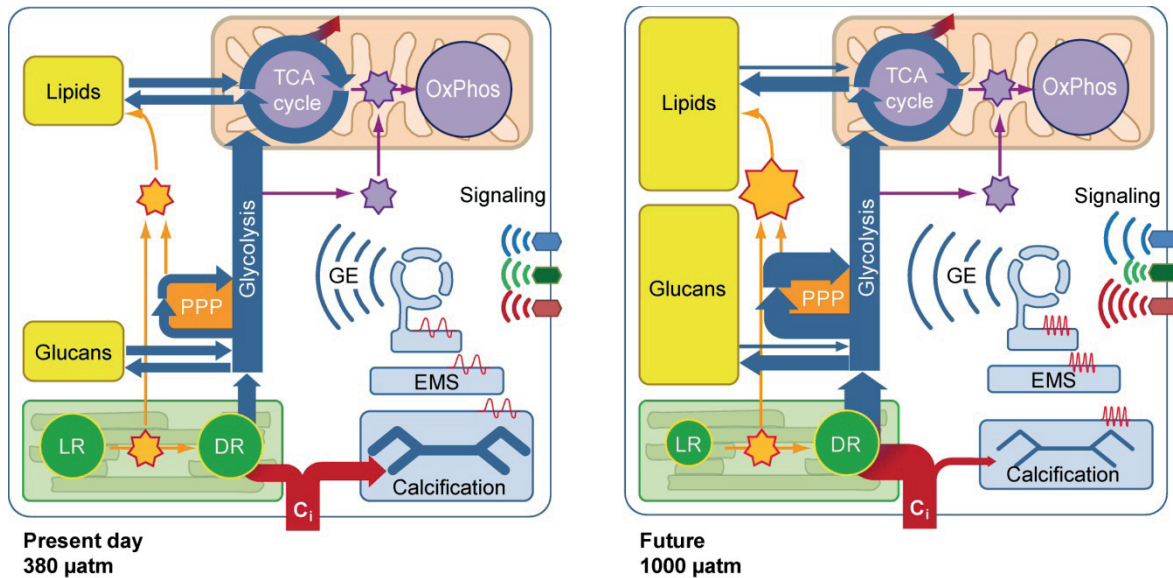
Figure 10: Proposed metabolic constellations in diploid *Emiliania huxleyi*: Under present-day conditions, calcification and photosynthetic dark reaction (DR) compete for inorganic carbon (C_i, red). DR produces organic carbon (C_{org}, blue) that is channeled through glycolysis towards oxidation in the mitochondrial tricarboxylic acid (TCA) cycle. NADH (purple star) produced in glycolysis and the TCA cycle is used to drive ATP generation in the mitochondrial oxidative phosphorylation. NADPH (orange star) produced in the pentose phosphate pathway (PPP) and photosynthetic light reactions (LR) is used to produce reduced storage compounds like glucans and lipids. Under future conditions, gene expression (GE) is altered and calcification is reduced, probably due to altered plasmalemmal signaling and action-potential signaling at the endomembrane system (EMS). Due to diminished calcification under ocean acidification, DR is enhanced. Besides the intense buildup of glucans, the stimulated activity of the PPP under OA provides more NADPH, promoting lipid synthesis. Due to elevated levels of NADPH, respective production of NADPH in the LR is down-regulated. Figure from publication III.

Major findings for the haploid life cycle stage

The haplont was shown to exhibit a pronounced expression of genes related to basic C and N metabolism, underlining that growth and biomass buildup are the dominating processes in haploid cells (Publication I). The expression of isocitrate lyase, a key indicator for mitochondrial lipid respiration, is significantly stronger than in the diploid stage. This suggests that mitochondrial energy generation plays an important role in the haplont, not only in energy balance but probably also as a carbon sink. The weak indication of pre-transcriptional regulation and the prominent up-regulation of protein

turnover (relative to the diplont) suggest that the haploid stage uses a radically different strategy of gene expression: The smaller genome likely requires less regulatory efforts and allows a more unrestricted gene expression. In contrast to the diplont, the proteome is then regulated in a 'top-down' manner, i.e., by ubiquitin-mediated protein breakdown (Publication I).

In response to OA, production rates of biomass as well as the cellular *in-situ* photosynthesis rates of the haplont were not significantly affected (Publication II). The apparent homeostasis must, however, be the result of regulatory efforts, as several physiological rearrangements were evident. For example, chlorophyll contents decreased under OA, indicating improved energy efficiency also in the haplont. Like in the diploid stage, responses were light modulated and typically most pronounced under low light-intensity. Transcriptome analyses have shown that under OA, the primary carbon metabolism is rearranged also in the haplont (Publication III). The PPP is amplified relative to GL and elevated levels of NADPH likely stimulate the synthesis of lipids and carotenoids. To achieve homeostasis under OA, the haplont up-regulates catabolic pathways, such as lipid catabolism (glyoxylate cycle), which have been shown to play a prominent role in this stage (Publication I). The haplont decreases photosynthetic energy generation by up-regulating xanthophyll-cycling (as seen similarly in the diplont) , by down-regulating chlorophyll synthesis as well as regeneration of ribulose-1,5-bisphosphate (a substrate of RubisCO).

Transcriptomics strongly support the view that a tripartite genome exists in *E. huxleyi* (Publication III; Von Dassow et al. 2009). This does not only harbor genes that are generic and constitutively expressed, but also genes that are selectively expressed in either the haploid or the diploid stage. The very different gene expression patterns (Publication I) and morphologies as well as responses to OA (Publication II) certainly originate from this differential utilization of genetic equipment (Publication III). The life-cycle stages use *distinct, but functionally equivalent* enzymes (e.g., stage-specific forms of glucose-6-phosphate dehydrogenases). Moreover, they use *functionally different* machinery (e.g., adenosinetriphosphate (ATP)-driven vs. pyrophosphate-driven H^+ pumps). It becomes clear that the tripartite architecture of the genome and its ploidy-dependent utilization constitute different cellular 'operating systems'. It is these operating systems that provide the cell types with distinct physiological properties and thereby 'streamline' them to thrive in contrasting environments and to occupy different ecological niches.

Emerging response patterns and unifying physiological concepts

On the phenomenological level, OA stimulated POC production and reduced PIC production in the diplont, a pattern that has been observed frequently in this (Langer et al. 2009) and other strains of *E. huxleyi* (Figure 11; Zondervan et al. 2001;

Hoppe et al. 2011). This finding contributes to the accumulating evidence that most strains of *E. huxleyi* react to OA with an unaffected or stimulated POC production and an unaffected or decreased PIC production, typically reflected by a decreased PIC:POC ratio. Interestingly, the gain in POC production often matches the decrease in PIC production (Zondervan et al 2001; Langer et al. 2009; publication II). As both processes are competing for the same substrates (energy and C_i), it can be hypothesized that biomass production and calcification are in principle antagonistic processes.

Study	Strain	Growth	P_{PIC}	P_{POC}	PIC:POC
Feng et al. 2008	CCMP371[c]				
Iglesias-Rodriguez et al. 2008	NZEH[R]				
Hoppe et al. 2011	RCC1256[A,C]				
	NZEH[R]				
Langer et al. 2009	RCC1212[B,O]				
	RCC1216[R,O]				
	RCC1238[A,C]				
	RCC1256[A,C]				
Lefebvre et al. 2012	CCMP371[A,C]				
Richier et al. 2011	RCC1216[R,O]				
Riebesell et al. 2000	PLYB92/11[A,C]				
Rokitta and Rost 2012 (Low light)	RCC1216[R,O]				
Rokitta and Rost 2012 (High light)	RCC1216[R,O]				
Sciandra et al. 2003	TW1				
Shi et al. 2009	NZEH[R]				
Sum		12 - 3 -	3 2 10 -	6 6 1 2	6 - 9 -

Figure 11: OA-responses in *Emiliania huxleyi* in growth and the production of POC and PIC (P_{POC}, P_{PIC}) as well as PIC:POC ratios. Modified after Hoppe et al. 2011.

Apparently, OA alters the relative competitivity of these processes for C_i and energy. In some strains of *E. huxleyi*, however, deviating patterns were observed (e.g., Langer et al. 2009, strain RCC1256). These non-conform OA-response patterns indicate that PIC and POC production exhibit different, strain-specific optima in $[CO_2]$ and/or $[H^+]$ (Bach et al. 2012). Nonetheless, most data sets from *E. huxleyi* strains (Zondervan et al. 2001; Sciandra et al. 2003; Feng et al. 2008; Lefebvre et al. 2012; Hoppe et al. 2011, publication II) have in fact shown opposing trends in PIC and POC production under OA, resulting in generally decreased PIC:POC ratios. Considering biogeochemistry, reduced calcification of *E. huxleyi* and possibly other coccolithophores is likely to be expected. Furthermore, OA was shown to cause floristic shifts in coccolithophore assemblages

from heavily towards lightly calcified morphotypes (Beaufort et al. 2011), i.e., it imposes selective pressure upon the degree of calcification (i.e., PIC per cell) that is largely determined on the level of cell physiology.

A second overarching pattern that emerges from the presented data is that cell-physiological responses to one varying environmental parameter are modulated by the constellation of other environmental parameters, such as energy availability. In both stages, the OA-responses were clearly dependent on light intensity, typically being more pronounced under low light. This can be explained when one regards environmental conditions as energetically beneficial or detrimental for a certain metabolic process that follows a typical Michaelis-Menten kinetic (Figure 12): The overall process rate is primarily determined by light intensity (i.e., cellular energization). Co-occurring changes in any energy-relevant environmental parameter ease or impede the process of interest and consequently alter the amount of energy that is required to drive it. With this abstraction it can be explained why the same treatment causes responses of different magnitudes depending on the light levels.
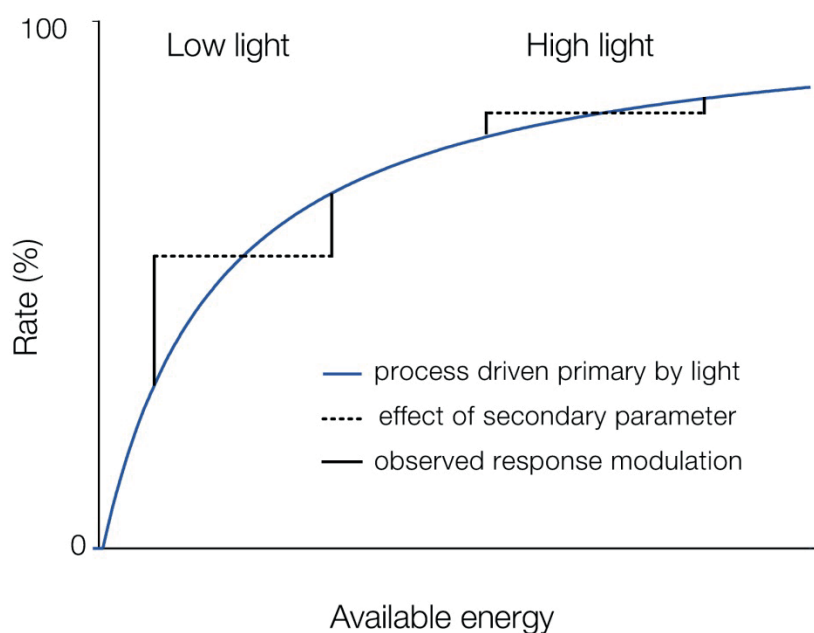
Figure 12: Concept of energy-modulated responses in physiological responses to varying environmental parameters.

Liebig's law of the minimum describes a particular situation, in which a process can *only* be stimulated by an increase in one rate-determining parameter (a resource or a condition), if a second rate-determining parameter (that would otherwise be co-limiting) also increases. Building on that foundation, concepts of co-limitation and co-amplification were formulated more recently (e.g., Saito et al. 2008; Figure 13A) that describe process rates in dependence of more than one parameter and can incorporate versatile mathematical descriptions of response curves. Because in this thesis energy was

used as the modulating parameter in the experimental matrix, the devised concept enables the interpretation of response pattern in the framework of 'substitutable co-limitation' (Saito et al. 2008, Figure 13B). In situations of substitutable co-limitation, effects of one varying parameter can be attenuated if the second parameter allows for energy re-allocation. The concept can therefore not only explain some of the variability in OA responses observed within the *E. huxleyi* morphospecies complex (Langer et al. 2009; Hoppe et al. 2011) or within a single strain (Langer et al. 2009; Richier et al. 2011; Publication II), but it can be extended to other experimental matrices, physiological processes or species. Studies have for example observed temperature-modulation of OA effects in *E. huxleyi* (De Bodt et al. 2011) and the coccolithophore *Syracosphaera pulchra* (Fiorini et al. 2011) as well as light-modulated responses in nitrogen fixation in the marine cyanobacterium *Trichodesmium erythraeum* (Kranz et al. 2010).
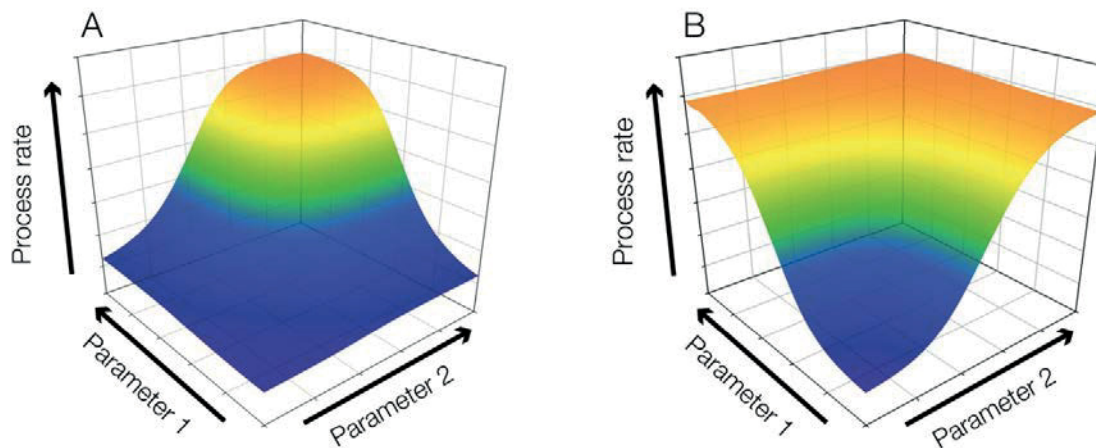
Figure 13: Scenarios of combined effects of varying environmental parameters. A: Constellation of rate-determining parameters that allows co-limitation and co-amplification (alterations in parameter 2 will be more effective when parameter 1 is high). B: Situation of substitutable co-limitation, allowing to overcome co-limitation by re-allocation of resources (increases in parameter 1 can compensate for low values parameter 2)

Regarding biogeochemistry, these findings imply that the impact of OA on calcification in *E. huxleyi* depends largely on the light regimes in future oceans. Especially during summer, i.e., in conditions of intensive irradiation and high stratification (the typical *E. huxleyi* blooming setting), the OA-induced decrease in calcification may be attenuated. In fact, as global warming increases stratification, more regimes may be created in which *E. huxleyi* can develop blooms (Tyrrell and Merico 2004), which could even over-compensate adverse effects of OA. However, models predict that non-blooming phytoplankton communities with only a moderately high fraction of calcifiers contribute strongest to the marine POC pump (Lam et al. 2011). Therefore, under these

conditions, impacts of OA on PIC formation and in consequence on overall POC export are likely to be significant.

The third overarching pattern is that in both life-cycle stages, OA affected signal transduction and ion homeostasis, as well as carbon metabolism and light physiology (Publication III). The effects on signal transduction and ion homeostasis occurred irrespective of light intensity, i.e., they were *energy-independent*. This is probably because these systems exhibit vital core functions in cells (environmental perception, Ca^{2+} signaling) that must not be subject to fluctuations in energy supply. The OA-effects on carbon metabolism and light physiology, on the other side, were clearly *energy-dependent*. The metabolic shift that is caused by altered levels and redox states of NAD and NADP affects the primal cellular redox-sensing systems, the so-called 'redox hub'. This hub represents an interconnected set of reactions and metabolites that are able to integrate redox signals from many different cellular sources. It also mediates molecular cross-talk between signaling pathways and bioenergetic processes and thereby coordinates organelle activities (Raghavendra and Padmasree 2003; Noctor et al. 2007; Publication III). The energy-dependent modulation of OA-effects on carbon metabolism and light physiology in *E. huxleyi* life-cycle stages apparently originates from efforts to assure balanced growth within the framework of altered biochemical pathways.

The low-light and high-light specific expression patterns indicate that cells tightly control carbon fluxes and redox levels when energy is scarce, but facilitate rapid mass fluxes of carbon skeletons and redox messengers between organelles when energy is plentiful. In other words, OA determines biochemical flux routes within carbon metabolism while light determines the throughput (Publication III). The downscaling of photosynthetic energy generation and light harvesting that was observed (Publication II) seems to be a mechanistic response to the overall increased levels of NADPH under OA (Publication III). In line with this, increased dissipation of light energy under OA was observed in diatom-dominated phytoplankton in assemblages (Gao et al. 2012), suggesting that phytoplankton generally apply such mechanistic response patterns. Lastly, re-routing of metabolic carbon fluxes and regulation of organelle activity in response to redox-relevant signals seems a universal feature of cells, as it is observed from unicellular protists like the pathogenic bacterium *Pseudomonas aeruginosa* (Price-Whelan et al. 2007) and baker's yeast *Saccharomyces cerevisae* (Ralser et al. 2007), over vascular plants like the tomato *Solanum lycopersicum* (Nunes-Nesi et al. 2005) even to proliferating human cancer cells (Cairns et al. 2011). Given the drastic differences between the life-cycle stages and the universality of 'redox-controlled metabolic fluxes', it may be proposed that a similar affection of carbon fluxes and redox state is likely to manifest in other species of unicellular phytoplankton.

Perspectives and research outlook

The presented data have contributed to the cell-biological understanding of microalgal metabolism in general and the physiology of calcification in particular. However, more research is necessary to bridge persisting knowledge gaps and to resolve the metabolic functioning of microalgae. In the following section, specific research questions are motivated and developed that will help to further deepen the understanding of the physiology of phytoplankton under global change.

The invasion of CO_2 into the oceans alters at least two major chemical parameters with numerical significance, especially $[H^+]$ ('Ocean Acidification') and $[CO_2]$ ('Ocean Carbonation'). OA-responses observed in microalgae (e.g., increased POC production) are, however, integrated physiological signals, deriving from differently sensitive subordinate processes (e.g., DIC uptake, light reactions, dark reaction) that are themselves differently sensitive to $[H^+]$ and $[CO_2]$, which complicates the identification of causality. To overcome this, experimental approaches can be used, in which carbonate chemistry parameters are uncoupled. Either TA is kept constant while pH is varied (i.e., simulating only acidification) or [DIC] is manipulated while pH is kept constant (i.e., simulating only carbonation). Using this approach, Bach and coworkers (2012) showed that the processes of POC and PIC production not only exhibit different $[CO_2]$ optima but are in fact differently influenced by $[H^+]$ and $[CO_2]$ at both sides of the optimum. For example, POC and PIC production were dependent on $[CO_2]$ at sub-saturating levels but were adversely affected by high $[H^+]$. These results highlight the need to examine the effects of carbonate system parameters in isolation.

An often neglected side-phenomenon of OA is the overall decreased buffer capacity of the seawater (Egleston et al. 2010) that will amplify the fluctuations in $[H^+]$ and $[CO_2]$ caused by invasion of atmospheric CO_2 and biological activity (Flynn et al. 2012). While physiological responses to OA are typically investigated after a sufficient acclimation under quasi-constant seawater chemistry, natural populations will experience a larger variability in pH regimes. Figure 14 exemplifies this, showing three scenarios of hypothetical blooms of calcifying phytoplankton. All algae are assumed to have an Redfield-like C:N stoichiometry of 6.625 mol mol^{-1} (Redfield et al. 1963), consume nitrate (NO_3^-) as N source and fix 250 µmol kg^{-1} DIC into particulate carbon. Scenario 1 (green arrow) shows the case of calcifiers in contemporary oceans (Present Day; pCO$_2$ = 380 µatm) exhibiting a PIC:POC ratio of 1. In such a scenario, $[H^+]$ would drift from 8.5 to 7.8 nmol kg^{-1} over the course of the bloom, i.e., 0.7 nmol kg^{-1}, an 8% reduction. In scenario two (blue arrow), the same bloom occurs under ocean acidification (Future; pCO$_2$ = 1000 µatm), where $[H^+]$ drifts from 19.1 to 17.6 nmol kg^{-1}, i.e. also an 8% reduction in $[H^+]$. However, due to 2-3 fold higher absolute concentration, $[H^+]$ drifts by 1.5 nmol kg^{-1}, i.e. double as much than in scenario 1. In scenario 3 (red arrow), the bloom occurs under OA (pCO$_2$ = 1000 µatm), but algae exhibit a lowered PIC:POC ratio of 0.3. Here, $[H^+]$ drops by 38% from 19.1 to 11.8 nmol kg^{-1} and cells experience an unprecedented range of pH.
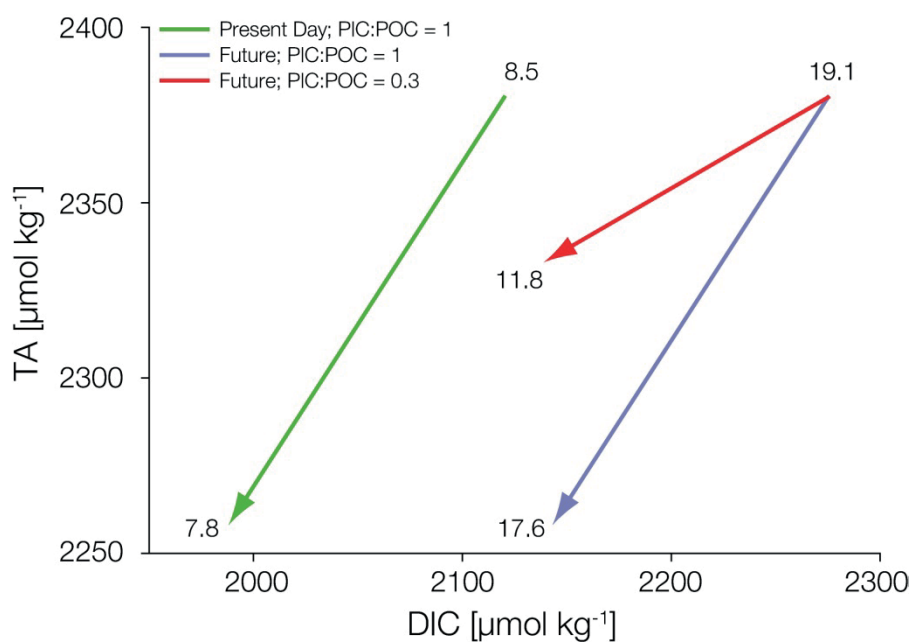
Figure 14: Bloom scenarios of calcifying algae fixing 125 µmol kg^{-1} DIC into POC and PIC (see text). Arrows indicate the concomitant shifts in the carbonate system. Numbers indicate [H$^+$] in nmol kg^{-1}. Constraints: temperature = 20°C, pressure = 1 dbar, salinity = 32 [PO$_4^{3-}$] = 3 µmol kg^{-1}; [H$_2$SiO$_4^{2-}$] = 1 µmol kg^{-1}; TA$_{initial}$ = 2380 µmol kg^{-1}; N-source: NO$_3^-$; POC:PON = 6.625 mol mol^{-1}.

The higher variability in [H$^+$] and [CO$_2$] in the future will potentially require more regulatory efforts by unicellular organisms. These efforts may constitute additional selective pressures and are likely to feedback on the species' ecology. It is important to characterize principal abilities to cope with the fluctuating carbonate chemistry and the potentially associated energetic costs. This may be accomplished by culturing algae under fluctuating or transient chemical conditions. Such investigations may allow an estimation of ecological long-term implications for microalgal life in the chemically fluctuating environments of the future.

The studies presented in this doctoral thesis have shown that cellular energy state determines the magnitude of responses to OA and certainly also to other environmental factors. This overarching pattern of energy-dependence prompts the investigation of other energetically-relevant environmental parameters. A prime candidate to investigate is the N-source utilized by cells. Whereas ammonia (NH$_4^+$) can be readily incorporated into amino acids, the reduction of NO$_3^-$ into usable NH$_4^+$ requires overall 8 electrons and is therefore much more energy intensive (Huppe and Turpin 1994). The required electrons are donated by NADH and NADPH, and experiments have shown that the utilized N-source affects the constellation of metabolic fluxes of carbon and nitrogen as well as the redox hub (Huppe et al. 1992). Investigating the effects of NH$_4^+$ and NO$_3^-$ in

81

combination with different levels of light or $p\text{CO}_2$ will improve the understanding of the relationships between energy budgeting, carbon allocation and phenomenological outcome that determine the biogeochemical impact of microalgae. It may also contribute to improved predictions for large scale carbon and nitrogen cycling in regions of new and recycled production that are fuelled by NO_3^- and NH_4^+ respectively (Eppley and Peterson 1979).

The so far outlined research perspectives may contribute to the understanding of the physiology of microalgae and the influences of the environment. Certainly, standard approaches (such as phenomenological assessments of elemental quotas and growth rates) should be flanked by state-of-the-art methodology, applying *in-vivo* physiology and 'functional -omics'. Only by extending data acquisition to the level of sub-cellular processes and biochemical activities, researchers will be able to make sound statements on what actually happens in cells, rather than solely describing the consequences. Here, gas-exchange measurements and functional transcriptomics were applied to characterize photosynthetic light reactions and carbon acquisition as wells as regulation of pathways and molecular functions. Future research efforts should be extended to proteomic and metabolomic techniques. Proteomics are able to resolve protein-protein interactions and post-translational modifications, which will deliver insights into interrelations and short-term (de-)activation of proteins (Dettmer et al. 2007; Jamers et al. 2009). Metabolomics can be applied to screen for target metabolites of biochemical pathways and to assess the relative throughput of these (i.e., flux-balance analyses; Fiehn 2002; Stitt et al. 2010). Protocols can be developed to separate and detected intermediates of carbon metabolism and also redox carriers like NAD^+, $NADP^+$, glutathione or ascorbate (Foyer and Noctor 2011; Fiehn 2002).

CONCLUSION

The use of experimental matrix approaches and holistic analytics permits the investigation of microalgae and their responses to environmental change with an unprecedented depth of detail. Supported by such multi-layered analytical frameworks, coccolithophores and other key phytoplankton groups should be further investigated. With information from the different hierarchical levels of biological organization (Figure 15), one can develop a system-biological understanding of microalgal physiology that is required for mathematical modeling of cells, ecosystem dynamics and global elemental fluxes (Follows et al. 2007, Marinov et al. 2010;).
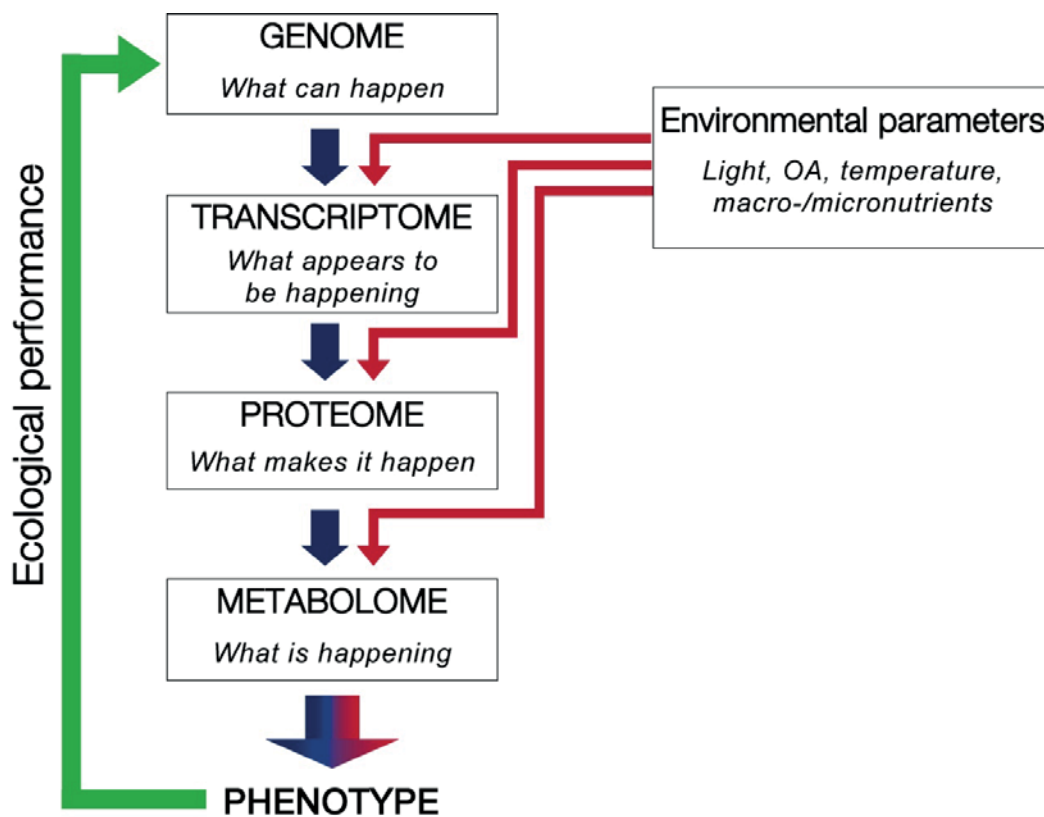
Figure 15: The '-omics cascade' adapted from Dettmer et al. (2007): The cascade comprises the hierarchical levels of cellular organization. Datasets from multiple levels can comprehensively describe the responses of organisms to environmental perturbations. The most powerful database will integrate data from all -omic levels and will enable a holistic understanding of environmental effects on organisms.

Such an improved understanding of phytoplankton physiology is a crucial prerequisite for reasonable predictions about the long-term effects of anthropogenic global change.

REFERENCES

Allen, M. R., D.J. Frame, C. Huntingford, C.D. Jones, J.A. Lowe, M. Meinshausen, and N. Meinshausen. 2009. Warming caused by cumulative carbon emissions towards the trillionth tonne. Nature **458:** 1163-1166.

Anning, T., N. Nimer, M. J. Merrett, and C. Brownlee. 1996. Costs and benefits of calcification in coccolithophorids. Journal of Marine Systems **9:** 45-56.

Bach, L. T., U. Riebesell, and K. G. Schulz. 2011. Distinguishing between the effects of ocean acidification and ocean carbonation in the coccolithophore *Emiliania huxleyi*. Limnology and Oceanography **56:** 2040-2050.

Balch, W. M., J. Fritz, and E. Fernandez. 1996. Decoupling of calcification and photosynthesis in the coccolithophore *Emiliania huxleyi* under steady-state light-limited growth. Marine Ecology Progress Series **142:** 87-97.

Balch, W., D. Drapeau, B. Bowler, and E. Booth. 2007. Prediction of pelagic calcification rates using satellite measurements. Deep Sea Research II **54:** 478-495.

Barker, G. L. A., J. C. Green, P. K. Hayes, and L. K. Medlin. 1994. Preliminary results using the rapd analysis to screen bloom populations of *Emiliania huxleyi* (Haptophyta). Sarsia **79:** 301-306.

Beaufort, L.,l. Probert, T. de Garidel-Thoron, E. M. Bendif, D. Ruiz-Pino, N. Metzl, C. Goyet, N. Buchet, P. Coupel, M. Grelaud, B. Rost, R. E. M. Rickaby, and C. de Vargas. 2011. Sensitivity of coccolithophores to carbonate chemistry and ocean acidification. Nature **476:** 80-83.

Benton, M. J., and R. J. Twitchett. 2003. How to kill (almost) all life: the end-Permian extinction event. Trends in Ecology & Evolution **18:** 358-365.

Bijma, J., M. Altabet, M. Conte, H. Kinkel, G. J. M. Versteegh, J. K. Volkman, S. G. Wakeham, and P. P. Weaver. 2001. Primary signal: Ecological and environmental factors - Report from Working Group 2. Geochemistry Geophysics Geosystems. **2:** 17pp.

Bown, P. R., J. A. Lees, and J. R. Young. 2004. Calcareous nannoplankton evolution and diversity through time, p. 451-508. *In* H. R. Thierstein and J. R. Young [eds.], Coccolithophores: From molecular processes to global impact. Springer-Verlag.

Bowring, S. A., D. H. Erwin, Y. G. Jin, M. W. Martin, K. Davidek, and W. Wang. 1998. U/Pb zircon geochronology and tempo of the end-permian mass extinction. Science **280:** 1039-1045.

Brand, L. E. 1982. Genetic variability and spatial patterns of genetic gifferentiation in the reproductive rates of the marine coccolithophores *Emiliania huxleyi* and *Gephyrocapsa oceanica*. Limnology and Oceanography **27:** 236-245.

Broecker, W. S., and T.-H. Peng. 1982. Tracers in the Sea. Eldigio Press, Palisades, N.Y., U.S.A.

Brownlee, C., N. Nimer, L. F. Dong, and M. J. Merrett. 1994. Cellular regulation during calcification in *Emiliana huxleyi*, p. 133-148. *In* J. C. Green and B. S. C. Leadbeater [eds.], The Haptophyte algae. Clarendon Press.

Buitenhuis, E. T., H. J. W. De Baar, and M. J. W. Veldhuis. 1999. Photosynthesis and calcification by *Emiliania huxleyi* (Prymnesiophyceae) as a function of inorganic carbon species. Journal of Phycology **35:** 949-959.

Castberg, T. , R. Thyrhaug, A. Larsen, R.-A. Sandaa, M. Heldal, J. L. Van Etten, and G. Bratbak. 2002. Isolation and characterization of a virus that infects *Emiliania huxleyi* (Haptophyta). Journal of Phycology **38:** 767-774.

Cairns, R. A., I. S. Harris, and T. W. Mak. 2011. Regulation of cancer cell metabolism. Nature Reviews Cancer **11:** 85-95.

Crutzen, P. J. 2002. Geology of mankind. Nature **415**.

De Bodt, C., N. Van Oostende, J. Harlay, K. Sabbe, and L. Chou. 2010. Individual and interacting effects of pCO_2 and temperature on *Emiliania huxleyi* calcification: study of the calcite production, the coccolith morphology and the coccosphere size. Biogeosciences **7:** 1401-1412.

De La Rocha, C. L., and U. Passow. 2007. Factors influencing the sinking of POC and the efficiency of the biological carbon pump. Deep Sea Research Part II: Topical Studies in Oceanography **54:** 639-658.

De Vargas, C., M. P. Aubry, I. Probert, and J. R. Young. 2004. Origin and evolution of coccolithophores: From coastal hunters to oceanic farmers, p. 251-281. *In* P. Falkowski and A. H. Knoll [eds.], Evolution of aquatic photoautotrophs. Elsevier Academic.

Dettmer, K., P. A. Aronov, and B. D. Hammock. 2007. Mass spectrometry-based metabolomics. Mass Spectrometry Reviews **26:** 51-78.

Dickson, A. G. 1981. An exact definition of total alkalinity and a procedure for the estimation of alkalinity and total inorganic carbon from titration data. Deep Sea Research I **28:** 609-623.

Dickson, A. G., and F. J. Millero. 1987. A comparison of the equilibrium constants for the dissociation of carbonic acid in seawater media. Deep Sea Research I **34:** 1733-1743.

Doney, S. C., W. M. Balch, V. J. Fabry, and R. A. Feely. 2009. Ocean acidification: a critical emerging problem for the ocean sciences. Oceanography **22:** 16-25.

Egleston, E. S., C. L. Sabine, and F. M. M. Morel. 2010. Revelle revisited: Buffer factors that quantify the response of ocean chemistry to changes in DIC and alkalinity. Global Biogeochemical Cycles **24:** GB1002.

Eppley, R. W., and B. J. Peterson. 1979. Particulate organic matter flux and planktonic new production in the deep ocean. Nature **282:** 677-680.

Etheridge, D.M., L.P. Steele, R.L. Langenfels, R.J. Francey, J.-M. Barnola, and V.I. Morgan. 1998. Historical CO_2 records from the Law Dome DE08, DE08-2, and DSS ice cores. *In* Trends: A Compendium of Data on Global Change. Carbon Dioxide Information Analysis Center, Oak Ridge National Laboratory, U.S. Department of Energy, Oak Ridge, Tennessee, U.S.A.

Falkowski, P., M. E. Katz, B. Van Den Schootbrugge, and A. H. Knoll. 2004. Why is the land green and the ocean red?, p. 429-453. *In* H. R. Thierstein and E. B. Young [eds.], Coccolithophores: from molecular processes to global impact. Amsterdam.

Feely, R. A., C. L. Sabine, K. Lee, W. Berelson, J. Kleypas, V. J. Fabry, and F. J. Millero. 2004. Impact of anthropogenic CO_2 on the $CaCO_3$ system in the Oceans. Science **305:** 362-366.

Feng, Y., .E. Warner, Y. Zhang, J. Sun, F. X. Fu, J. M. Rose, and D. A. Hutchins. 2008. Interactive effects of increased pCO_2, temperature and irradiance on the marine coccolithophore *Emiliania huxleyi* (Prymnesiophyceae). European Journal of Phycology **43:** 78-98.

Fiehn, O. 2002. Metabolomics – the link between genotypes and phenotypes. Plant Molecular Biology **48:** 155-171.

Field, C. B., M. J. Behrenfeld, J. T. Randerson, and P. Falkowski. 1998. Primary Production of the Biosphere: Integrating Terrestrial and Oceanic Components. Science **281:** 237-240.

Fiorini, S., J. J. Middelburg, and J. P. Gattuso. 2011. Effects of elevated CO_2 partial pressure and temperature on the coccolithophore *Syracosphaera pulchra*. Aquatic Microbial Ecology **64:** 221-232.

Fischer, H., M. Wahlen, J. Smith, D. Mastroianni, and B. Deck. 1999. Ice core records of atmospheric CO_2 around the last three glacial terminations. Science **283:** 1712-1714.

Flynn, K. J., J. C. Blackford, M. E. Baird, J. A. Raven, D. R. Clark, J. Beardall, C. Brownlee, H. Fabian, and G. L. Wheeler. 2012. Changes in pH at the exterior surface of plankton with ocean acidification. Nature Climate Change **2:** 510-513.

Follows, M. J., S. Dutkiewicz, S. Grant, and S. W. Chisholm. 2007. Emergent Biogeography of Microbial Communities in a Model Ocean. Science **315:** 1843-1846.

Foyer, C. H., and G. Noctor. 2011. Ascorbate and Glutathione: The Heart of the Redox Hub. Plant Physiology **155:** 2-18.

Frada, M., I. Probert, M. J. Allen, W. H. Wilson, and C. De Vargas. 2008. The 'Cheshire Cat' escape strategy of the coccolithophore *Emiliania huxleyi* in response to viral infection. PNAS **105:** 15944-15949.

Frada, M. J., K. D. Bidle, I. Probert, and C. De Vargas. 2012. In situ survey of life cycle phases of the coccolithophore *Emiliania huxleyi* (Haptophyta). Environmental Microbiology **14:** 1558-1569.

Gao, K., J. Xu, G. Gao, Y. Li, D. A. Hutchins, B. Huang, L. Wang, Y. Zheng, P. Jin, X. Cai, D.-P. Hader, W. Li, K. Xu, N. Liu, and U. Riebesell. 2012. Rising CO_2 and increased light exposure synergistically reduce marine primary productivity. Nature Climate Change **2:** 519-523.

Green, J. C., P. A. Course, and G. A. Tarran. 1996. The life-cycle of *Emiliania huxleyi*: A brief review and a study of relative ploidy levels analysed by flow cytometry. Journal of Marine Systems **9:** 33-44.

Hagino, K., E. M. Bendif, J. R. Young, K. Kogame, I. Probert, Y. Takano, T. Horiguchi, C. de Vargas, and H. Okada. 2011. New evidence for morphological and genetic variation in the cosmopolitan coccolithophore *Emiliania huxleyi* (Prymnesiophyceae) from the COX1b-ATP4 genes. Journal of Phycology **47:** 1164-1176.

Harris, R. P. 1994. Zooplankton grazing on the coccolithophore *Emiliania huxleyi* and its role in inorganic carbon flux. Marine Biology **119:** 431-439.

Honjo, S., S. J. Manganini, R. A. Krishfield, and R. Francois. 2008. Particulate organic carbon fluxes to the ocean interior and factors controlling the biological pump: A synthesis of global sediment trap programs since 1983. Progress in Oceanography **76:** 217-285.

Hoppe, C. J. M., G. Langer, and B. Rost. 2011. *Emiliania huxleyi* shows identical responses to elevated pCO_2 in TA and DIC manipulations. Journal of Experimental Marine Biology and Ecology **406:** 54-62.

Huppe, H. C., and D. H. Turpin. 1994. Integration of Carbon and Nitrogen Metabolism in Plant and Algal Cells. Annual Review of Plant Molecular Biology **45:** 577-607.

Huppe, H. C., G. C. Vanlerberghe, and D. H. Turpin. 1992. Evidence for activation of the oxidative pentose phosphate pathway during photosynthetic assimilation of NO_3^- but not NH_4^+ by a green alga. Plant Physiology **100:** 2096-2099.

IPCC. 1995. The science of climate change: contribution of Working group I. *In* J. T. Houghton et al. [eds.], Climate change 1995. 2nd assessment report of the Intergovernmental Panel on Climate change. Cambridge University Press.

Jamers, A., R. Blust, and W. De Coen. 2009. Omics in algae: Paving the way for a systems biological understanding of algal stress phenomena? Aquatic Toxicology **92:** 114-121.

James, S. R., R. W. Dennell, A. S. Gilbert, H. T. Lewis, J. A. J. Gowlett, T. F. Lynch, W. C. McGrew, C. R. Peters, G. G. Pope, and A. B. Stahl. 1989. Hominid use of fire in the lower and middle pleistocene: A review of the evidence [and comments and replies]. Current Anthropology **30:** 1-26.

Kegel, J. U., M. Blaxter, M. J. Allen, K. Metfies, W. H. Wilson, and K. Valentin. 2010. Transcriptional host-virus interaction of *Emiliania huxleyi* (Haptophyceae) and EhV-86 deduced from combined analysis of expressed sequence tags and microarrays. European Journal of Phycology **45:** 1-12.

Keeling, C.D., and T.P. Whorf. 2004. Atmospheric CO_2 records from sites in the SIO air sampling network. *In* Trends: A Compendium of Data on Global Change. Carbon Dioxide Information Analysis Center, Oak Ridge National Laboratory, U.S. Department of Energy, Oak Ridge, Tennessee, U.S.A.

Klaas, C., and D. E. Archer. 2002. Association of sinking organic matter with various types of mineral ballast in the deep sea: Implications for the rain ratio. Global Biogeochemical Cycles **16:** 1116-1130.

Klaveness, D. 1972. *Coccolithus huxleyi* (Lohm.) Kamptn II. The flagellate cell, aberrant cell types, vegetative propagation and life cycles. British Phycological Journal **7:** 309-318.

Knoll, A. H. 2003. Biomineralization and evolutionary history. Reviews in mineralogy and geochemistry **54:** 329-356.

Kranz, S. A., O. Levitan, K.-U. Richter, O. Prasil, I. Berman-Frank, and B. Rost. 2010. Combined Effects of CO_2 and Light on the N_2-Fixing Cyanobacterium *Trichodesmium* IMS101: Physiological Responses. Plant Physiology **154:** 334-345.

Kroeker, K. J., R. L. Kordas, R. N. Crim, and G. G. Singh. 2010. Meta-analysis reveals negative yet variable effects of ocean acidification on marine organisms. Ecology Letters **13:** 1419-1434.

Kump, L. R., T. J. Bralower, and A. J. Ridgwell. 2009. Ocean acidification in deep time. Oceanography **22:** 94-107.

Lacis, A. A., G. A. Schmidt, D. Rind, and R. A. Ruedy. 2010. Atmospheric CO_2: principal control knob governing Earth´s temperature. Science **330:** 356-359.

Lam, P. J., S. C. Doney, and J. K. B. Bishop. 2011. The dynamic ocean biological pump: Insights from a global compilation of particulate organic carbon, $CaCO_3$, and opal concentration profiles from the mesopelagic. Global Biogeochemical Cycles **25:** 1-14.

Langer, G., M. Geisen, K. H. Baumann, J. Kläs, U. Riebesell, S. Thoms, and J. R. Young. 2006. Species-specific responses of calcifying algae to changing seawater carbonate chemistry. Geochemistry Geophysics Geosystems **7:** 12pp.

Langer, G., G. Nehrke, I. Probert, J. Ly, and P. Ziveri. 2009. Strain-specific responses of *Emiliania huxleyi* to changing seawater carbonate chemistry. Biogeosciences **6:** 2637-2646.

Lefebvre, S. C., I. Benner, J. H. Stillman, A. E. Parker, M. K. Drake, P. E. Rossignol, K. M. Okimura, T. Komada, and E. J. Carpenter. 2012. Nitrogen source and pCO_2 synergistically affect carbon allocation, growth and morphology of the coccolithophore

Emiliania huxleyi: potential implications of ocean acidification for the carbon cycle. Global Change Biology **18:** 493-503.

Leonardos, N., B. Read, B. Thake, and J. R. Young. 2009. No mechanistic dependence of photosynthesis on calcification in the coccolithophorid *Emiliania huxleyi* (Haptophyta). Journal of Phycology **45:** 1046-1051.

Löbl, M., A. M. Cockshutt, D. Campbell, and Z. V. Finkel. 2010. Physiological basis for high resistance to photoinhibition under nitrogen depletion in *Emiliania huxleyi*. Limnology and Oceanography **55:** 2150-2160.

Lüthi, D., M. Le Floch, B. Bereiter, T. Blunier, J.-M. Barnola, U. Siegenthaler, D. Raynaud, J. Jouzel, H. Fischer, K. Kawamura, and T. F. Stocker. 2008. High-resolution carbon dioxide concentration record 650,000 - 800,000 years before present. Nature **453:** 379-382.

Marinov, I., S. C. Doney, and I. D. Lima. 2010. Response of ocean phytoplankton community structure to climate change over the 21st century: partitioning the effects of nutrients, temperature and light. Biogeosciences **7:** 3941-3959.

Martínez, J. M., D. C. Schroeder, A. Larsen, G. Bratbak, and W. H. Wilson. 2007. Molecular dynamics of *Emiliania huxleyi* and cooccurring viruses during two separate mesocosm studies. Applied and Environmental Microbiology **73:** 554-562.

Mauna Loa Observatory, Scripps Institution of Oceanography via www.CO2NOW.org.

Medlin, L. K., G. L. A. Barker, L. Campbell, J. C. Green, P. K. Hayes, D. Marie, S. Wrieden, and D. Vaulot. 1996. Genetic characterisation of *Emiliania huxleyi* (Haptophyta). Journal of Marine Systems **9:** 13-31.

Mehrbach, C., C. H. Culberson, J. E. Hawley, and R. M. Pytkowicz. 1973. Measurement of the apparent dissociation constants of carbonic acid in seawater at atmospheric pressure. Limnology and Oceanography **18:** 897-907.

Milliman, J. D. 1993. Production and accumulation of calcium carbonate in the ocean: budget of a non-steady state. Global Biogeochemical Cycles **7:** 927-957.

Mohan, R., L. P. Mergulhao, M. V. S. Guptha, A. Rajakumar, M. Thamban, N. Anil Kumar, M. Sudhakar, and R. Ravindra. 2008. Ecology of coccolithophores in the Indian sector of the Southern Ocean. Marine Micropaleontology **67:** 30-45.

Monnin, E., E. J. Steig, U. Siegenthaler, K. Kawamura, J. Schwander, B. Stauffer, T. F. Stocker, D. L. Morse, J.-M. Barnola, B. Bellier, D. Raynaud, and H. Fischer. 2004. Evidence for substantial accumulation rate variability in Antarctica during the Holocene, through synchronization of CO_2 in the Taylor Dome, Dome C and DML ice cores. Earth and Planetary Science Letters **224:** 45-54.

Nanninga, H. J., and T. Tyrrell. 1996. Importance of light for the formation of algal blooms by *Emiliania huxleyi*. Marine Ecology Progress Series **136:** 195-203.

Neftel, A., H. Friedli, E. Moor, H. Lötscher, U. Siegenthaler, and B. Stauffer. 1994. Historical CO_2 record from the Siple Station ice core. *In* Trends: A Compendium of Data on Global Change. Carbon Dioxide Information Analysis Center, Oak Ridge National Laboratory, U.S. Department of Energy, Oak Ridge, Tennessee, U.S.A.

Nejstgaard, J. C., I. Gismervik, and P. T. Solberg. 1997. Feeding and reproduction by *Calanus finmarchicus*, and microzooplankton grazing during mesocosm blooms of diatoms and the coccolithophore *Emiliania huxleyi*. Marine Ecology Progress Series **147:** 197-217.

Nielsen, M. V. 1995. Photosynthetic characteristics of the coccolithophorid *Emiliania huxleyi* (Prymnesiophyceae) exposed to elevated concentrations of dissolved inorganic carbon. Journal of Phycology **31:** 715-719.

Nisumaa, A. M., S. Pesant, R. G. J. Bellerby, B. Delille, J. J. Middelburg, J. C. Orr, U. Riebesell, T. Tyrrell, D. Wolf-Gladrow, and J. P. Gattuso. 2011. EPOCA/EUR-OCEANS data compilation on the biological and biogeochemical responses to ocean acidification. Earth System Science Data **2:** 167-175.

Noctor, G., R. De Paepe, and C. H. Foyer. 2007. Mitochondrial redox biology and homeostasis in plants. Trends in Plant Science **12:** 125-134.

Nunes-Nesi, A., F. Carrari, A. Lytovchenko, A. M. O. Smith, M. Ehlers Loureiro, R. G. Ratcliffe, L. J. Sweetlove, and A. R. Fernie. 2005. Enhanced photosynthetic performance and growth as a consequence of decreasing mitochondrial malate dehydrogenase activity in transgenic tomato plants. Plant Physiology **137:** 611-622.

Orr, J. C., V. J. Fabry, O. Aumont, L. Bopp, S. C. Doney, R. A. Feely, A. Gnanadesikan, N. Gruber, A. Ishida, F. Joos, R. M. Key, K. Lindsay, E. Maier-Reimer, R. Matear, P. Monfray, A. Mouchet, R. G. Najjar, G.-K. Plattner, K. B. Rodgers, C. L. Sabine, J. L. Sarmiento, R. Schlitzer, R. D. Slater, I. J. Totterdell, M.-F. Weirig, Y. Yamanaka, and A. Yool. 2005. Anthropogenic ocean acidification over the twenty-first century and its impact on calcifying organisms. Nature **437:** 681-686.

Paasche, E., and S. Brubak. 1994. Enhanced calcification in the coccolithophorid *Emiliania huxleyi* (Haptophyceae) under phosphorus limitation. Phycologia **33:** 324-330.

Paasche, E. 1998. Roles of nitrogen and phosphorus in coccolith formation in *Emiliania huxleyi* (Prymnesiophyceae). European Journal of Phycology **33:** 33-42.

Paasche, E. 2002. A review of the coccolithophorid *Emiliania huxleyi* (Prymnesiophyceae), with particular reference to growth, coccolith formation, and calcification-photosynthesis interactions. Phycologia **40:** 503-529.

Peters, G. P., G. Marland, C. Le Quere, T. Boden, J. G. Canadell, and M. R. Raupach. 2012. Rapid growth in CO_2 emissions after the 2008-2009 global financial crisis. Nature Climate Change **2:** 2-4.

Petit, J. R., J. Jouzel, D. Raynaud, N. I. Barkov, J. M. Barnola, I. Basile, M. Bender, J. Chappellaz, M. Davis, G. Delaygue, M. Delmotte, V. M. Kotlyakov, M. Legrand, V. Y. Lipenkov, C. Lorius, L. Pepin, C. Ritz, E. Saltzman, and M. Stievenard. 1999. Climate and atmospheric history of the past 420,000 years from the Vostok ice core, Antarctica. Nature **399:** 429-436.

Pierrehumbert, R. T. 2011. Infrared radiation and planetary temperature. Physics today **64:** 33-38.

Price-Whelan, A., L. E. P. Dietrich, and D. K. Newman. 2007. Pyocyanin alters redox homeostasis and carbon flux through central metabolic pathways in *Pseudomonas aeruginosa* PA14. Journal of Bacteriology **189:** 6372-6381.

Raghavendra, A. S., and K. Padmasree. 2003. Beneficial interactions of mitochondrial metabolism with photosynthetic carbon assimilation. Trends in Plant Science **8:** 546-553.

Ralser, M. , M. Wamelink, A. Kowald, B. Gerisch, G. Heeren, E. Struys, E. Klipp, C. Jakobs, M. Breitenbach, H. Lehrach, and S. Krobitsch. 2007. Dynamic rerouting of the carbohydrate flux is key to counteracting oxidative stress. Journal of Biology **6:** 10.

Raven, J. A., L. A. Ball, J. Beardall, M. Giordano, and S. C. Maberly. 2005. Algae lacking carbon-concentrating mechanisms. Canadian Journal of Botany **83:** 879-890.

Read, B., J. Kegel, M.J. Klute, A. Kuo, S.C. Lefebvre, F. Maumus, C. Mayer, J. Miller, A. Allen, K.D. Bidle, M. Borodovsky, C. Bowler, C. Brownlee, J.-M. Claverie, M. Cock, C. De Vargas, M. Elias, S. Frickenhaus, V.N. Gladyshev, K. Gonzalez, M. Groth, C. Guda, A.R. Hadaegh, E.K. Herman, D. Iglesias-Rodriguez, B. Jones, T. Lawson, F. Leese, Y.C. Lin, E. Lindquist, A. Lobanov, S. Lucas, S.B. Malik, M.E. Marsh, T.E. Mock, A. Monier, B. Mueller-Roeber, J. Napier, H. Ogata, A. Pagarete, M. Parker, I. Probert, H. Quesneville, C.A. Raines, S. Rensing, D.M. Riano-Pachon, S. Richier, S.D. Rokitta, A. Salamov, A.F. Sarno, J. Schmutz, D. Schroeder, Y. Shiraiwa, D.M. Soanes, K. Valentin, M. van der Giezen, Y. Van der Peer, F. Verret, P. Von Dassow, T.M. Wahlund, G. Wheeler, B. Williams, W.H. Wilson, G. Wolfe, L.L. Wurch, J.R. Young, J.B. Dacks, C.F. Delwiche, S. Dhyrman, G. Glöckner, U. John, T. Richards, A.Z. Worden, X. Zhan, and I.V. Grigoriev. In Review. *Emiliania's* pan genome drives the phytoplankton's global distribution.

Redfield, A. C., B. H. Ketchum, and F. A. Richards. 1963. The influence of organisms on the composition of sea-water. *In* M. N. Hill [ed.], Comparative and descriptive oceanography. The sea: ideas and observations on progress in the study of the seas.

Revelle, R., and H. E. Suess. 1957. Carbon dioxide exchange between atmosphere and ocean and the question of an increase of atmospheric CO_2 during the past decades. Tellus B **9:** 18-27.

Richier, S., S. Fiorini, M.-E. Kerros, P. Von Dassow, and J.-P. Gattuso. 2011. Response of the calcifying coccolithophore *Emiliania huxleyi* to low pH/high pCO_2: from physiology to molecular level. Marine Biology **158:** 551-560.

Ridgwell, A., and R. E. Zeebe. 2005. The role of the global carbonate cycle in the regulation and evolution of the Earth system. Earth and Planetary Science Letters **234:** 299-315.

Riebesell, U., I. Zondervan, B. Rost, P. D. Tortell, E. Zeebe, and F. M. M. Morel. 2000. Reduced calcification in marine plankton in response to increased atmospheric CO_2. Nature **407:** 634-637.

Riegman, R., W. Stolte, A. A. M. Noordeloos, and D. Slezak. 2000. Nutrient uptake and alkaline phosphatase (EC 3.1.3.1) activity of *Emiliania huxleyi* (Prymnesiophyceae) during growth under N and P limitation in continuous cultures. Journal of Phycology **36:** 87-96.

Rohde, R. A. 2006. Carbon_Dioxide_400kyr_Rev. The Global Warming Art Project. http://commons.wikimedia.org.

Rokitta, S. D., L. J. De Nooijer, S. Trimborn, C. De Vargas, B. Rost, and U. John. 2011. Transcriptome analyses reveal differential gene expression patterns between life-cycle stages of *Emiliania huxleyi* (Haptophyta) and reflect specialization to different ecological niches. Journal of Phycology **47:** 829-838.

Rokitta, S. D., and B. Rost. 2012. Effects of CO_2 and their modulation by light in the life-cycle stages of the coccolithophore *Emiliania huxleyi*. Limnology and Oceanography **57:** 607-618.

Rokitta, S. D., U. John and B. Rost. 2012b. Ocean Acidification Affects Redox-Balance and Ion-Homeostasis in the Life-Cycle Stages of *Emiliania huxleyi*. PLoS ONE 7(12): e52212. doi:10.1371/journal.pone.0052212

Rost, B., I. Zondervan, and U. Riebesell. 2002. Light-dependent carbon isotope fractionation in the coccolithophorid *Emiliania huxleyi*. Limnology and Oceanography **47:** 120-128.

Rost, B., and U. Riebesell. 2004. Coccolithophores and the biological pump: responses to environmental changes, p. 76–99. *In* H. R. Thierstein and J. R. Young [eds.], Coccolithophores—From Molecular Processes to Global Impact. Springer.

Rost, B., U. Riebesell, and D. Sültemeyer. 2006. Carbon acquisition of marine phytoplankton: effect of photoperiod length. Limnology and Oceanography **51:** 12-20.

Rost, B., I. Zondervan, and D. Wolf-Gladrow. 2008. Sensitivity of phytoplankton to future changes in ocean carbonate chemistry: Current knowledge, contradictions and research directions. Marine Ecology Progress Series **373:** 227-237.

Saito, M. A., T. J. Goepfert, and T. R. Jason. 2008. Some thoughts on the concept of colimitation: Three definitions and the importance of bioavailability. Limnology and Oceanography **53:** 276-290.

Sciandra, A., J. Harlay, D. Lefèvre, R. Lemée, P. Rimmelin, M. Denis, and J.-P. Gattuso. 2003. Response of coccolithophorid *Emiliania huxleyi* to elevated partial pressure of CO_2 under nitrogen limitation. Marine Ecology Pogress Series. **261:** 111-122.

Sikes, C. S., R. D. Roer, and K. M. Wilbur. 1980. Photosynthesis and coccolith formation: inorganic carbon sources and net inorganic reaction of deposition. Limnology and Oceanography **25:** 248-261.

Staats, N., L. Stal, J., B. D. Winder, and L. Mur, R. 2000. Oxygenic photosynthesis as driving process in exopolysaccharide production of benthic diatoms. Marine Ecology Progress Series **193:** 261-269.

Stanley, S. M., and L. A. Hardie. 1998. Secular oscillations in the carbonate mineralogy of reef-building and sediment-producing organisms driven by tectonically forced shifts in seawater chemistry. Palaeogeography, Palaeoclimatology, Palaeoecology **144:** 3-19.

Steffen, W., A. Sanderson, P. D. Tyson, J. Jäger, P. A. Matson, B. I. Moore, F. Oldfield, K. Richardson, H. J. Schellnhuber, B. L. Turner, and R. J. Wasson. 2004. Executive summary: Global change and the earth system - A planet under pressure.

Stitt, M., R. Sulpice, and J. Keurentjes. 2012. Metabolic networks: how to identify key components in the regulation of metabolism and growth. Plant Physiology **152:** 428-444.

Smit, J., and J. Hertogen. 1980. An extraterrestrial event at the Cretaceous-Tertiary boundary. Nature **285:** 198-200.

Tanner, L. H., S. G. Lucas, and M. G. Chapman. 2004. Assessing the record and causes of Late Triassic extinctions. Earth-Science Reviews **65:** 103-139.

Thierstein, H. R. 1976. Mesozoic calcareous nannoplankton biostratigraphy of marine sediments. Marine Micropaleontology **1:** 325-362.

Townsend, D. W., M. D. Keller, P. M. Holligan, S. G. Ackleson, and W. M. Balch. 1994. Blooms of the coccolithophore *Emiliania huxleyi* with respect to hydrography in the Gulf of Maine. Continental Shelf Research **14:** 979-1000.

Trimborn, S., G. Langer, and B. Rost. 2007. Effect of varying calcium concentrations and light intensities on calcification and photosynthesis in *Emiliania huxleyi*. Limnology and Oceanography **52:** 2285-2293.

Tyrrell, T., and A. Merico. 2004. *Emiliania huxleyi*: bloom observations and the conditions that induce them, p. 75-97. *In* H. R. Thierstein and J. R. Young [eds.], Coccolithophores: From molecular processes to global impact. Springer-Verlag.

Valero, M., S. Richerd, V. R. Perrot, and C. Destombe. 1992. Evolution of alternation of haploid and diploid phases in life cycles. Trends in Ecology & Evolution **7:** 25-29.

Von Dassow, P. , H. Ogata, I. Probert, P. Wincker, C. Da Silva, S. Audic, J.-M. Claverie, and C. De Vargas. 2009. Transcriptome analysis of functional differentiation between

haploid and diploid cells of *Emiliania huxleyi*, a globally significant photosynthetic calcifying cell. Genome Biology **10:** R114.

Westbroek, P., and F. Marin. 1998. A marriage of bone and nacre. Nature **392:** 861-862.

Winter, A., and W. G. Siesser. 1994. Atlas of living coccolithophores, p. 107-159. *In* A. Winter and W. G. Siesser [eds.], Coccolithophores. Cambridge University Press.

Wolf-Gladrow, D. A., U. Riebesell, S. Burkhardt, and J. Bijma. 1999. Direct effects of CO_2 concentration on growth and isotopic composition of marine plankton. Tellus B **51:** 461-476.

Wolf-Gladrow, D. A., R. E. Zeebe, C. Klppaseaas, A. Koertzinger, and A. G. Dickson. 2007. Total alkalinity: The explicit conservative expression and its application to biogeochemical processes. Marine Chemistry **106:** 287-300.

Xu, Y., J. M. Boucher, and F. M. M. Morel. 2010. Expression and diversity of alkaline phosphatase EHAP1 in *Emiliania huxleyi* (Prymnesiophyceae). Journal of Phycology **46:** 85-92.

Young, J. R. 1994. Functions of coccoliths, p. 63-82. *In* A. Winter and W. G. Siesser [eds.], Coccolithophores. Cambridge University Press.

Young, J. R., M. Geisen, L. Cros, A. Kleijne, C. Sprengel, I. Probert, and J. B. Ostergaard. 2003. A guide to extant coccolithophore taxonomy. Journal of Nannoplankton Research - Special Issue **1:** 1-125.

Zeebe, R. E., and D. A. Wolf-Gladrow. 2001. CO_2 in seawater: equilibrium, kinetics, isotopes. Elsevier Science B.V., Amsterdam.

Zondervan, I., R. E. Zeebe, B. Rost, and U. Riebesell. 2001. Decreasing marine biogenic calcification: A negative feedback on rising atmospheric pCO_2. Global Biogeochemical Cycles **15:** 507-516.

APPENDIX

Publication: Implications of observed inconsistencies in carbonate chemistry measurements for ocean acidification studies

Biogeosciences

Implications of observed inconsistencies in carbonate chemistry measurements for ocean acidification studies

C. J. M. Hoppe, G. Langer, S. D. Rokitta, D. A. Wolf-Gladrow, and B. Rost

Alfred Wegener Institute for Polar and Marine Research, 27570 Bremerhaven, Germany

Correspondence to: C. J. M. Hoppe (clara.hoppe@awi.de)

Abstract. The growing field of ocean acidification research is concerned with the investigation of organism responses to increasing pCO_2 values. One important approach in this context is culture work using seawater with adjusted CO_2 levels. As aqueous pCO_2 is difficult to measure directly in small-scale experiments, it is generally calculated from two other measured parameters of the carbonate system (often A_T, C_T or pH). Unfortunately, the overall uncertainties of measured and subsequently calculated values are often unknown. Especially under high pCO_2, this can become a severe problem with respect to the interpretation of physiological and ecological data. In the few datasets from ocean acidification research where all three of these parameters were measured, pCO_2 values calculated from A_T and C_T are typically about 30 % lower (i.e. ∼300 µatm at a target pCO_2 of 1000 µatm) than those calculated from A_T and pH or C_T and pH. This study presents and discusses these discrepancies as well as likely consequences for the ocean acidification community. Until this problem is solved, one has to consider that calculated parameters of the carbonate system (e.g. pCO_2, calcite saturation state) may not be comparable between studies, and that this may have important implications for the interpretation of CO_2 perturbation experiments.

1 Introduction

Since the beginning of the Industrial Revolution, CO_2 emissions from the burning of fossil fuels and changes in land use have increased atmospheric CO_2 levels from preindustrial values of 280 ppm to currently 390 ppm (www.esrl.noaa.gov/gmd/ccgg/trends; data by Tans and Keeling, NOAA/ESRL). Values are expected to rise to 750 ppm (IPCC scenario IS92a,

IPCC, 2007) or even beyond 1000 ppm by the end of this century (Raupach et al., 2007). In addition to its contribution to the broadly discussed greenhouse effect, about 25 % of anthropogenic CO_2 has been taken up by the ocean (Canadell et al., 2007), causing a shift of the carbonate chemistry towards higher CO_2 concentrations and lower pH (Broecker et al., 1971). This process, commonly referred to as ocean acidification (OA), is already occurring and is expected to intensify in the future (Kleypas et al., 1999; Wolf-Gladrow et al., 1999; Caldeira and Wickett, 2003). Ocean acidification will affect marine biota in many different ways (for reviews see Fabry et al., 2008; Rost et al., 2008).

To shed light on potential responses of organisms and ecosystems, numerous national and international research projects have been initiated (see Doney et al., 2009). An essential part of OA research is based on CO_2 perturbation experiments, which represent the primary tool for studying responses of key species and marine communities to acidification of seawater. Marine biologists working in this field have to deal with several problems associated with this type of experiment: being especially interested in high pCO_2 scenarios, seawater carbonate chemistry needs to be adjusted and kept quasi-constant over the duration of an experiment (in many cases, the carbonate chemistry is not at all controlled after initial adjustment). Also, the correct determination of at least two parameters is necessary to obtain a valid description of the whole carbonate system and hence correctly interpret organism responses.

Aqueous pCO_2 is difficult to measure in small-scale experiments, and also pH has been under debate due to intricacies concerning pH scales and measurement protocols (Dickson, 2010; Liu et al. 2011). Total alkalinity (A_T) and dissolved inorganic carbon (C_T) are usually favoured as

input parameters for carbonate chemistry calculations, because sample preservation and measurements are relatively straightforward. This combination of parameters had also been thought to lead to the most accurate calculations of CO_2 concentrations and carbonate saturation states (Riebesell et al., 2010). Still, there is no agreement of which two parameters are to be measured, and, as a consequence, carbonate system calculations in different studies are often based on different input parameters. As will be shown here, this may severely impair comparability of different datasets.

Even though detailed literature on measurement protocols has been published (Dickson et al., 2007; Gattuso et al., 2010), potential pitfalls and problems with uncertainty estimations remain and, as certified reference materials (CRMs) are only available for current surface ocean conditions, the quality of carbonate chemistry measurements at high pCO_2 levels is often unknown. Uncertainties of estimated pCO_2 values are generally considered to be smaller than 10 % (c.f. Gattuso et al., 2010; Hydes et al., 2010). An examination of the few over-determined datasets assessed in OA laboratories (including data from our own laboratory; reported in the Supplement) reveals up to 30 % discrepancies between estimated pCO_2 levels derived from different input pairs (A_T C_T; A_T pH; C_T pH). This potentially widespread phenomenon has major implications for the comparability and quantitative validity of studies in the OA community. In view of the growing body of OA literature and its impact on public opinion and policy makers (Raven et al., 2005), the identification, quantification and prevention of common errors has to be an issue of high priority.

This publication is based on an earlier manuscript entitled On CO_2 perturbation experiments: Over-determination of carbonate chemistry reveals inconsistencies (Hoppe et al. 2010).

2   Results

We present here a comparison of over-determined carbonate chemistry datasets found in the literature together with our own datasets. Only one dataset with more than two parameters of the carbonate system measured in OA-laboratories was found in the list of EPOCA relevant publications archived in the PANGEA® database (Nisumaa et al., 2010; http://www.epoca-project.eu/index.php/data.html): Schneider and Ere , (200); another study was excluded from this analysis because of con icting values between database and manuscript. In addition, the data from Iglesias-Rodrigue et al. (2008), Thomsen et al. (2010) and our own laboratory (Hoppe et al. 2010) are shown. For all datasets, values reported for relevant parameters (e.g. salinity, temperature, pH scale, etc.) and the dissociation constants of carbonic acid of Mehrbach et al. (1973; as refit by Dickson and Millero, 1987) were used to calculate pCO_2 values at 15 °C using the program CO_2sys (Pierrot et al., 200). As infor-
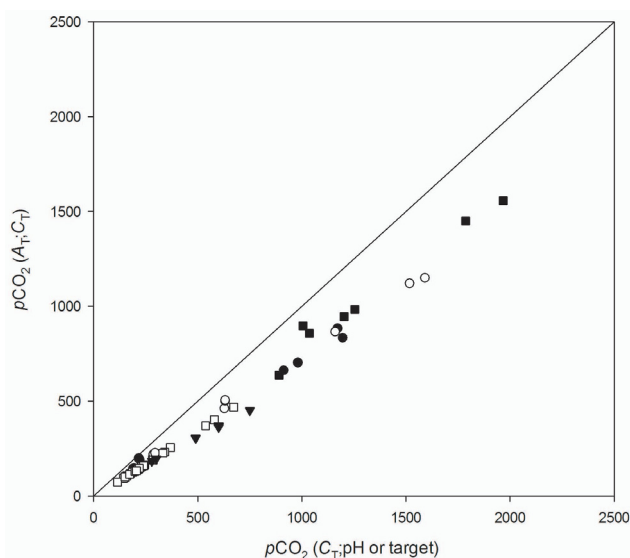
Fig. 1. Calculated pCO_2 (A_T; C_T) versus calculated pCO_2 (C_T; pH) in μatm from this study (closed circles, natural seawater; open circles, artificial seawater), Schneider and Ere , 200 (open squares), Thomsen et al., 2010 (closed squares) and Iglesias-Rodr gue et al., 2008 (closed triangles; here pCO_2(target) instead of $pCO_2(C_T$; pH) is given). pCO_2 values were calculated for the respective salinity, nutrients and carbonate chemistry parameters at 15 °C for all datasets.

mation on nutrient concentrations was lacking in the datasets used, values were based on appropriate literature data (see Supplement for details).

These calculations revealed discrepancies in the pCO_2 calculated from different input pairs, which increased systematically with increasing pCO_2 (Fig. 1). The pCO_2 calculated from C_T and A_T was $\sim$ 30 % lower than the pCO_2 calculated from either C_T and pH or from A_T and pH, the latter pairs yielding comparable results ($\pm$5 %). The carbonate system of Iglesias-Rodrigue et al. (2008; as shown in the PANGEA® database) was not strictly over-determined. However, if one assumes equilibration of the aerated seawater with the gas mixtures used (280–750 ppm), the deviation of the pCO_2 values (calculated from A_T and C_T) from the target pCO_2 reveals a similar relationship to that observed in the other datasets (Fig. 1). Even though outgassing in C_T samples cannot be completely excluded as a potential source of the discrepancies in this particular study, the consistent pattern among studies argues strongly against this explanation.

With respect to our own dataset, further information is available. Discrepancies of $\sim$30 % were observed irrespective of whether C_T or A_T was manipulated, and in both natural and artificial seawaters (NSW and ASW, respectively; Supplement, Table 2).

3 Discussion

Underestimation of $p\text{CO}_2$ calculated from measured values of A_T and C_T has been described in a number of studies from the marine chemistry community, in which direct measurements over a range of $p\text{CO}_2$ levels (approx. 200–1800 µatm) were compared to calculations from A_T and C_T (Lee et al., 199 ,2000; Wanninkhof et al., 1999; Luecker et al., 2000; Millero et al., 2002). The magnitude of these deviations is, however, much smaller than found in our study (5–10 %; cf. Fig. 4 in Luecker et al., 2000). The latter datasets and those from the OA community differ in the magnitude of the discrepancies (∼5–10 % and ∼30 %, respectively). Thus, the phenomenon observed in our study seems to be different from the one documented by marine chemists.

Currently, we do not have an explanation for the discrepancies described here, although a few simple explanations, such as the uncertainties of dissociation constants or uncertainties attributed to A_T, C_T or pH measurements, can be ruled out: Systematic errors in measured A_T (5 µmol kg^{-1}; based on repeated CRM measurements, our own data), C_T (7 µmol kg^{-1}; based on repeated CRM measurements, our own data), pH (0.02; Liu et al., 2011) and in equilibrium constants (0.01 in pK$_1^*$, 0.02 in pK$_2^*$; Dickson, 2010) would be much too small to explain the large discrepancies in calculated $p\text{CO}_2$.

The contribution of dissolved organic matter (DOM) to alkalinity has recently gained a lot of attention (Kim and Lee, 2009; Koeve et al., 2010). However, changes in A_T due to DOM cannot cause the discrepancies described here, since the phenomenon was also observed in an experiment in which artificial seawater without any organic compounds or organisms was used (Supplement, Table 2). Furthermore, experiments with nutrient-enriched North Sea seawater (our data), probably DOM-rich water from Kiel Bight (Thomsen et al., 2010) and from the oligotrophic Red Sea (Schneider and Ere , 200) show essentially identical discrepancies (Fig. 1). Nonetheless, DOM contributions can become a significant source of error in high biomass cultures (Kim and Lee, 2009).

It remains pu ling that these discrepancies are observed in experiments involving both A_T and C_T adjustments, different seawater compositions, as well as in several datasets produced with different equipment and procedures (e.g. coulometric, colourimetric and manometric C_T measurements). The fact that several independent studies carried out within the framework of ocean acidification research show similar discrepancies between calculated $p\text{CO}_2$ values (Fig. 1) suggests a systematic, as opposed to a random, deviation that will hinder a realistic judgement of the quality of datasets.

Regardless of the reasons for its occurrence, this phenomenon will have consequences for ocean acidification research. Firstly, published $p\text{CO}_2$ values may not be comparable if different input parameters were measured and used to calculate $p\text{CO}_2$. Secondly, if calculated $p\text{CO}_2$ values are underestimated by up to 30 %, an organism s respective sensitivity to acidification might be severely overestimated. This is especially important at $p\text{CO}_2$ levels $\geq$750 µatm, which are typically applied for the year 2100 scenario and therefore crucial for all CO_2 perturbation experiments. As an example, one might refer to the responses of four *Emiliania huxleyi* strains to different $p\text{CO}_2$ levels reported by Langer et al. (2009). For strain RCC125 , the authors report strongly decreasing calcification rates above $p\text{CO}_2$ values of 00 µatm ($p\text{CO}_2$ values were derived from A_T and C_T measurements). As the study of Langer et al. (2009) was conducted in the same laboratory as this one, the presence of the described discrepancies can be assumed. If the $p\text{CO}_2$ values from Langer et al. (2009) are indeed ∼30 % lower than the ones calculated from A_T and pH (or C_T and pH), our study could suggest that calcification increases until a $p\text{CO}_2$ of 750 µatm and only declines at values above 800 µatm. Predictions for this strain for the often proposed 2100 scenario of 750 µatm would thus differ substantially. The discrepancies in calculated $p\text{CO}_2$ values described here might also explain the differing results reported by Langer et al. (2009) and Hoppe et al. (2011) with respect to the sensitivity of this strain. Thirdly, depending on the input pair chosen, the calculated carbonate ion concentration and hence the calcite and aragonite saturation states might differ significantly. In this study, discrepancies in saturation states were found to be in the range of 15–30 %.

Care must therefore be taken when comparing studies that use different pairs of input parameters or when reporting threshold levels of $p\text{CO}_2$ harmful to an organism. To improve comparability between future studies, it may be useful to agree on a certain pair of input parameters as long as the described discrepancies remain. We suggest, for the time being, that the OA community should use A_T and pH as input parameters when calculating the carbonate chemistry and, whenever possible, measure and report additional parameters. This suggestion does, however, not mean that the resulting $p\text{CO}_2$ values are correct . Although choosing a particular pair of parameters provides a pragmatic approach to dealing with such discrepancies, it is unsatisfying and – if the choice results in inaccurate calculations of $p\text{CO}_2$ and CO_3^{2-} – may lead to inappropriate interpretations of organism responses. Currently, we have neither sufficient understanding of the uncertainties of carbonate chemistry measurements, nor a clear demonstration that it is possible to get thermodynamically consistent data of A_T, C_T, pH and $p\text{CO}_2$ for seawater samples with $p\text{CO}_2 >$ 00 µatm (A. Dickson personal communication, 2011). Further investigations on source and occurrence of this phenomenon are necessary. Certified reference material with high $p\text{CO}_2$, as well as calculation programs including the propagation of errors, could improve estimations of uncertainties in carbonate chemistry measurements and therewith calculations of $p\text{CO}_2$ values. It should become common practise to provide and defend

estimates of uncertainty. A large-scale inter-comparison of the quality of carbonate chemistry measurements between different laboratories (from the OA but also from the marine chemistry community) would help revealing whether the phenomenon described here is indeed widespread.

Supplementary material related to this article is available online at: http://www.biogeosciences.net/9/ 2401/2012/bg-9-2401-2012-supplement.zip.

References

Broecker, W. S., Li, . H., and Peng, T. H.: Carbon Dioxide – Man s Unseen Artifact, in: Impingement of Man on the Ocean, edited by: Hood, D. W., Wiley, New ork, USA, 287–324, 1971.

Caldeira, K. and Wickett, M. E.: Oceanography: Anthropogenic carbon and ocean pH, Nature, 425, p. 3 5, 2003.

Canadell, J. G., C. Le uere, C., Raupach, M. R., Field, C. B., Buitenhuis, E. T., Ciais, P., Conway, T. J., Gillett, N. P., Houghton, R. A. and Marland, G.: Contributions to accelerating atmospheric CO(2) growth from economic activity, carbon intensity, and efficiency of natural sinks, P. Natl. Acad. Sci. USA, 104, 188 –188702007.

Dickson, A. G.: The carbon dioxide system in sea water: equilibrium chemistry and measurements, in: Guide for Best Practices in Ocean Acidification Research and Data Reporting, edited by: Riebesell U., Fabry V. J., Hansson L. and Gattuso J.-P., Office for Official Publications of the European Union, Luxembourg, 2010.

Dickson, A. G. and Millero F. J.: A comparison of the equilibrium constants for the dissociation of carbonic acid in seawater media, Deep-Sea Res., 34, 1733–1743, 1987.

Dickson, A. G., Sabine, C. L., and Christian, J. R. (Eds.): Guide to best practices for ocean CO$_2$ measurements, PICES Special Publication, 3, Sidney, Canada, 2007.

Doney, S. C., Balch, W. M. Fabry, V. J., and Feely, R. A.: Ocean Acidification: A Critical Emerging Problem for the Ocean Sciences, Oceanography, 22, 1 –25, 2009.

Fabry, V. J., Seibel, B. A., Feely, R. A., and Orr, J. C.: Impacts of ocean acidification on marine fauna and ecosystem processes, ICES J. Mar. Sci., 5, 414–432, 2008.

Gattuso, J.-P., Lee, K., Rost, B., and Schul , K.: Approaches and tools to manipulate the carbonate chemistry, in: Guide for Best Practices in Ocean Acidification Research and Data Reporting, edited by: Riebesell, U., Fabry, V. J., Hansson, L., and Gattuso, J.-P., Office for Official Publications of the European Union, Luxembourg, 2010.

Hoppe, C. J. M., Langer, G., Rokitta, S. D., Wolf-Gladrow, D. A., and Rost, B.: On CO$_2$ pertubation experiments: over-determination of carbonate chemistry reveals inconsistencies, Biogeosciences Discuss., 7, 1707–172 , doi:10.5194/bgd-7-1707-2010, 2010.

Hoppe, C. J. M., Langer, G., and Rost, B.: *Emiliania huxleyi* shows identical responses to elevated pCO$_2$ in TA and DIC manipulations, J. Exp. Mar. Biol. Ecol., 40 , 54– 2, 2011.

Hydes, D. J., Loucaides, S., and Tyrrell, T.: Report on a desk study to identify likely sources of error in the measurements of carbonate system parameters and related calculations, Supplement to DEFRA contract ME4133 DEFRApH monitoring project. National Oceanography Centre, Southampton Research and Consultancy Report, No.x, 54 pp., 2010.

Iglesias-Rodrigue , M. D., Buitenhuis, E. T., Raven, J. A., Schofield, O. M., Poulton, A. J., Gibbs, S., Halloran, P. R., and Baar, H. J. W. d.: Phytoplankton Calcification in a High-CO$_2$ world, Science, 322, 33 –340, 2008.

IPPC: Climate Change 2007: Synthesis Report, Contribution of Working Groups I, II and III to the Fourth Assessment Report of the Intergovernmental Panel on Climate Change (Core Writing Team Pachauri, R. K. and Reisinger, A. (Eds.)) IPCC, Geneva, Swit erland, 2007.

Kim, H.-C. and Lee, K.: Significant contribution of dissolved organic matter to seawater alkalinity, Geophys. Res. Lett., 3 , L20 03, 5 pp., 2009.

Kleypas, J. A., Buddemeier, R. W., Archer, D. E., Gattuso, J.-P., Langdon, C., and Opdyke, B. N.: Geochemical consequences of increased atmospheric carbon dioxide on coral reefs, Science, 284, 118–120, 1999.

Koeve, W., Kim, H.-C., Lee, K., and Oschlies, A.: Potential impact of DOC accumulation on fCO$_2$ and carbonate ion computations in ocean acidification experiments, Biogeosciences Discuss., 8, 3797–3827, doi:10.5194/bgd-8-3797-2011, 2011.

Langer, G., Nehrke, G., Probert, I., Ly, J., and iveri, P.: Strain-specific responses of *Emiliania huxleyi* to changing seawater carbonate chemistry, Biogeosciences, , 2 37–2 4 , 2009, http://www.biogeosciences.net/ /2 37/2009/.

Lee, K., Millero, F. J., and Campbell, D. M.: The reliability of the thermodynamic constants for the dissociation of carbonic acid in seawater, Mar. Chem., 55, 233–245, 199 .

Lee, K., Millero, F. J., Byrne, R. H., Feely, R. A., and Wanninkhof, R.: The recommended dissociation constants for carbonic acid in sea water, Geophys. Res. Lett., 27, 229–232, 2000.

Liu, ., Patsavas, M. C., and Byrne, R. H.: Purification and Characteri ation of meta-Cresol Purple for Spectrophotometric Seawater pH Measurements, Environ. Sci. Technol., 45, 48 2–48 8, 2011.

Lueker, T. J., Dickson, A. G., and Keeling, C. D.: Ocean pCO$_2$ calculated from dissolved inorganic carbon, alkalinity, and equations for K$_1$ and K$_2$: validation based on laboratory measurements of CO$_2$ in gas and seawater at equilibrium, Mar. Chem., 70, 105–119, 2000.

Mackey, K. R., Rivlin, T., Grossman, A. R., Post, A. F., and Paytan, A.: Picophytoplankton responses to changing nutrient and light regimes during a bloom, Mar. Biol., 158, 1531–154 , 2009.

Mehrbach, C., Culberson, C. H., Hawley, J. E., and Pytkow-ic , R. M.: Measurement of the apparent dissociation constants of carbonic acid in seawater at atmospheric pressure, Limnol. Oceanogr., 18, 897–907, 1973.

Millero, F. J., Pierrot, D., Lee, K., Wanninkhof, R., Feely, R., Sabine, C. L., Key, R. M., and Takahashi, T.: Dissociation constants for carbonic acid determined from field measurements, Deep-Sea Res., 49, 1705–1723, 2002.

Pierrot, D. E., Lewis, E., and Wallace, D. W. R.: MS Exel Program Developed for CO_2 System Calculations, ORNL/CDIAC-105aCarbon Dioxide Information Analysis Centre, Oak Ridge National Laboratory, US Department of Energy, 200 .

Raupach, M. R., Marland, G., Ciais, P., Le uere, C., Canadell, J. G., Klepper, G., and Field, C. B.: Global and regional drivers of accelerating CO_2 emissions, Proc. Natl. Acad. Sci. USA, 104, 10288–10293, 2007.

Raven, J. A., Caldeira, K., Elderfield, H., Hoegh-Guldberg, O., Liss, P., Riebesell, U., Shepherd, J., Turley, C., and Watson, A.: Ocean acidification due to increasing atmospheric carbon dioxide, The Royal Society, Cardiff, UK, 2005.

Riebesell U., Fabry V. J., Hansson L., and Gattuso J.-P. (Eds.): Guide for Best Practices in Ocean Acidification Research and Data Reporting, Office for Official Publications of the European Union, Luxembourg, 2010.

Rost, B., ondervan, I., and Wolf-Gladrow, D. A.: Sensitivity of phytoplankton to future changes in ocean carbonate chemistry: current knowledge, contradictions and research directions, Mar. Ecol. Prog. Ser., 373, 227–237, 2008.

Schneider, K. and Ere , J.: The effect of carbonate chemistry on calcification and photosynthesis in the hermatypic coral *Acropora eurystoma*, Limnol. Oceanogr., 51, 1284–1293, 200 .

Thomsen, J., Gutowska, M. A., Saphorster, J., Heinemann, A., Trubenbach, K., Fiet ke, J., Hiebenthal, C., Eisenhauer, A., Kort inger, A., Wahl, M., and Mel ner, F.: Calcifying invertebrates succeed in a naturally CO_2 enriched coastal habitat but are threatened by high levels of future acidification, Biogeosciences Discuss., 7, 5119–515 , doi:10.5194/bgd-7-5119-2010, 2010.

Wanninkhof, R., Lewis, E., Feely, R. A., and Millero, F. J.: The optimal carbonate dissociation constants for determining surface water pCO_2 from alkalinity and total inorganic carbon, Mar. Chem., 5,291–301, 1999.

Wolf-Gladrow, D. A., Riebesell, U., Burkhardt, S., and Bijma, J.: Direct effects of CO_2 on growth and isotopic composition of marine plankton, Tellus, 51, 4 1–47 , 1999.

Bookchapter: Mechanism of coccolith synthesis

Lena-Maria Holtz[*,1]
Gerald Langer[2]
Sebastian D. Rokitta[1]
Silke Thoms[1]

[*] Corresponding author, Lena-Maria.Holtz@awi.de, +49(471)4831-2093,

[1] Alfred Wegener Institute for Polar and Marine Research, Am Handelshafen 12, 27570 Bremerhaven, Germany
[2] Department of Earth Sciences, Cambridge University, Downing St., Cambridge. CB2 3EQ, UK.

Embargoed

Publication: *Emiliania´s* pan genome drives the phytoplankton´s global distribution

Betsy A. Read[1], Jessica Kegel[2*], Mary J. Klute[3*], Alan Kuo[4*], Stephane C. Lefebvre[5*], Florian Maumus[6*], Christoph Mayer[7*], John Miller[8*], Andy Allen, Kay Bidle, Mark Borodovsky, Chris Bowler, Colin Brownlee, Jean-Michel Claverie, J. Mark Cock, Colomban de Vargas, Marek Elias, Stephan Frickenhaus, Vadim N.Gladyshev, Karina Gonzalez, Marco Groth, Chittibabu Guda, Ahmad Hadaegh, Emily K. Herman, Deborah Iglesias-Rodriguez, Bethan Jones, Tracey Lawson, Florian Leese, Yao-Cheng Lin, Erica Lindquist, Alexei Lobanov, Susan Lucas, Shehre- Banoo Malik, Mary E. Marsh, Thomas Mock, Adam Monier, Bernd Mueller-Roeber, Johnathan Napier, Hiroyuki Ogata, Antonio Pagarete, Micaela Parker, Ian Probert, Hadi Quesneville, Christine Raines, Stefan Rensing, Diego Mauricio Riano-Pachon, Sophie Richier, Sebastian Rokitta, Asaf Salamov, Analissa F. Sarno, Jeremy Schmutz, Declan Schroeder, Yoshihiro Shiraiwa, Darren M. Soanes, Klaus Valentin, Mark van der Giezen, Yves Van der Peer, Frederic Verret, Peter von Dassow, Thomas M. Wahlund, Glen Wheeler, Bryony Williams, Willie Wilson, Gordon Wolfe, Louie L. Wurch, Jeremy Young, Joel B. Dacks[3*], Charles F. Delwiche[8*], Sonya Dyhrman[9*], Gernot Glöckner[10*], Uwe John[2*], Thomas Richards[11*], Alexandra Z. Worden[12*], Xiaoyu Zhang[13*], and Igor V. Grigoriev[4]

[1] Biological Sciences, California State University, San Marcos, California. [2] Department of Polar Oceanography, Alfred Wegener Institute for Polar and Marine Research, Bremerhaven, Germany. [3] Department of Cell Biology, University of Alberta, Canada. [4] US Department of Energy Joint Genome Institute, Walnut Creek, California. [5] J. Craig Venter Institute, San Diego, California. [6] Institut National de la Recherché Agronomique, Unité de Recherche en Génomique-Info, Versailles, France. [7] Department of Animal Ecology, Evolution and Biodiversity, Ruhr-Universitat Bochum, Bonn, Germany. [8] Cell Biology and Molecular Genetics, University of Maryland, College Park, Maryland. [9] Biology Department, Woods Hole Oceanographic Institution, Woods Hole, Massachusetts. [10] Leibniz-Institute of Freshwater Ecology and Inland Fisheries, Berlin, Germany. [11] Department of Zoology, The Natural History Museum, London, United Kingdom. [12] Monterey Bay Aquarium Research Institute, Moss Landing, California. [13] Department of Computer Science, California State University, San Marcos, California.

* These lead authors contributed equally to this work.

Embargoed